

# Excitation spectra of quantum matter without quasiparticles

Boston College  
October 15, 2020  
Subir Sachdev

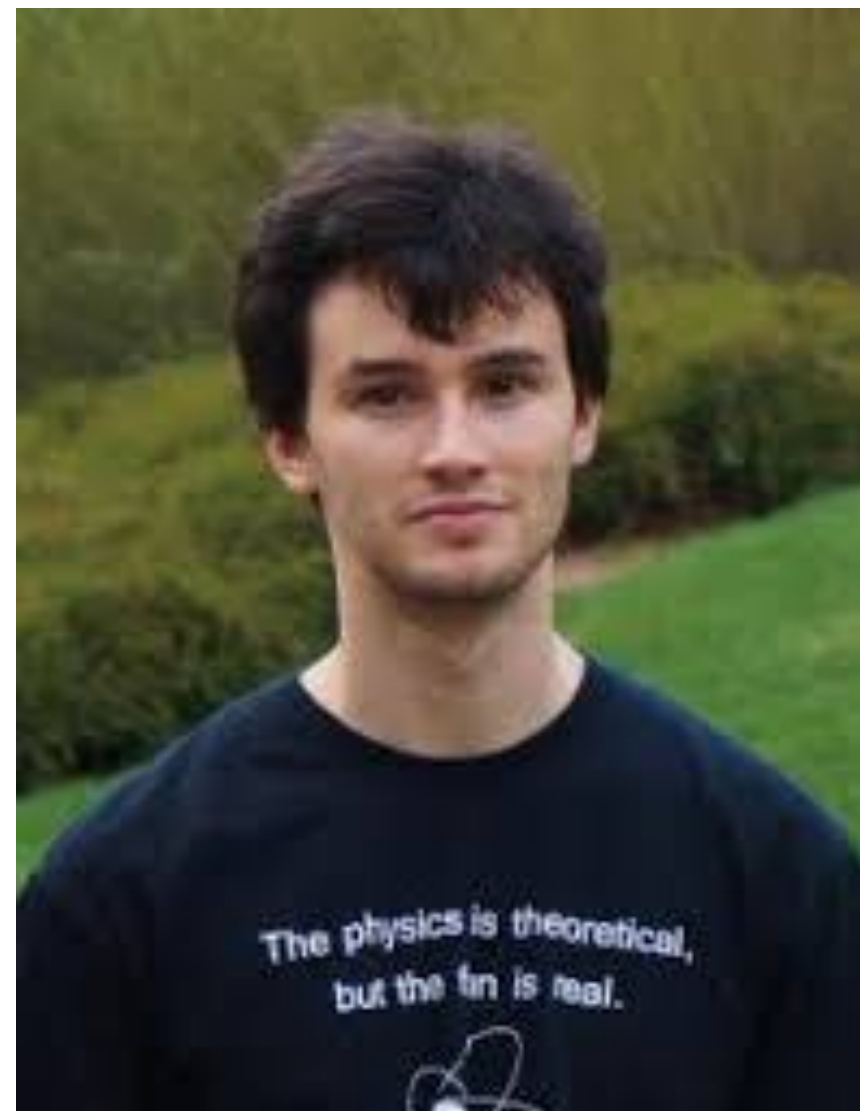


Talk online: [sachdev.physics.harvard.edu](https://sachdev.physics.harvard.edu)





Darshan Joshi



Grigory Tarnopolsky

Physical Review X  
10, 021033 (2020)



Chenyuan Li

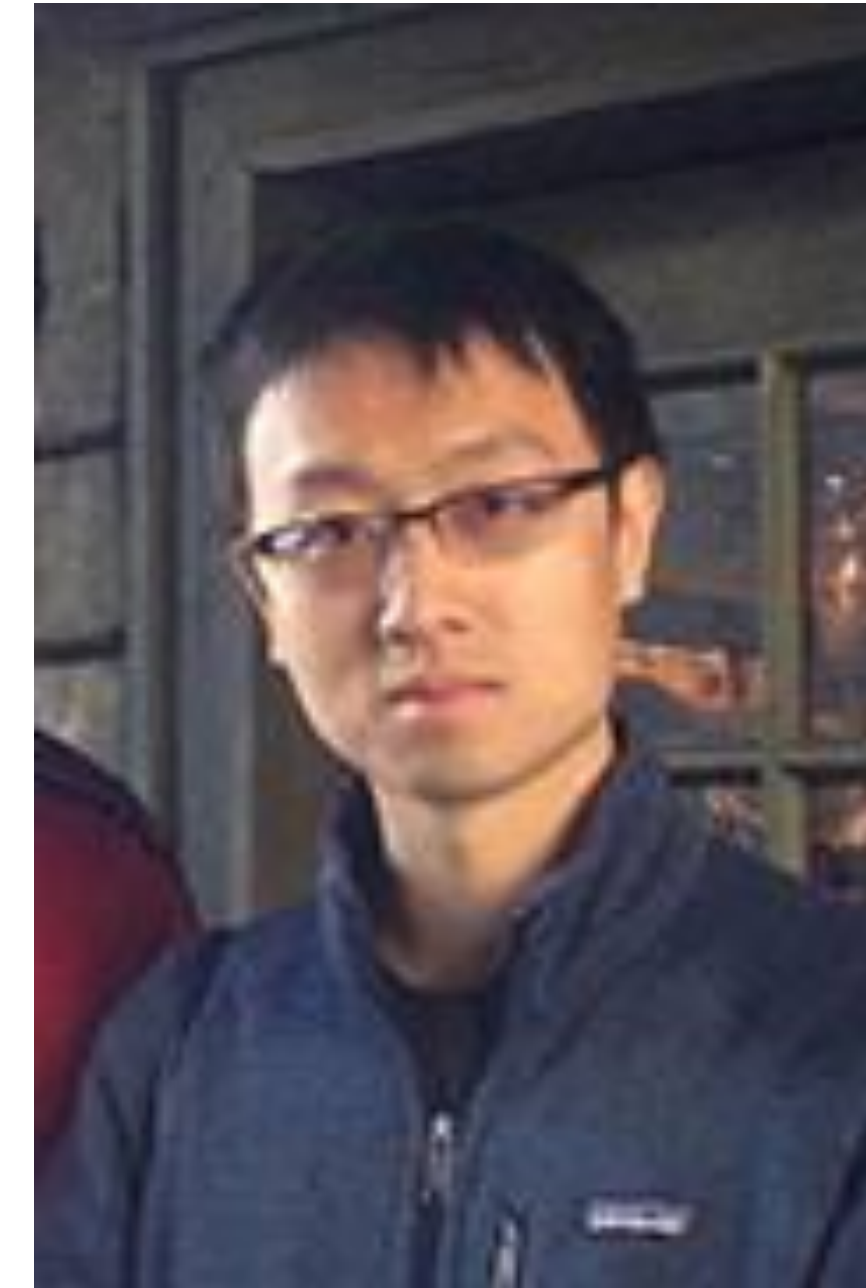


Antoine Georges



Haoyu Guo

Annals of Physics,  
**418**, 168202 (2020)



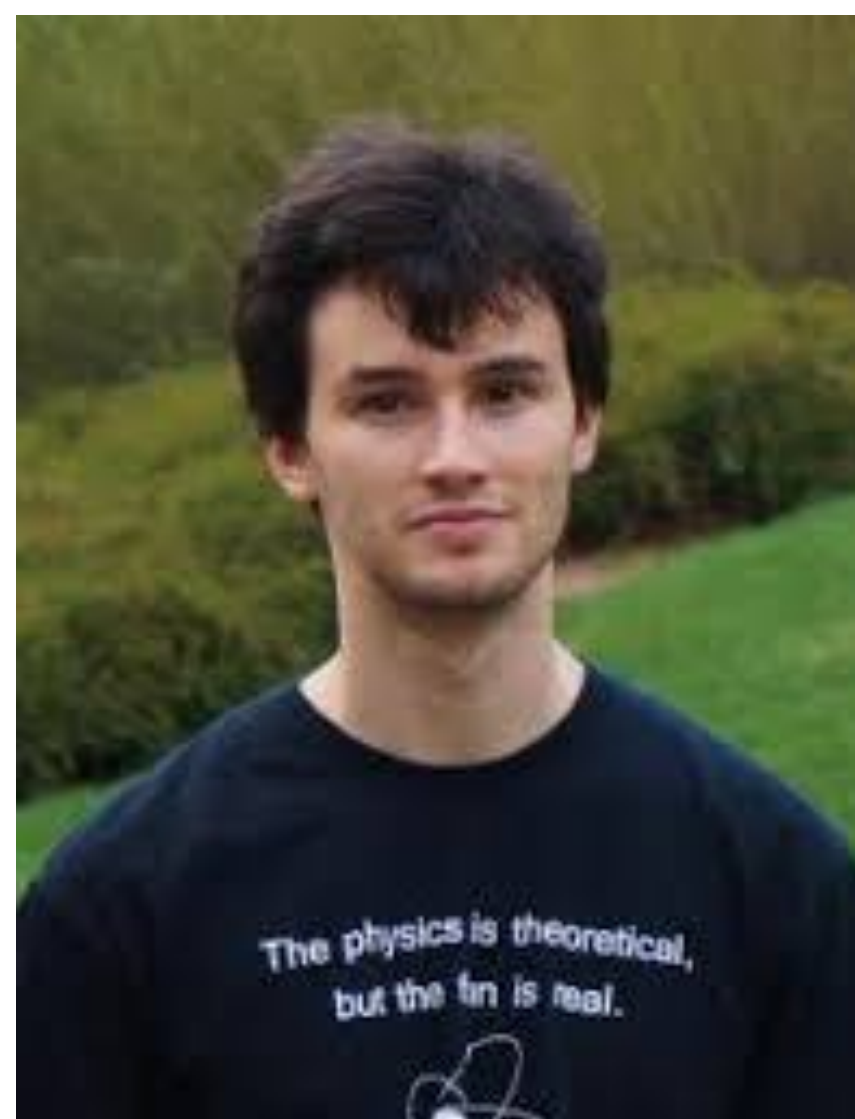
Yingfeu Gu



Maria Tikhanovskaya



Haoyu Guo



Grigory Tarnopolsky

to appear....



Henry Shackleton



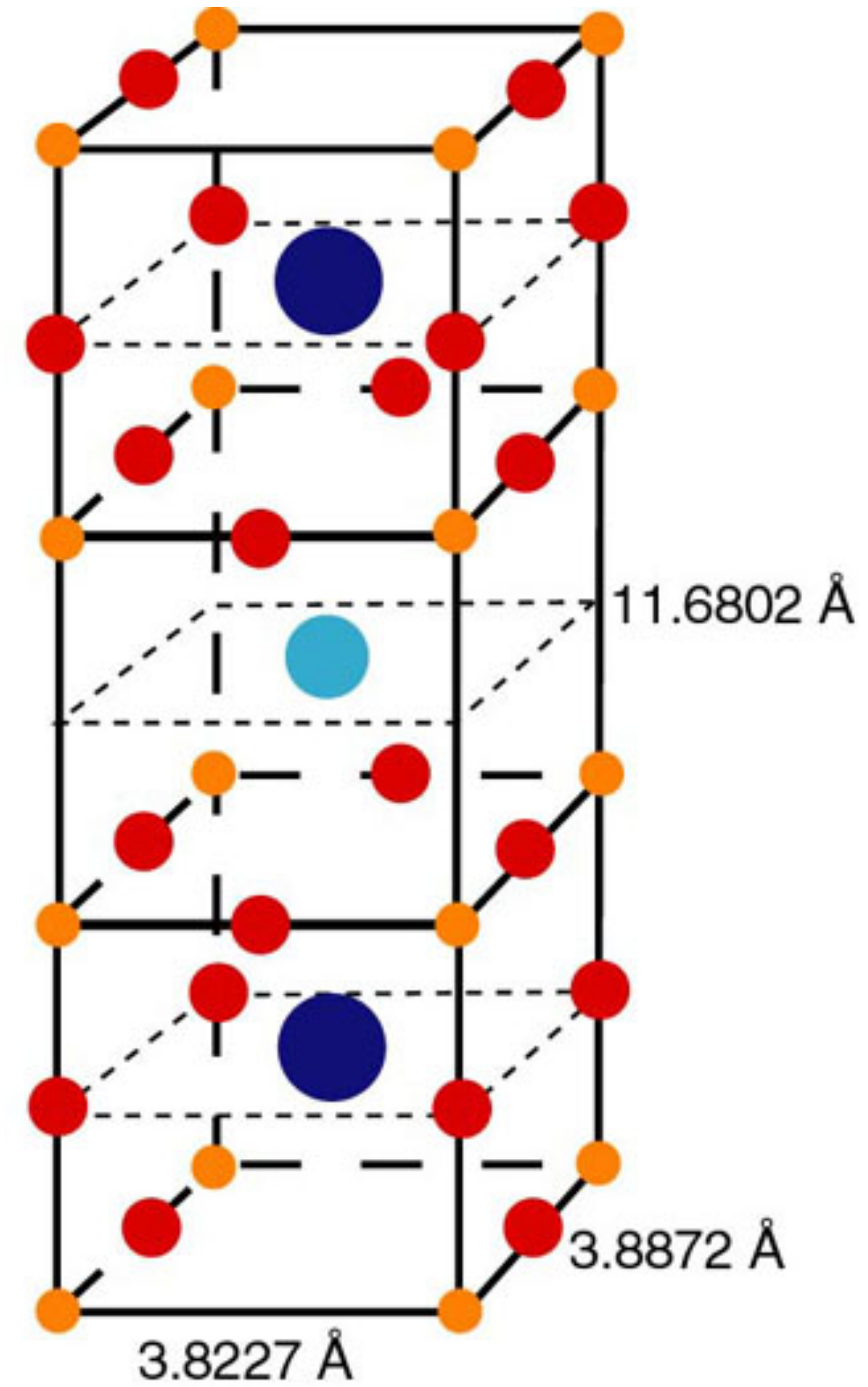
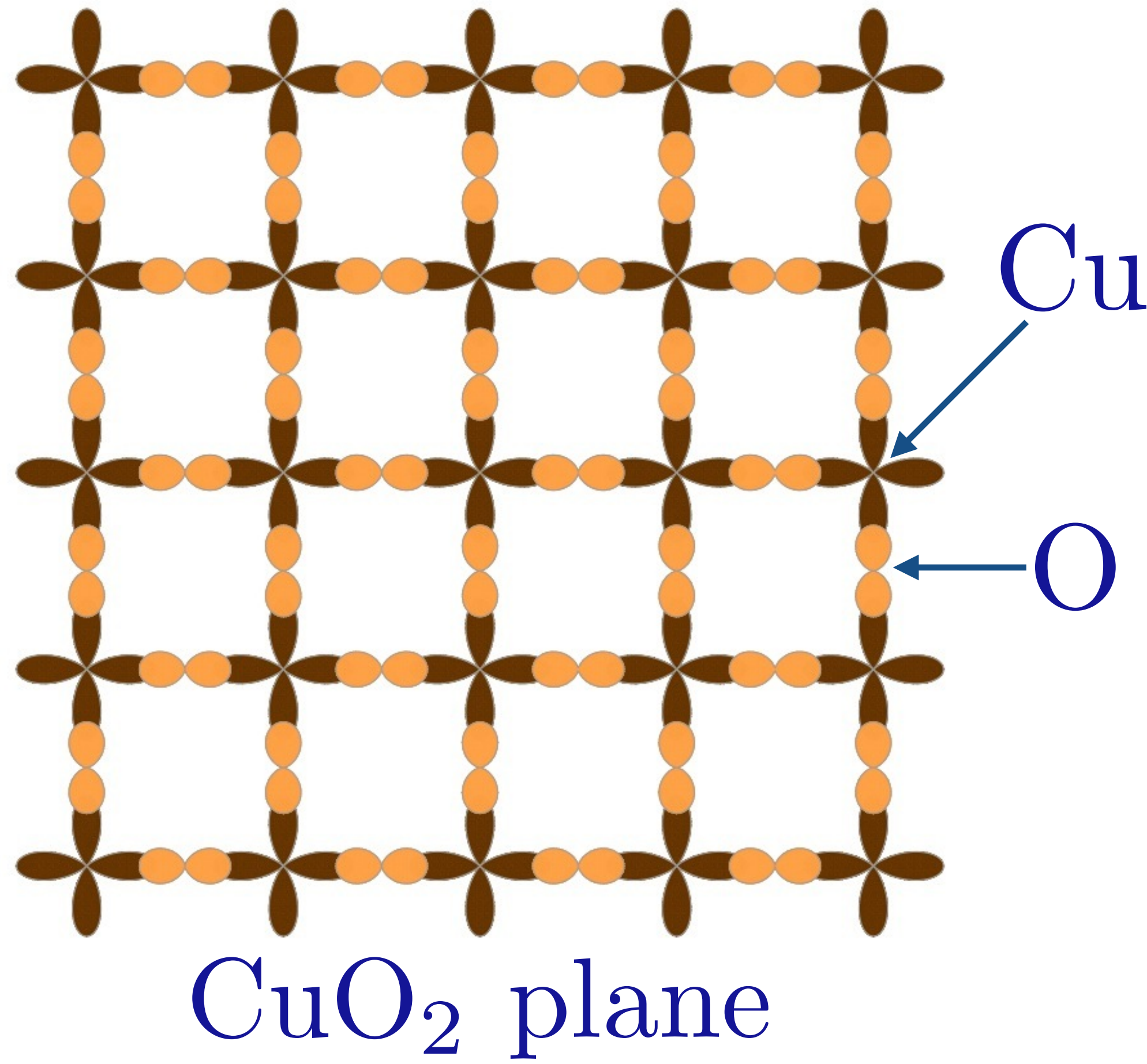
Alexander Wietek

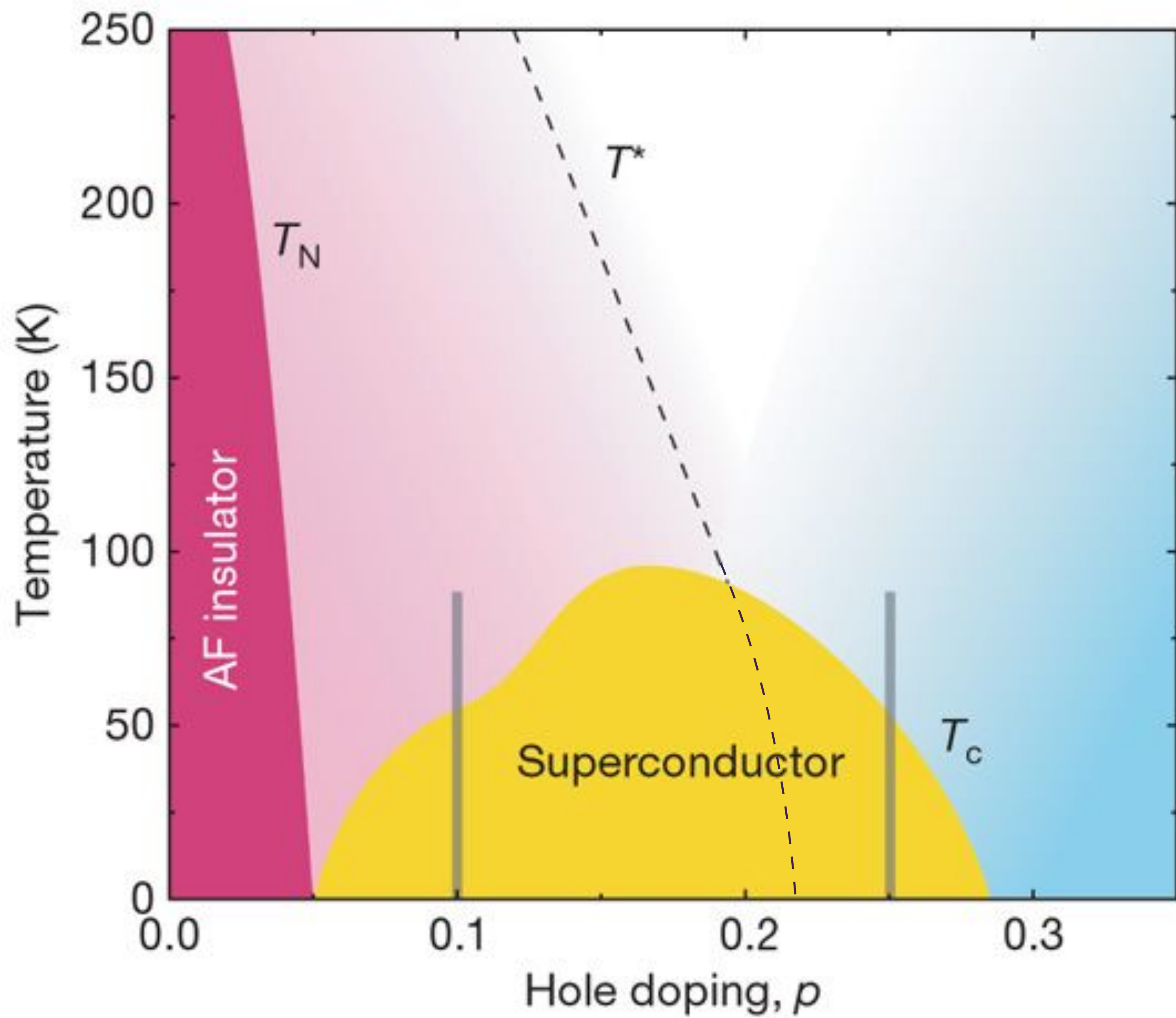


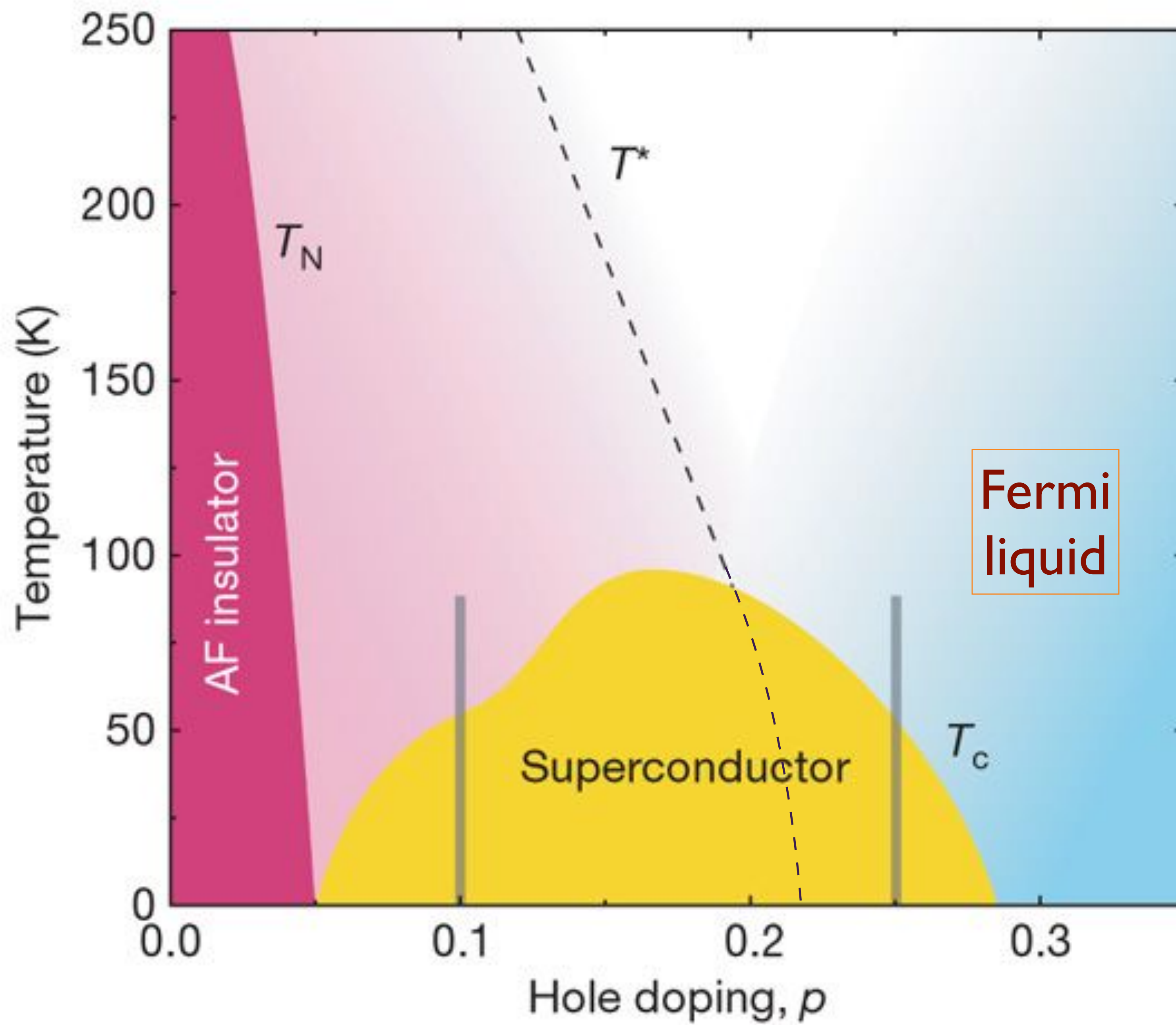
Antoine Georges

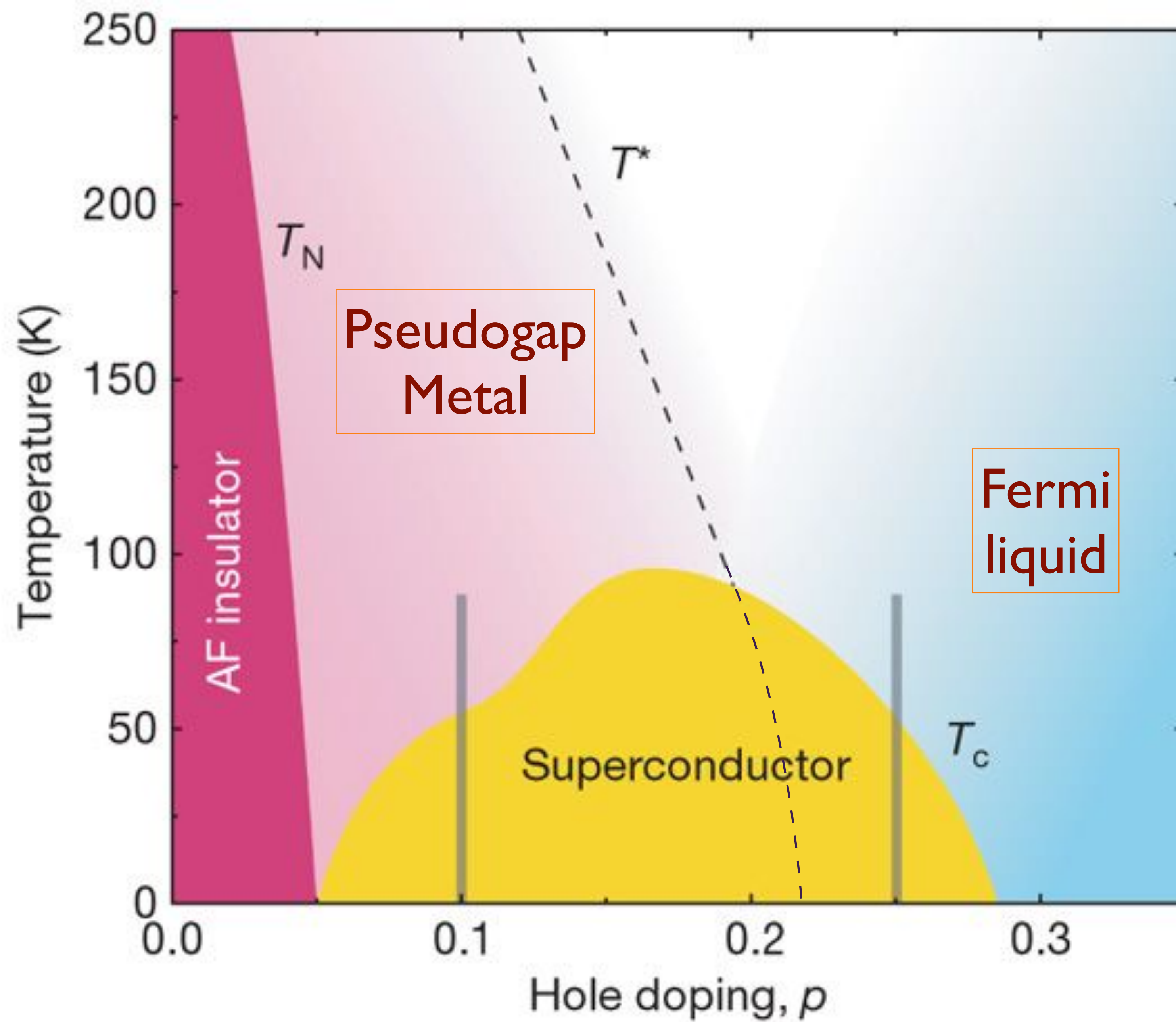
to appear....

# High temperature superconductors





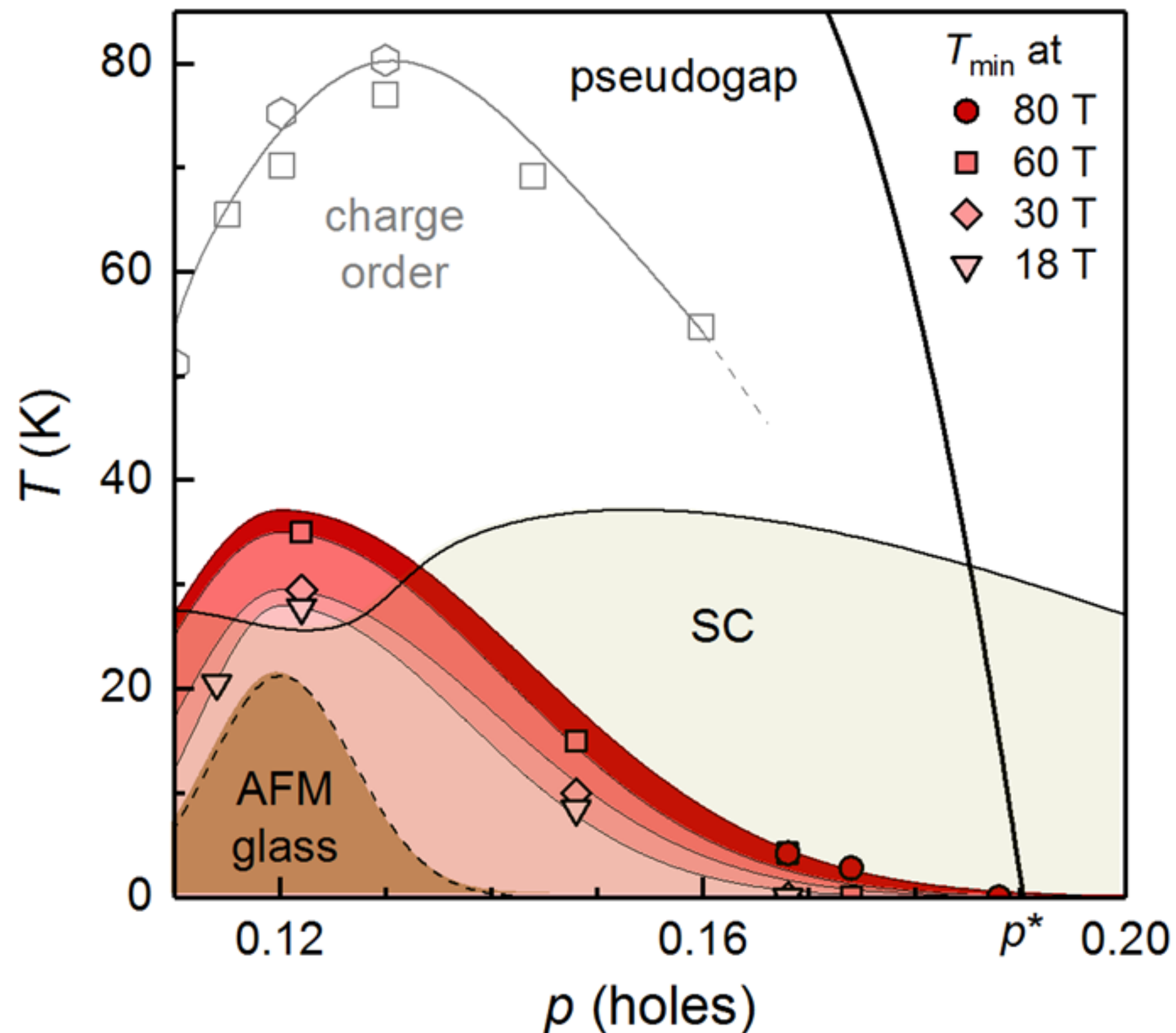




# Hidden magnetism at the pseudogap critical point of a high temperature superconductor

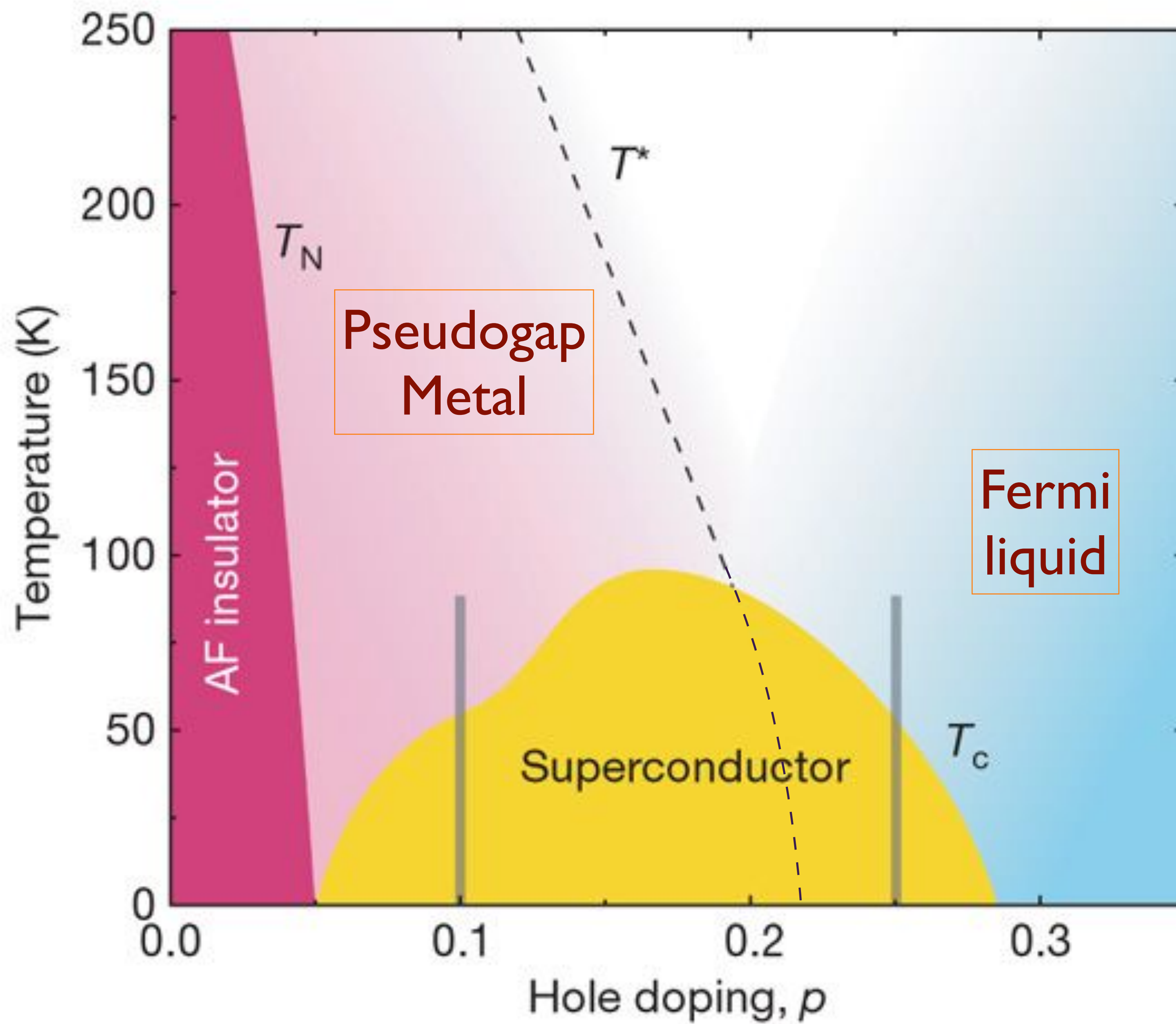
Nature Physics doi: 10.1038/s41567-020-0950-5

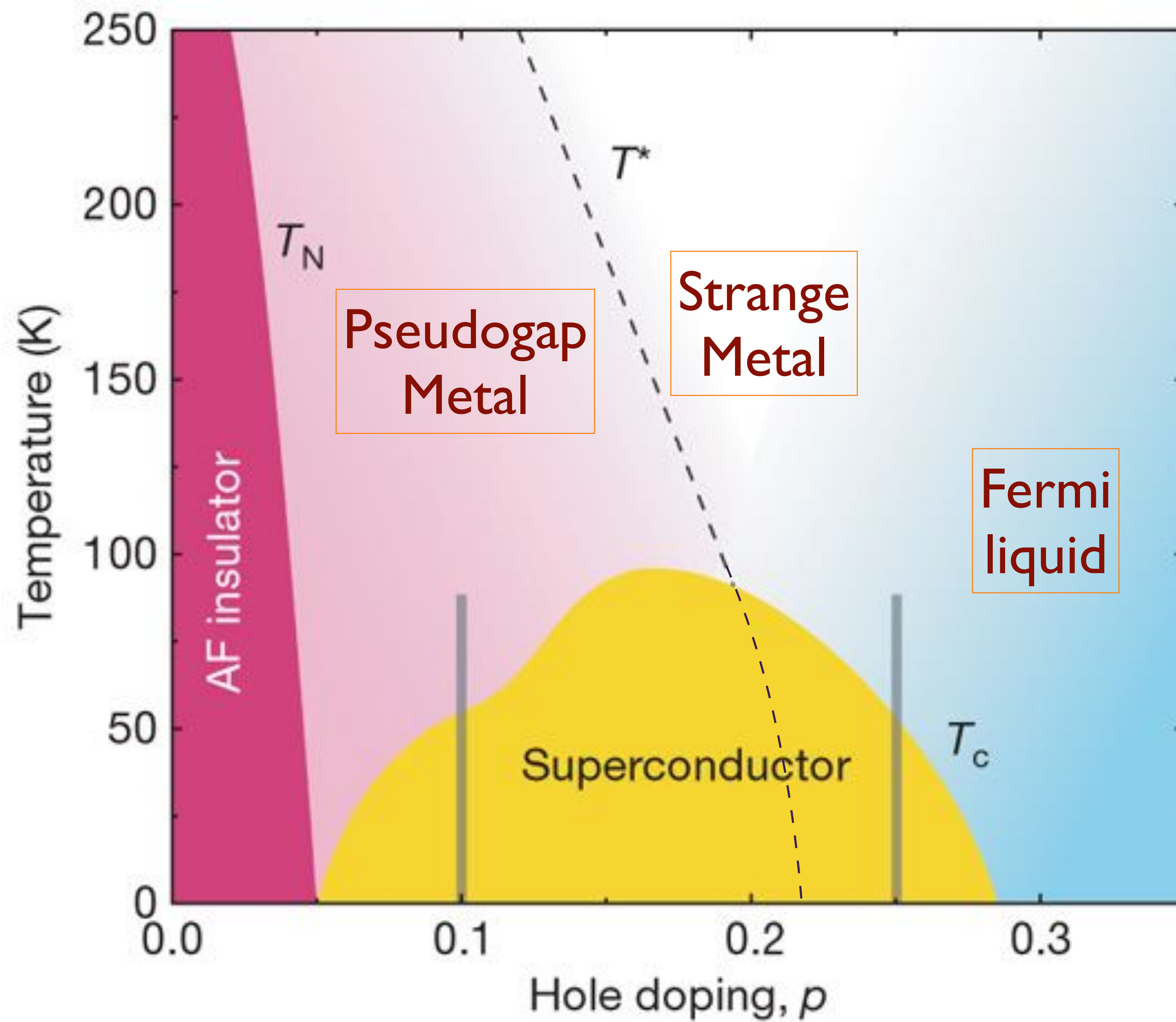
Mehdi Frachet<sup>1†</sup>, Igor Vinograd<sup>1†</sup>, Rui Zhou<sup>1,2</sup>, Siham Benhabib<sup>1</sup>, Shangfei Wu<sup>1</sup>, Hadrien Mayaffre<sup>1</sup>, Steffen Krämer<sup>1</sup>, Sanath K. Ramakrishna<sup>3</sup>, Arneil P. Reyes<sup>3</sup>, Jérôme Debray<sup>4</sup>, Tohru Kurosawa<sup>5</sup>, Naoki Momono<sup>6</sup>, Migaku Oda<sup>5</sup>, Seiki Komiya<sup>7</sup>, Shimpei Ono<sup>7</sup>, Masafumi Horio<sup>8</sup>, Johan Chang<sup>8</sup>, Cyril Proust<sup>1</sup>, David LeBoeuf<sup>1\*</sup>, Marc-Henri Julien<sup>1\*</sup>

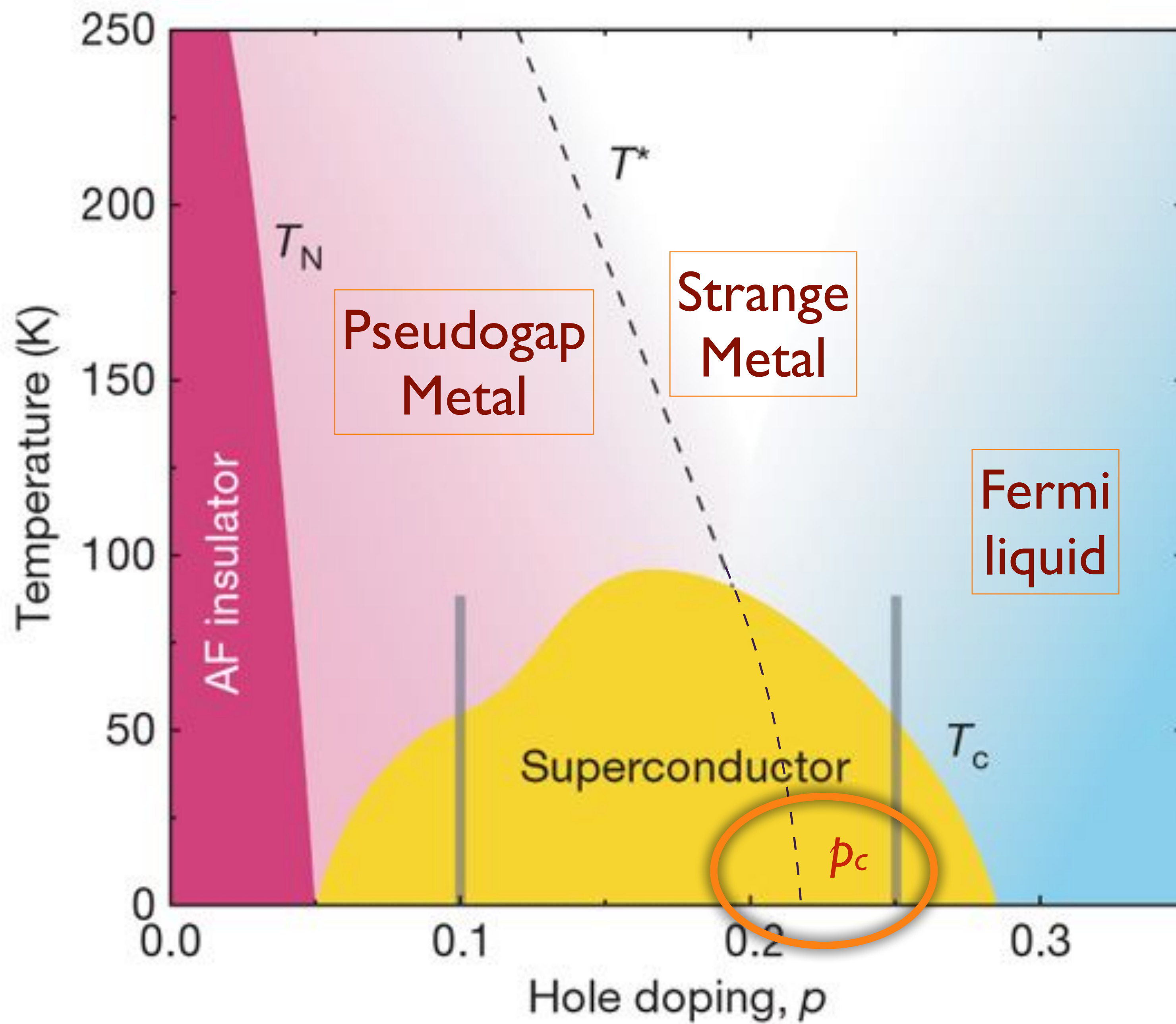


## Quasi-static magnetism in the pseudogap state of $\text{La}_{2-x}\text{Sr}_x\text{CuO}_4$ .

Temperature – doping phase diagram representing  $T_{min}$ , the temperature of the minimum in the sound velocity, at different fields. Since superconductivity precludes the observation of  $T_{min}$  in zero-field, the dashed line (brown area) represents the extrapolated  $T_{min}(B=0)$ . While not exactly equal to the freezing temperature  $T_f$  (see Fig. 2),  $T_{min}$  is closely tied to  $T_f$  and so is expected to have the same doping dependence, including a peak around  $p = 0.12$  in zero/low fields (ref. 2). Onset temperatures of charge order are from ref. 33 (squares) and 35 (hexagons).







Remarkable recent observation of ‘Planckian’ strange metal transport in cuprates, pnictides, magic-angle graphene, and ultracold atoms: the resistivity,  $\rho$ , is linear in  $T$  down to very low  $T$ .

Using the Drude formula

$$\rho = \frac{m^*}{ne^2} \frac{1}{\tau_D}$$

a universal Drude scattering rate is observed

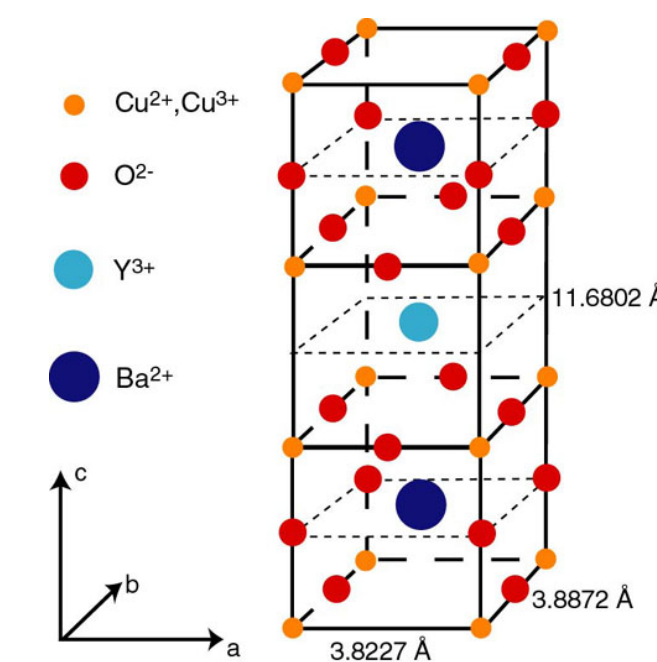
$$\frac{1}{\tau_D} \approx \frac{k_B T}{\hbar},$$

independent of the strength of interactions,  
as  $T \rightarrow 0$

Material		$n$ ( $10^{27} \text{ m}^{-3}$ )	$m^*$ ( $m_0$ )	$A_1 / d$ ( $\Omega / \text{K}$ )	$h / (2e^2 T_F)$ ( $\Omega / \text{K}$ )	$\alpha$
Bi2212	$p = 0.23$	6.8	$8.4 \pm 1.6$	$8.0 \pm 0.9$	$7.4 \pm 1.4$	$1.1 \pm 0.3$
Bi2201	$p \sim 0.4$	3.5	$7 \pm 1.5$	$8 \pm 2$	$8 \pm 2$	$1.0 \pm 0.4$
LSCO	$p = 0.26$	7.8	$9.8 \pm 1.7$	$8.2 \pm 1.0$	$8.9 \pm 1.8$	$0.9 \pm 0.3$
Nd-LSCO	$p = 0.24$	7.9	$12 \pm 4$	$7.4 \pm 0.8$	$10.6 \pm 3.7$	$0.7 \pm 0.4$
PCCO	$x = 0.17$	8.8	$2.4 \pm 0.1$	$1.7 \pm 0.3$	$2.1 \pm 0.1$	$0.8 \pm 0.2$
LCCO	$x = 0.15$	9.0	$3.0 \pm 0.3$	$3.0 \pm 0.45$	$2.6 \pm 0.3$	$1.2 \pm 0.3$
TMTSF	$P = 11 \text{ kbar}$	1.4	$1.15 \pm 0.2$	$2.8 \pm 0.3$	$2.8 \pm 0.4$	$1.0 \pm 0.3$

**Slope of  $T$ -linear resistivity vs Planckian limit in seven materials.**

$$\frac{1}{\tau_D} = \alpha \frac{k_B T}{\hbar}$$



A. Legros, S. Benhabib, W. Tabis, F. Laliberté, M. Dion, M. Lizaire, B. Vignolle, D. Vignolles, H. Raffy, Z. Z. Li, P. Auban-Senzier, N. Doiron-Leyraud, P. Fournier, D. Colson, L. Taillefer, and C. Proust, *Nature Physics* **15**, 142 (2019)

## Challenge for theory:

A model of a metal in which the resistivity,  $\rho$ , obeys

$$\lim_{T \rightarrow 0} \frac{d\rho}{dT} \neq 0$$

$$\rho(T) = \rho(0) + AT + \dots, \quad T \rightarrow 0.$$

Why random and all-to-all couplings ?

# Why random and all-to-all couplings ?

- Randomness is present in the real system.

# Why random and all-to-all couplings ?

- Randomness is present in the real system.
- Randomness self-averages (except for certain correlators in spin-glass phase) — Green's functions are the same on every site.

# Why random and all-to-all couplings ?

- Randomness is present in the real system.
- Randomness self-averages (except for certain correlators in spin-glass phase) — Green's functions are the same on every site.
- The pseudogap-Fermi liquid transition is primarily a transition in many-body entanglement which survives presence of randomness.

# Why random and all-to-all couplings ?

- Randomness is present in the real system.
- Randomness self-averages (except for certain correlators in spin-glass phase) — Green's functions are the same on every site.
- The pseudogap-Fermi liquid transition is primarily a transition in many-body entanglement which survives presence of randomness.
- Introducing randomness removes the “distractions” of other parameters.

# Why random and all-to-all couplings ?

- Randomness is present in the real system.
- Randomness self-averages (except for certain correlators in spin-glass phase) — Green's functions are the same on every site.
- The pseudogap-Fermi liquid transition is primarily a transition in many-body entanglement which survives presence of randomness.
- Introducing randomness removes the “distractions” of other parameters.
- The problem maps onto a model of a “quantum impurity” in a self-consistent environment. Closely related models are obtained in non-random models in the limit of large spatial dimension in extended dynamical mean-field theory.

# Why random and all-to-all couplings ?

- Randomness is present in the real system.
- Randomness self-averages (except for certain correlators in spin-glass phase) — Green's functions are the same on every site.
- The pseudogap-Fermi liquid transition is primarily a transition in many-body entanglement which survives presence of randomness.
- Introducing randomness removes the “distractions” of other parameters.
- The problem maps onto a model of a “quantum impurity” in a self-consistent environment. Closely related models are obtained in non-random models in the limit of large spatial dimension in extended dynamical mean-field theory.
- Analytic and numeric progress is possible, and we can compare their results !

1. Random  $J$  model (insulator)

*Operator spectrum and numerics*

2. Random  $t$ - $J$  model (metals)

*Deconfined criticality and numerics*

3. Random  $t$ - $J$ - $U$  model

1. Random  $J$  model (insulator)

*Operator spectrum and numerics*

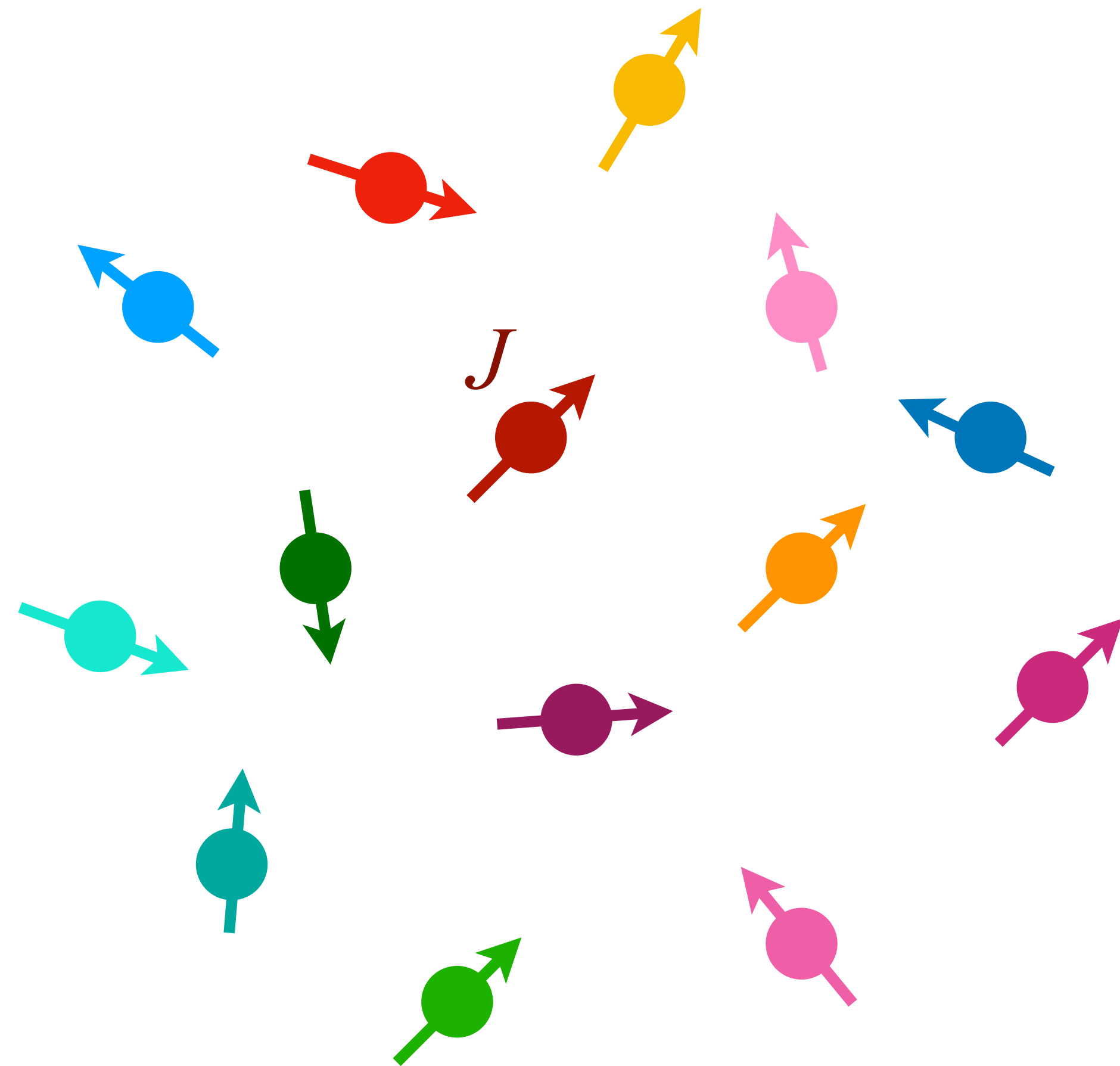
2. Random  $t$ - $J$  model (metals)

*Deconfined criticality and numerics*

3. Random  $t$ - $J$ - $U$  model

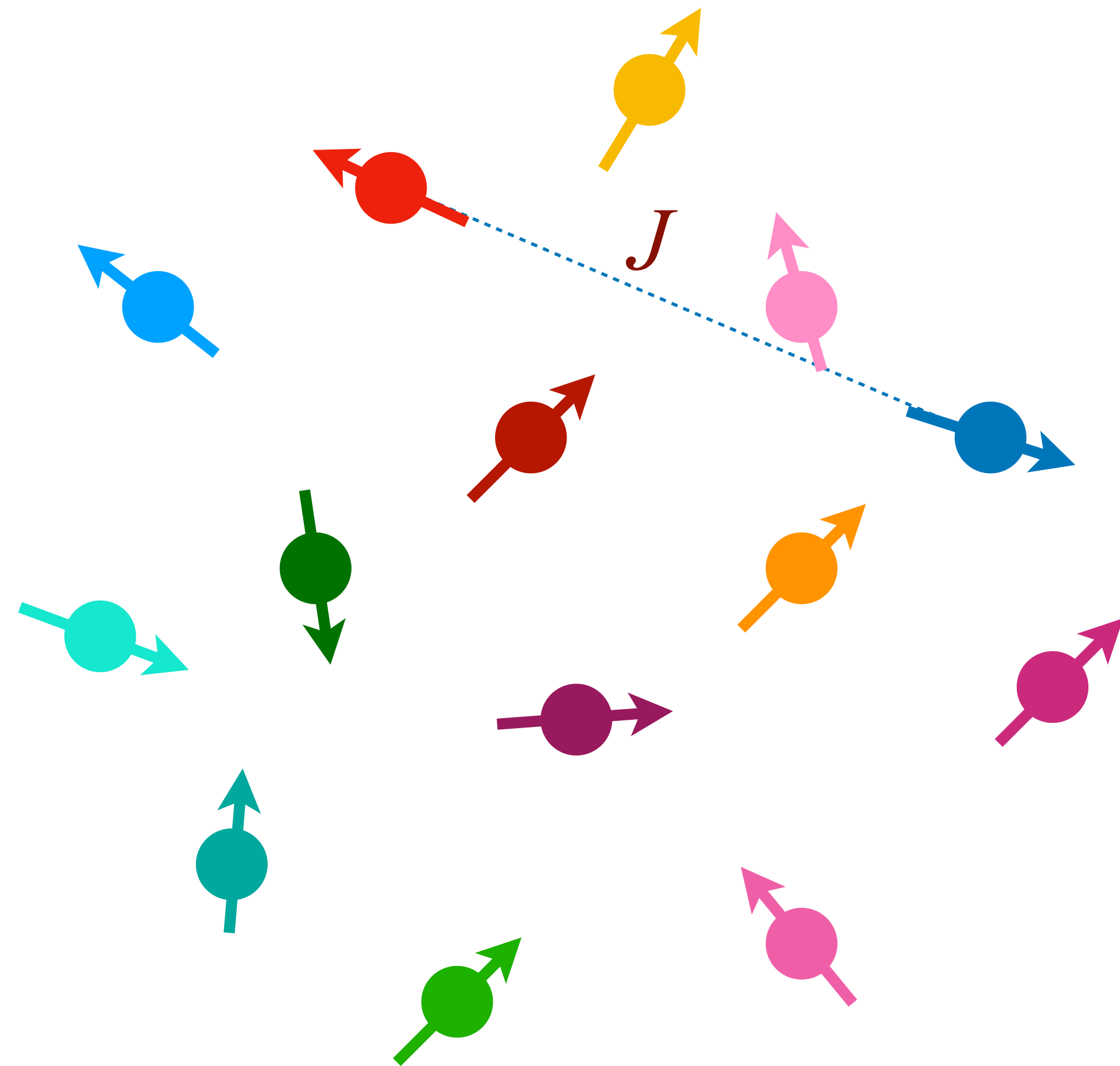
# Random $J$ model (insulator)

$$H = \frac{1}{\sqrt{N}} \sum_{i < j=1}^N J_{ij} \vec{S}_i \cdot \vec{S}_j$$



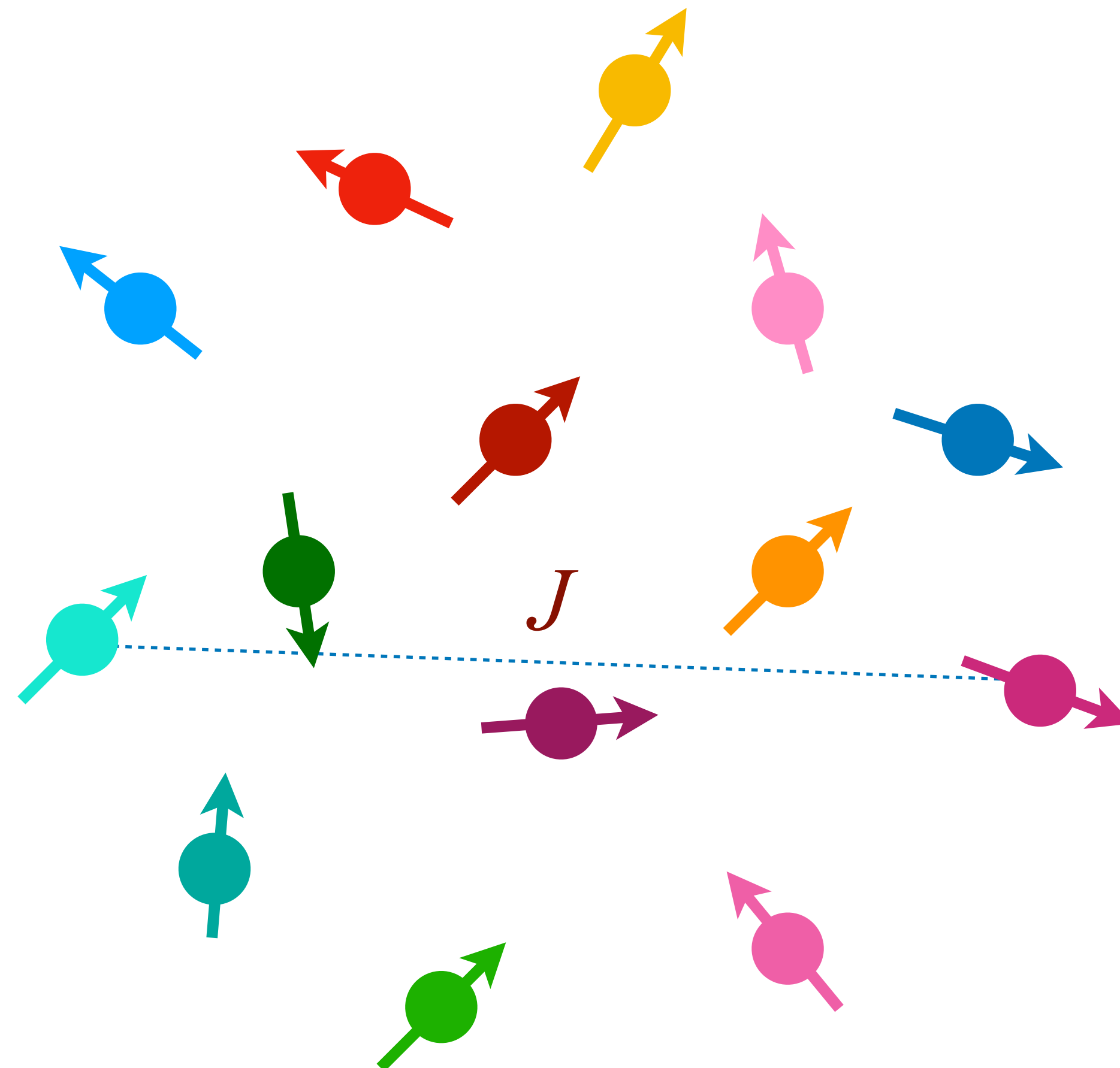
# Random $J$ model (insulator)

$$H = \frac{1}{\sqrt{N}} \sum_{i < j=1}^N J_{ij} \vec{S}_i \cdot \vec{S}_j$$



# Random $J$ model (insulator)

$$H = \frac{1}{\sqrt{N}} \sum_{i < j=1}^N J_{ij} \vec{S}_i \cdot \vec{S}_j$$



# Random $J$ model (insulator)

$$H = \frac{1}{\sqrt{N}} \sum_{i < j=1}^N J_{ij} \vec{S}_i \cdot \vec{S}_j$$

$$\alpha = \uparrow, \downarrow, \quad \vec{S}_i = \frac{1}{2} f_{i\alpha}^\dagger \vec{\sigma}_{\alpha\beta} f_{i\beta}, \quad \sum_{\alpha} f_{i\alpha}^\dagger f_{i\alpha} = 1$$

$$J_{ij} \text{ random, } \overline{J_{ij}} = 0, \overline{J_{ij}^2} = J^2$$

Fermionic spinons

# Random $J$ model (insulator): $SU(M)$ symmetry

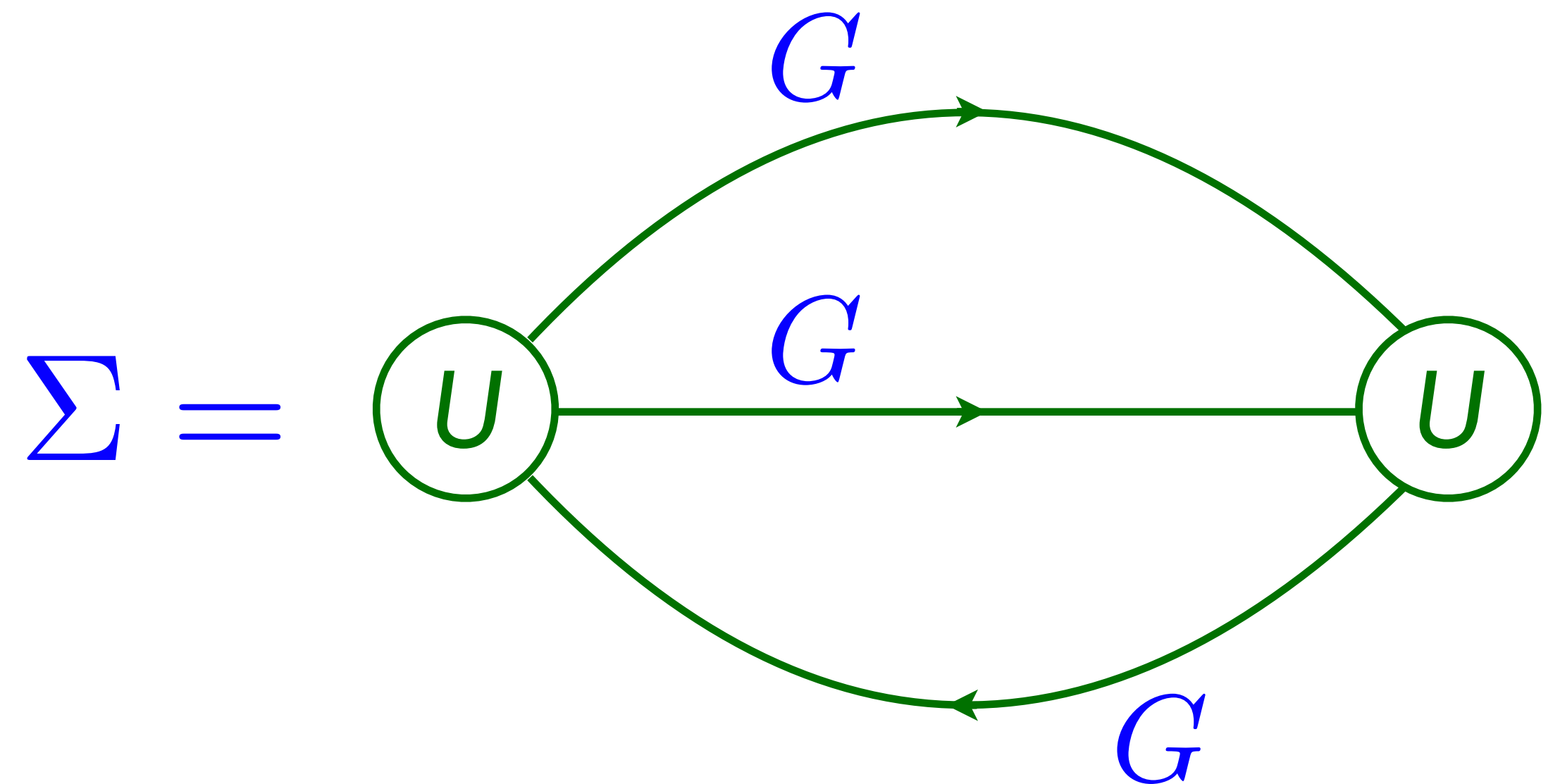
Express the spin operator in terms of fermionic spinons  $\vec{S} = (1/2)f_\alpha^\dagger \vec{\sigma}_{\alpha\beta} f_\beta$ , and let  $\alpha = 1 \dots M$ . The fermions obey the constraint

$$\sum_{\alpha=1}^M f_\alpha^\dagger f_\alpha = \frac{M}{2}$$

In the limit of large  $N$ , *followed* by large  $M$ , we obtain the SYK equations for the spinon Green's function  $G$  and self energy  $\Sigma$ :

$$G(i\omega) = \frac{1}{i\omega - \Sigma(i\omega)}$$

$$\Sigma(\tau) = -J^2 G^2(\tau) G(-\tau)$$



## Random $J$ model (insulator)

$$G(i\omega) = \frac{1}{i\omega - \Sigma(i\omega)} \quad , \quad \Sigma(\tau) = -J^2 G^2(\tau) G(-\tau)$$

The solution at  $T = 0$  for  $|\tau| \gg 1/J$  is

$$G(\tau) \sim \frac{\text{sgn}(\tau)}{\sqrt{\tau}} \quad , \quad \langle \vec{S}(\tau) \cdot \vec{S}(0) \rangle \sim \frac{1}{|\tau|}$$

or for  $|z| \ll J$

$$G(z) = \frac{A}{\sqrt{z}} \quad , \quad \Sigma(z) = -\frac{1}{A} \sqrt{z}$$

# Time reparameterization symmetry

$$G(i\omega) = \frac{1}{i\omega - \Sigma(i\omega)} \quad , \quad \Sigma(\tau) = -J^2 G^2(\tau) G(-\tau)$$

At frequencies  $\ll J$ , the  $i\omega$  can be dropped, and without it the SYK equations are invariant under time reparameterization and gauge transformations. The singular part of the self-energy and the Green's function obey

$$\int_0^\beta d\tau_2 \Sigma(\tau_1, \tau_2) G(\tau_2, \tau_3) = -\delta(\tau_1 - \tau_3)$$
$$\Sigma(\tau_1, \tau_2) = -J^2 G^2(\tau_1, \tau_2) G(\tau_2, \tau_1)$$

These equations can be solved exactly at  $T = 0$  and  $T > 0$ .

# Time reparameterization symmetry

$$\int_0^\beta d\tau_2 \Sigma(\tau_1, \tau_2) G(\tau_2, \tau_3) = -\delta(\tau_1 - \tau_3)$$

$$\Sigma(\tau_1, \tau_2) = -J^2 G^2(\tau_1, \tau_2) G(\tau_2, \tau_1)$$

These equations are invariant under

$$\tau = f(\sigma)$$

$$G(\tau_1, \tau_2) = [f'(\sigma_1) f'(\sigma_2)]^{-1/4} \frac{g(\sigma_1)}{g(\sigma_2)} \tilde{G}(\sigma_1, \sigma_2)$$

$$\Sigma(\tau_1, \tau_2) = [f'(\sigma_1) f'(\sigma_2)]^{-3/4} \frac{g(\sigma_1)}{g(\sigma_2)} \tilde{\Sigma}(\sigma_1, \sigma_2)$$

where  $f(\sigma)$  and  $g(\sigma)$  are arbitrary functions.

By using  $f(\sigma) = \tan(\pi T \sigma) / (\pi T)$  we can obtain the  $T > 0$  solution. A. Kitaev, 2015

S. Sachdev, PRX **5**, 041025 (2015)

# Time reparameterization symmetry

Let us write the large  $N$  saddle point solutions as

$$\begin{aligned}G_s(\tau_1 - \tau_2) &\sim (\tau_1 - \tau_2)^{-1/2} \\ \Sigma_s(\tau_1 - \tau_2) &\sim (\tau_1 - \tau_2)^{-3/2}.\end{aligned}$$

and so  $G(\tau_1, \tau_2) = G_s(\tau_1 - \tau_2)$ . Now when we transform to  $\sigma$  co-ordinates,  $\tilde{G}(\sigma_1, \sigma_2)$  will not in general be a function of  $\sigma_1 - \sigma_2$ : so time reparameterization symmetry is spontaneously broken by the saddle point.

# Time reparameterization symmetry

Let us write the large  $N$  saddle point solutions as

$$\begin{aligned} G_s(\tau_1 - \tau_2) &\sim (\tau_1 - \tau_2)^{-1/2} \\ \Sigma_s(\tau_1 - \tau_2) &\sim (\tau_1 - \tau_2)^{-3/2}. \end{aligned}$$

and so  $G(\tau_1, \tau_2) = G_s(\tau_1 - \tau_2)$ . Now when we transform to  $\sigma$  co-ordinates,  $\tilde{G}(\sigma_1, \sigma_2)$  will not in general be a function of  $\sigma_1 - \sigma_2$ : so time reparameterization symmetry is spontaneously broken by the saddle point.

We search for the transformations under which  $\tilde{G}(\sigma_1, \sigma_2) = G_s(\sigma_1 - \sigma_2)$ : this is true only for the  $\text{SL}(2, \mathbb{R})$  transformations under which

$$f(\tau) = \frac{a\tau + b}{c\tau + d}, \quad ad - bc = 1.$$

So the (approximate) time reparameterization symmetry is spontaneously broken down to  $\text{SL}(2, \mathbb{R})$  by the saddle point.

# Random $J$ model (insulator)

$$G(i\omega) = \frac{1}{i\omega - \Sigma(i\omega)} \quad , \quad \Sigma(\tau) = -J^2 G^2(\tau) G(-\tau)$$

The conformal (SL(2,R) invariant) solution for  $|\tau| \gg 1/J$  and  $T \ll J$  is

$$G(\tau) \sim \text{sgn}(\tau) \left| \frac{\pi T}{\sin(\pi T \tau)} \right|^{1/2} \quad , \quad G(\omega) \sim \frac{-i}{\sqrt{T}} \frac{\Gamma\left(\frac{1}{4} - \frac{i\hbar\omega}{2\pi T}\right)}{\Gamma\left(\frac{3}{4} - \frac{i\hbar\omega}{2\pi T}\right)}$$

and the local spin susceptibility  $\chi_L(i\omega_n) = \int_0^\beta d\tau \langle \vec{S}(\tau) \cdot \vec{S}(0) \rangle$  is

$$\text{Im}\chi_L(\omega) \sim \tanh\left(\frac{\hbar\omega}{2T}\right)$$

# Corrections to $SL(2,R)$ conformal invariance

The irrelevant  $f_\alpha^\dagger \partial_\tau f_\alpha$  term will induce corrections proportional to conformal primaries

$$S_{\text{SYK}} = S_{\text{CFT}} + \sum_h g_h \int_0^\beta d\tau O_h(\tau),$$

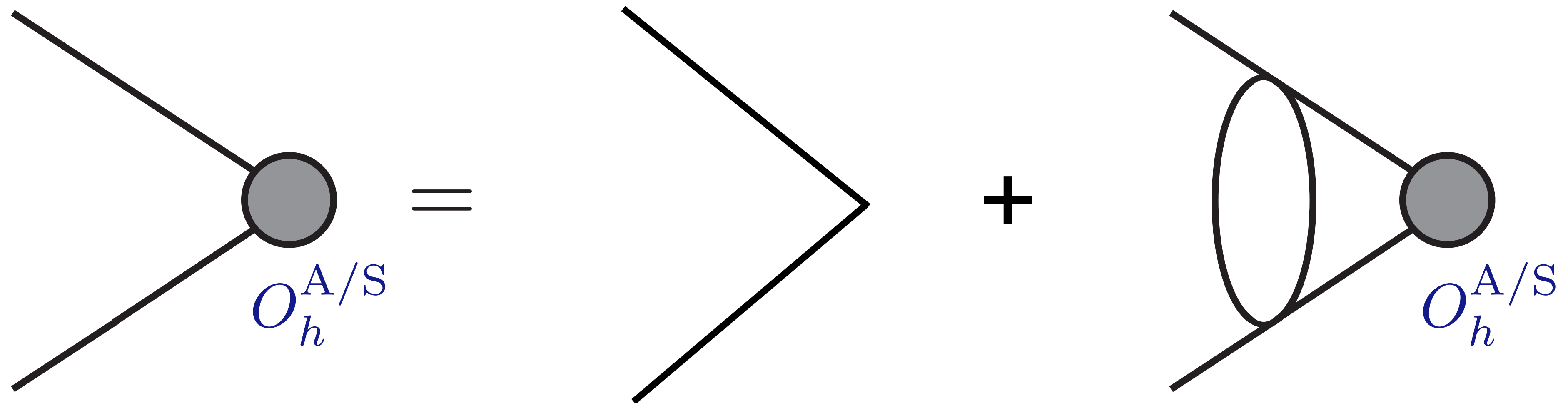
where  $O_h$  has scaling dimension  $h$  with  $\langle O_h(\tau) O_h(0) \rangle \sim |\tau|^{-2h}$ . Note that  $\dim[g_h] = 1 - h$ , so  $h > 1$  is an irrelevant perturbation. This will induce a correction

$$G(\tau) = G_{\text{conformal}}(\tau) \left[ 1 - \frac{\alpha_h}{|J_\tau|^{h-1}} + \dots \right],$$

where we can relate  $\alpha_h$  to  $g_h$  by computing the conformal 3-point correlator  $\langle f_\alpha^\dagger(\tau_1) f_\alpha(\tau_2) O_h(\tau_3) \rangle$ . All expressions can be generalized to  $T > 0$  by a conformal mapping.

# Corrections to $SL(2,R)$ conformal invariance

There are an infinite set of bilinear primary operators  $O_h^A(\tau)$  and  $O_h^S(\tau)$ , which descend from the UV operators  $O_{h_n}^A = f_\alpha^\dagger \partial_\tau^{2n+1} f_\alpha$  and  $O_{h_n}^S = f_\alpha^\dagger \partial_\tau^{2n} f_\alpha$  for  $n = 0, 1, 2, \dots$ . To compute the scaling dimensions of the operators  $O_h^{A/S}(\tau)$  we consider three point functions

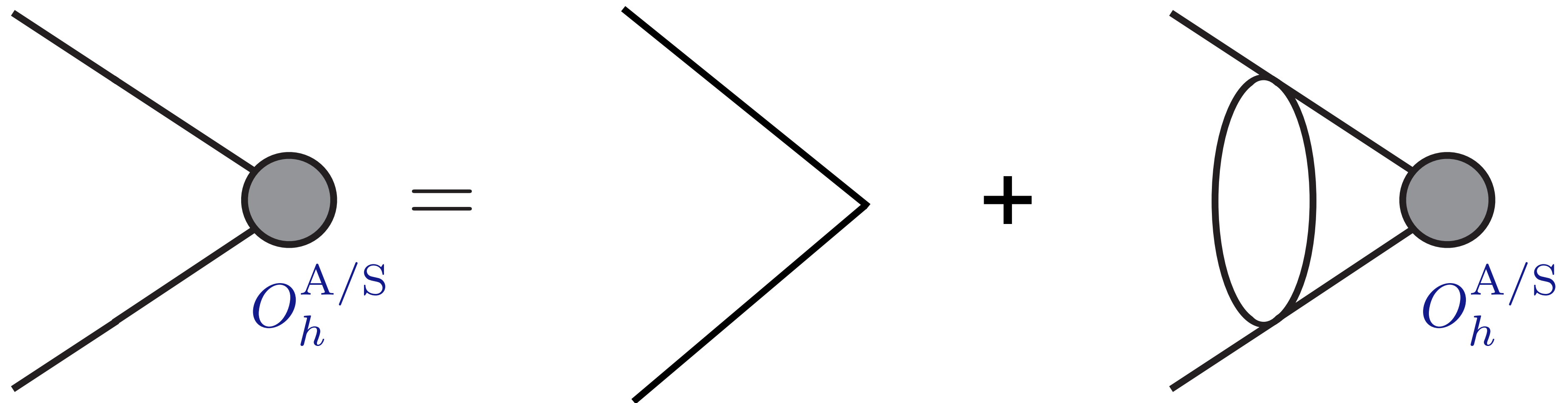


Solution of this integral equation yields the conditions  $k_A(h) = 1$  and  $k_S(h) = 1$  where

$$k_A(h) = \frac{3(1 - \sin(\pi h))}{\cos(\pi h)(2h - 1)} \quad , \quad k_S(h) = \frac{(1 + \sin(\pi h))}{\cos(\pi h)(1 - 2h)}$$

# Corrections to $SL(2,R)$ conformal invariance

There are an infinite set of bilinear primary operators  $O_h^A(\tau)$  and  $O_h^S(\tau)$ , which descend from the UV operators  $O_{h_n}^A = f_\alpha^\dagger \partial_\tau^{2n+1} f_\alpha$  and  $O_{h_n}^S = f_\alpha^\dagger \partial_\tau^{2n} f_\alpha$  for  $n = 0, 1, 2, \dots$ . To compute the scaling dimensions of the operators  $O_h^{A/S}(\tau)$  we consider three point functions



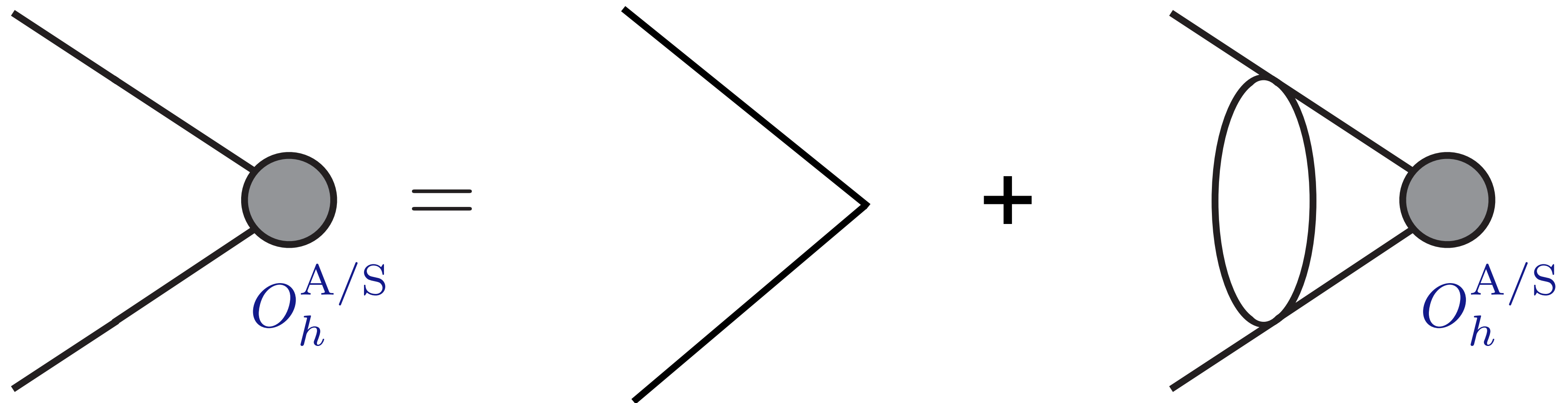
Solution of this integral equation yields the conditions  $k_A(h) = 1$  and  $k_S(h) = 1$  where

$$k_A(h) = \frac{3(1 - \sin(\pi h))}{\cos(\pi h)(2h - 1)}, \quad k_S(h) = \frac{(1 + \sin(\pi h))}{\cos(\pi h)(1 - 2h)}$$

‘Protected’ operators:  $k_A(h = 2) = 1$ : time reparameterization operator

# Corrections to $SL(2,R)$ conformal invariance

There are an infinite set of bilinear primary operators  $O_h^A(\tau)$  and  $O_h^S(\tau)$ , which descend from the UV operators  $O_{h_n}^A = f_\alpha^\dagger \partial_\tau^{2n+1} f_\alpha$  and  $O_{h_n}^S = f_\alpha^\dagger \partial_\tau^{2n} f_\alpha$  for  $n = 0, 1, 2, \dots$ . To compute the scaling dimensions of the operators  $O_h^{A/S}(\tau)$  we consider three point functions



Solution of this integral equation yields the conditions  $k_A(h) = 1$  and  $k_S(h) = 1$  where

$$k_A(h) = \frac{3(1 - \sin(\pi h))}{\cos(\pi h)(2h - 1)}, \quad k_S(h) = \frac{(1 + \sin(\pi h))}{\cos(\pi h)(1 - 2h)}$$

‘Protected’ operators:

$k_A(h = 2) = 1$ : time reparameterization operator

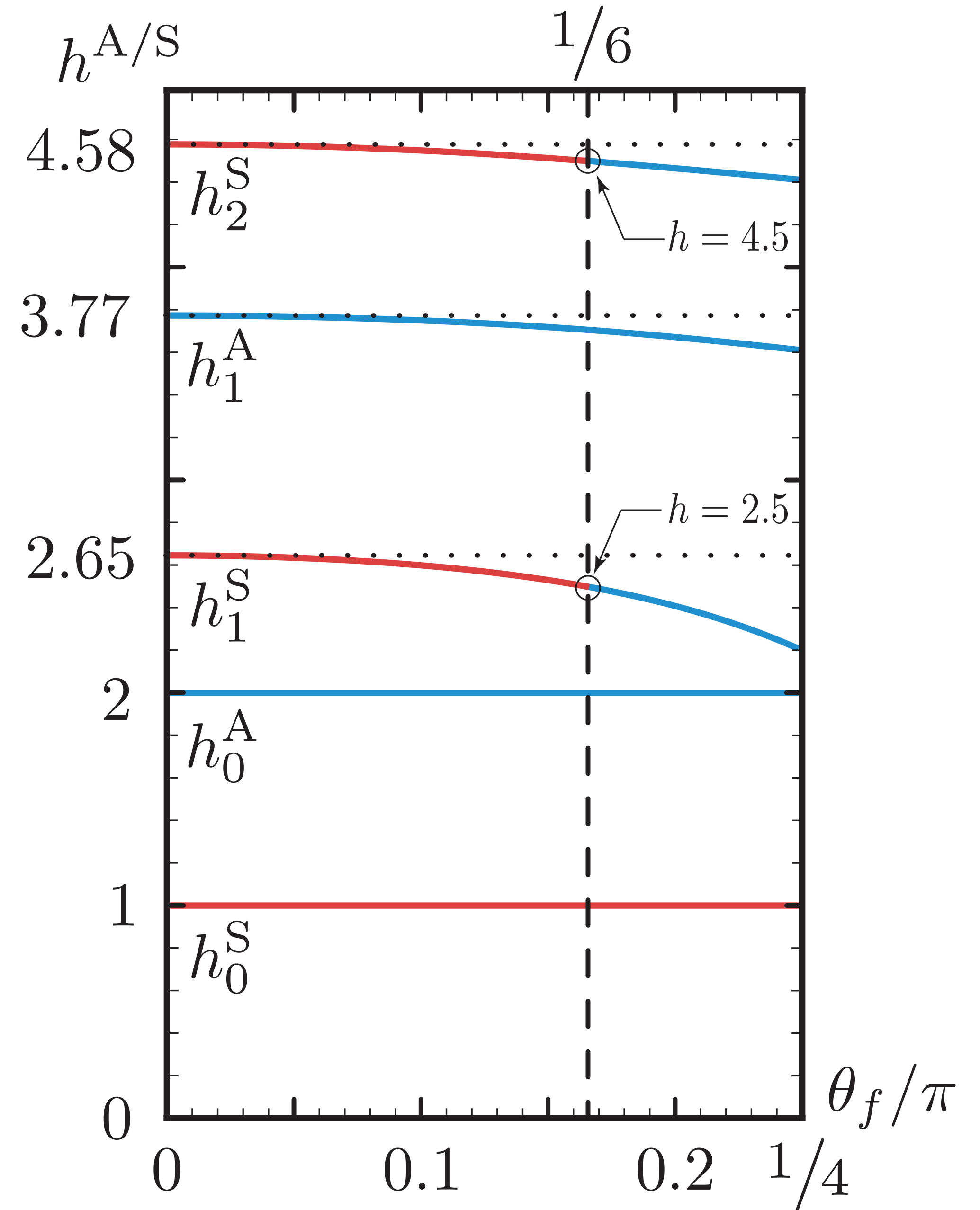
$k_S(h = 1) = 1$ : emergent  $U(1)$  gauge symmetry.

# Corrections to SL(2,R) conformal invariance

We can also consider more general models with  $\sum_{\alpha} f_{i\alpha}^{\dagger} f_{i\alpha} = \kappa M$  (the particle-hole symmetric case is  $\kappa = 1/2$ ). These are characterized by

$$G(\omega) = \begin{cases} \frac{C e^{-i\pi/4 - i\theta_f}}{\sqrt{\omega}}, & \omega > 0 \\ \frac{-C e^{i\pi/4 - i\theta_f}}{\sqrt{|\omega|}}, & \omega < 0 \end{cases}$$

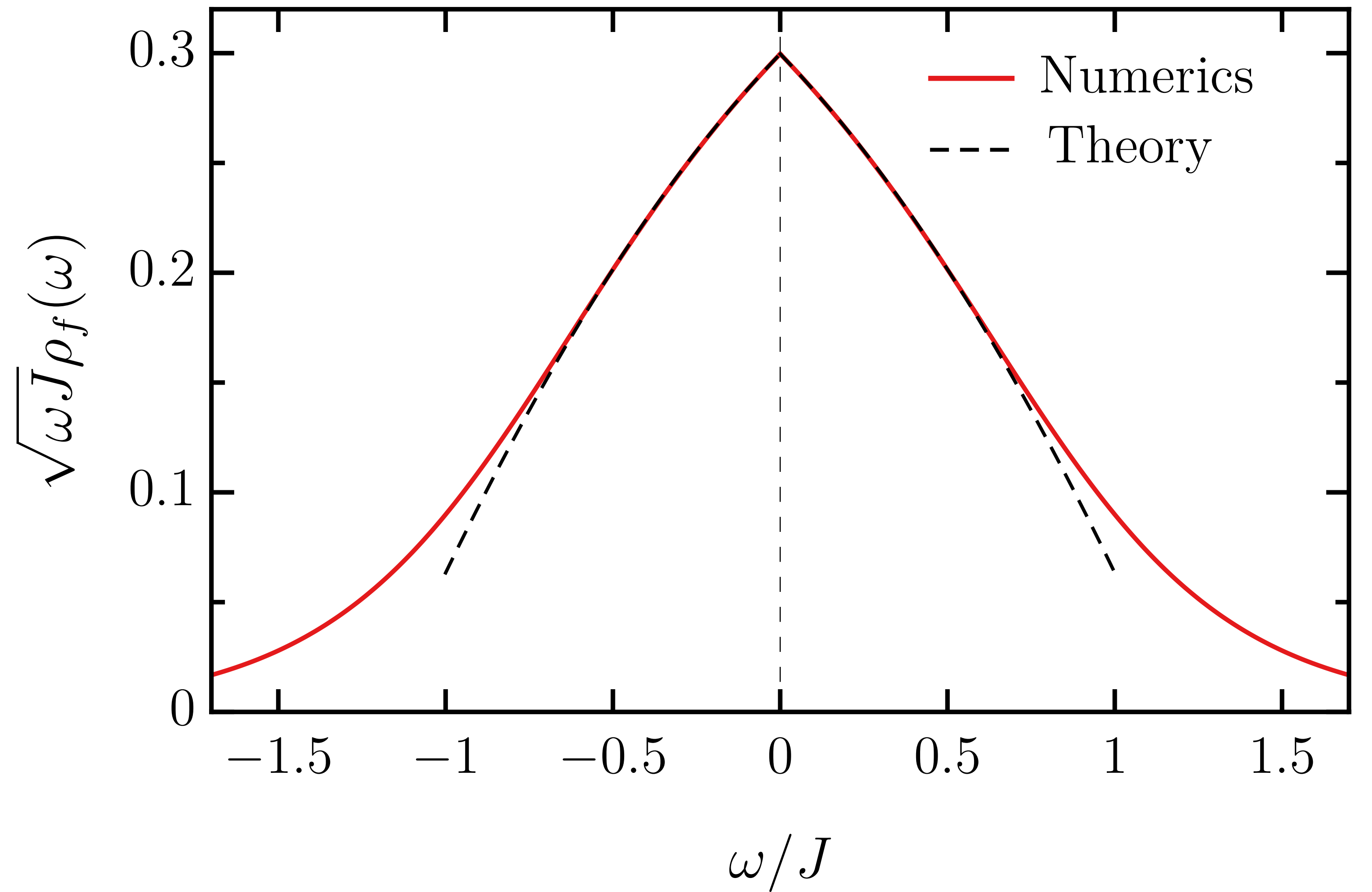
with  $\theta_f$  determined exactly from  $\kappa$  via a Luttinger relation ( $\theta_f = 0$  at  $\kappa = 1/2$ ).



Comparison of  $T = 0$   
spectral density with  
numerical solution  
of SYK equations

$$g_f(\omega) = \sqrt{|\omega|} \text{Im} G(\omega)$$

Fermionic spectral density for  $\theta_f = 0$

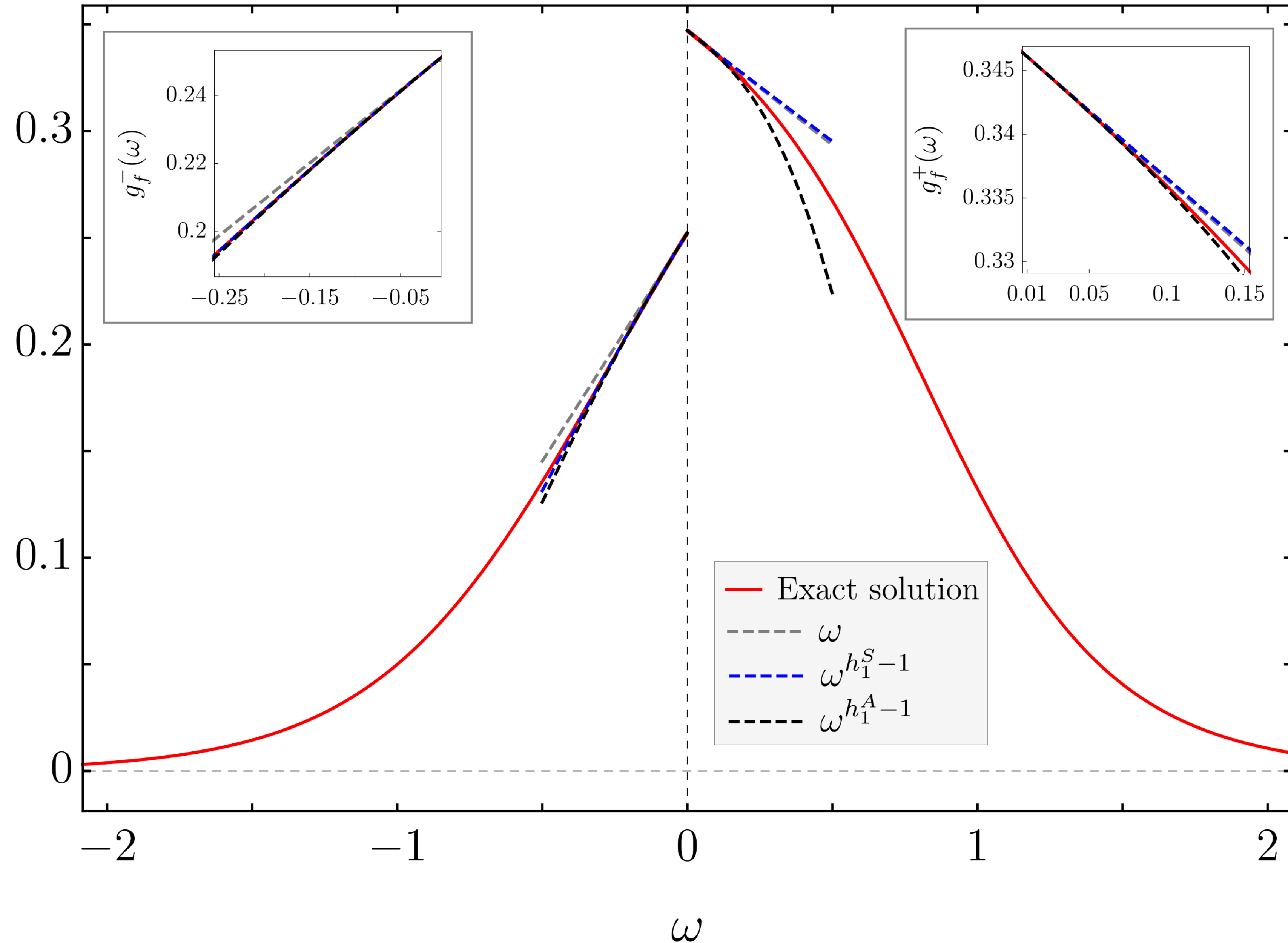


$$g(\omega) = \frac{1}{(4\pi^3)^{\frac{1}{4}} J} \left( 1 - 2\alpha_0^A \frac{\omega}{J} - 3(\alpha_0^A)^2 \left(\frac{\omega}{J}\right)^2 - 0.68\alpha_1^A \left(\frac{\omega}{J}\right)^{2.77} + \frac{26}{3}(\alpha_0^A)^3 \left(\frac{\omega}{J}\right)^3 - \dots \right)$$

Comparison of  $T = 0$  spectral density with numerical solution of SYK equations

$$g_f(\omega) = \sqrt{|\omega|} \text{Im} G(\omega)$$

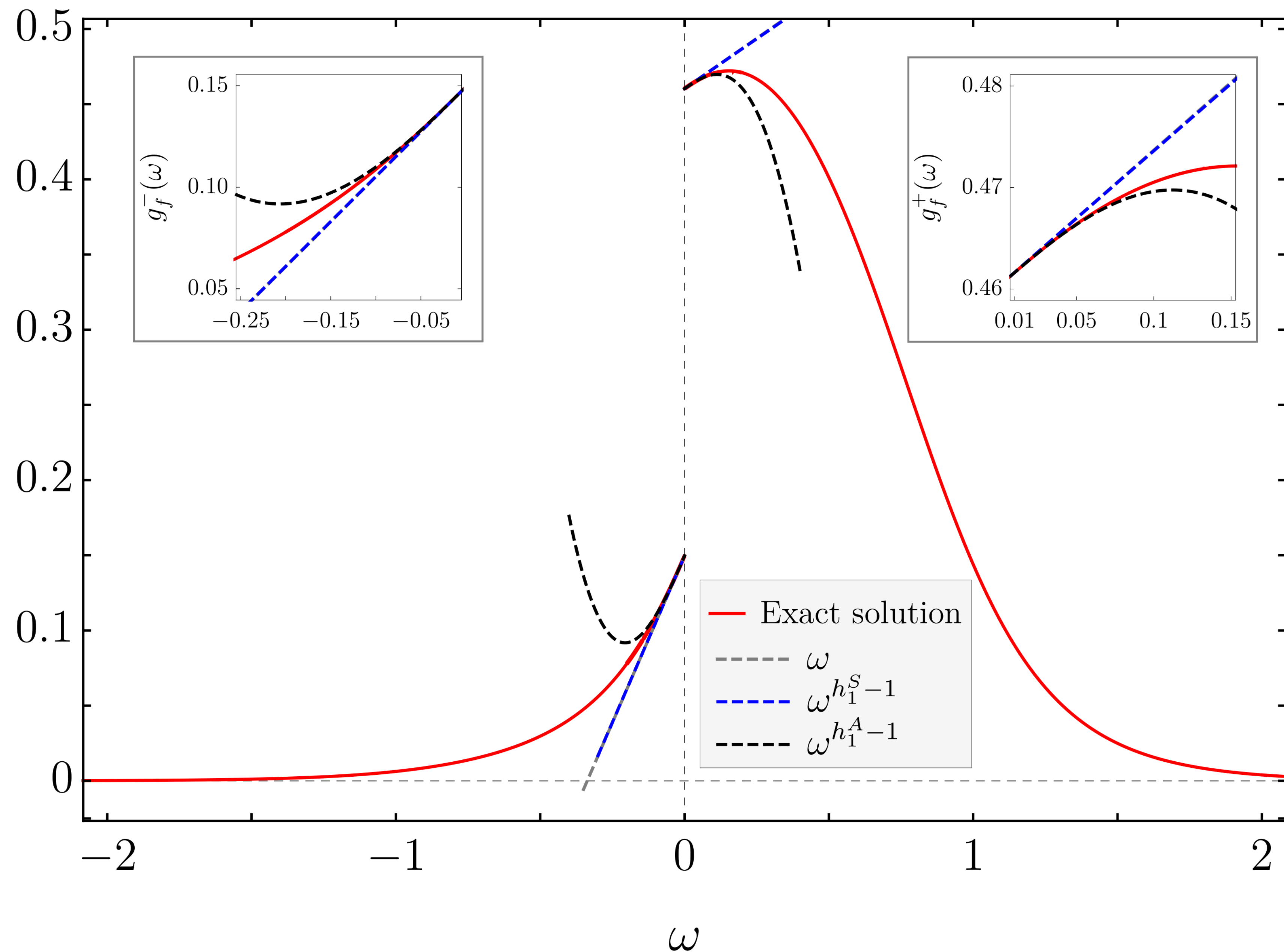
$g_f(\omega) = \sqrt{\omega} \rho_f$  as a function of  $\omega$  at  $\theta_f = 0.05\pi$



Comparison of  $T = 0$  spectral density with numerical solution of SYK equations

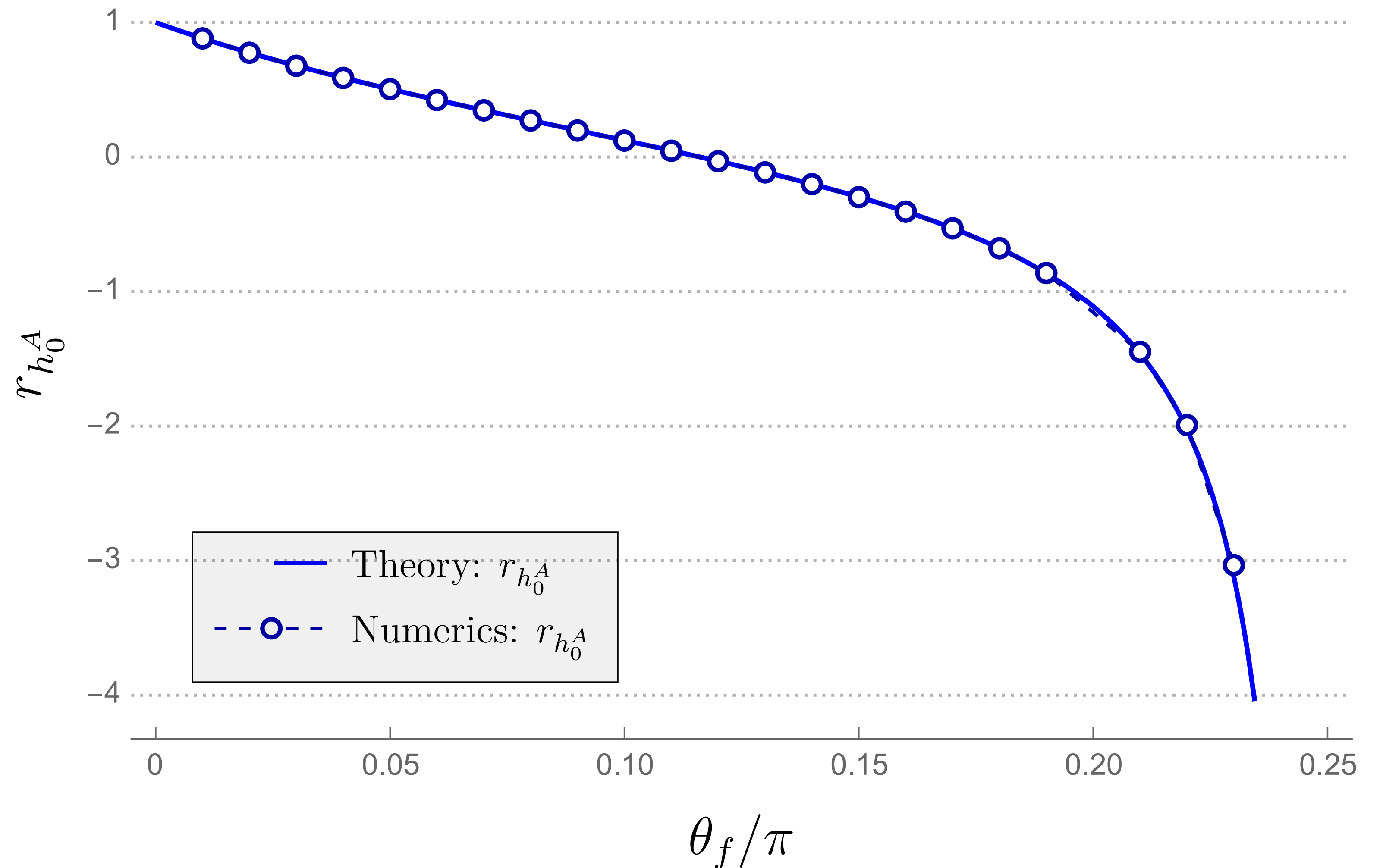
$$g_f(\omega) = \sqrt{|\omega|} \text{Im} G(\omega)$$

$g_f(\omega) = \sqrt{\omega} \rho_f$  as a function of  $\omega$  at  $\theta_f = 0.15\pi$



Comparison of  $T = 0$  spectral density with numerical solution of SYK equations

$$\text{Im } G(\omega) = \frac{g_f(\omega)}{\sqrt{|\omega|}}$$



Ratios of  $h = 2$  corrections at  $\omega > 0$  and  $\omega < 0$  compared with conformal perturbation theory

# Corrections to $SL(2,R)$ conformal invariance

The  $h = 2$  correction to the local spin susceptibility is

$$\text{Im}\chi_L(\omega) \sim \tanh\left(\frac{\hbar\omega}{2T}\right) \left[ 1 - \mathcal{C}\gamma \hbar\omega \tanh\left(\frac{\hbar\omega}{2T}\right) + \dots \right]$$

where the specific heat per spin component  $= \gamma T$ , and

$$\mathcal{C} = \frac{24}{\pi(2 + 3\pi)}$$

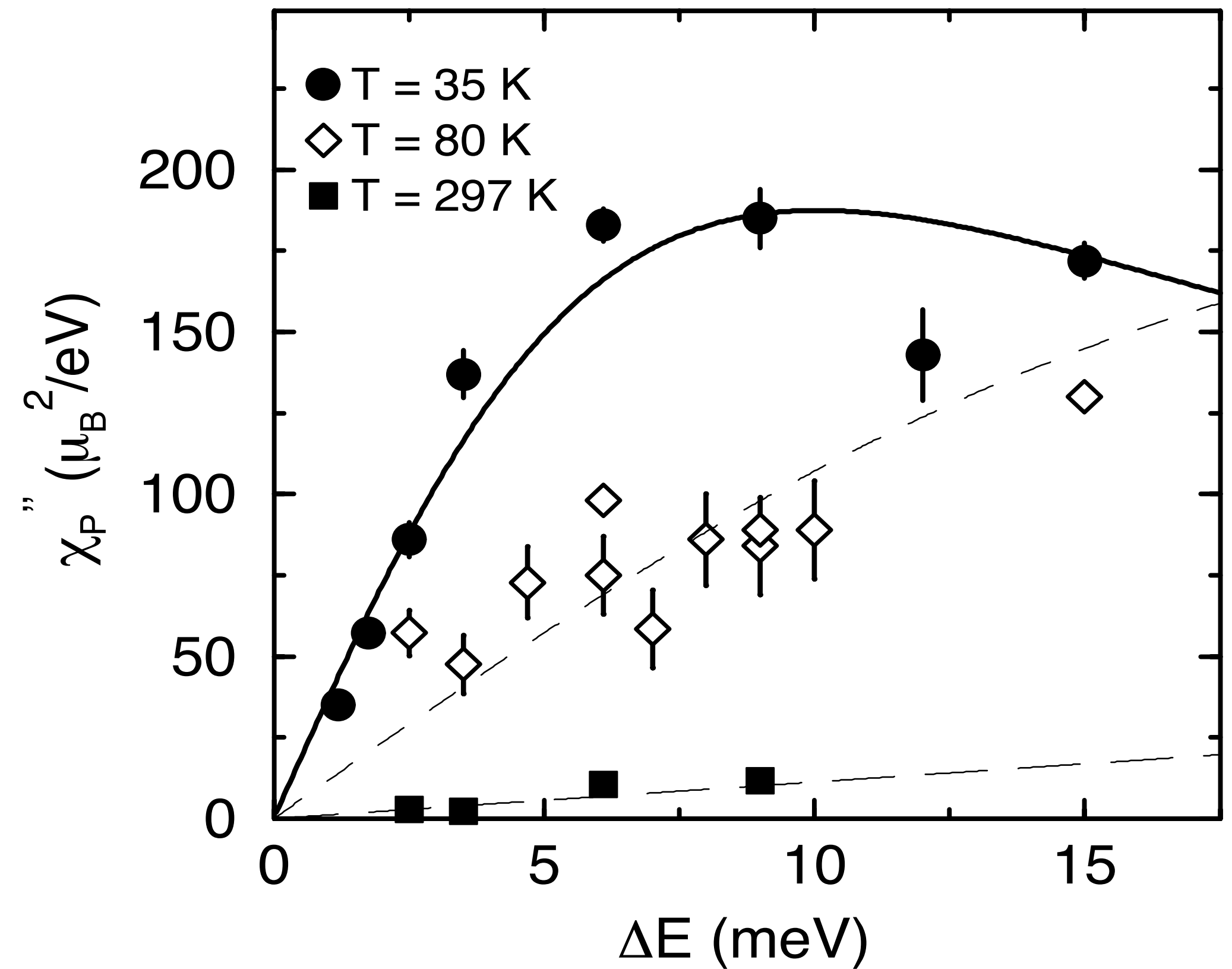
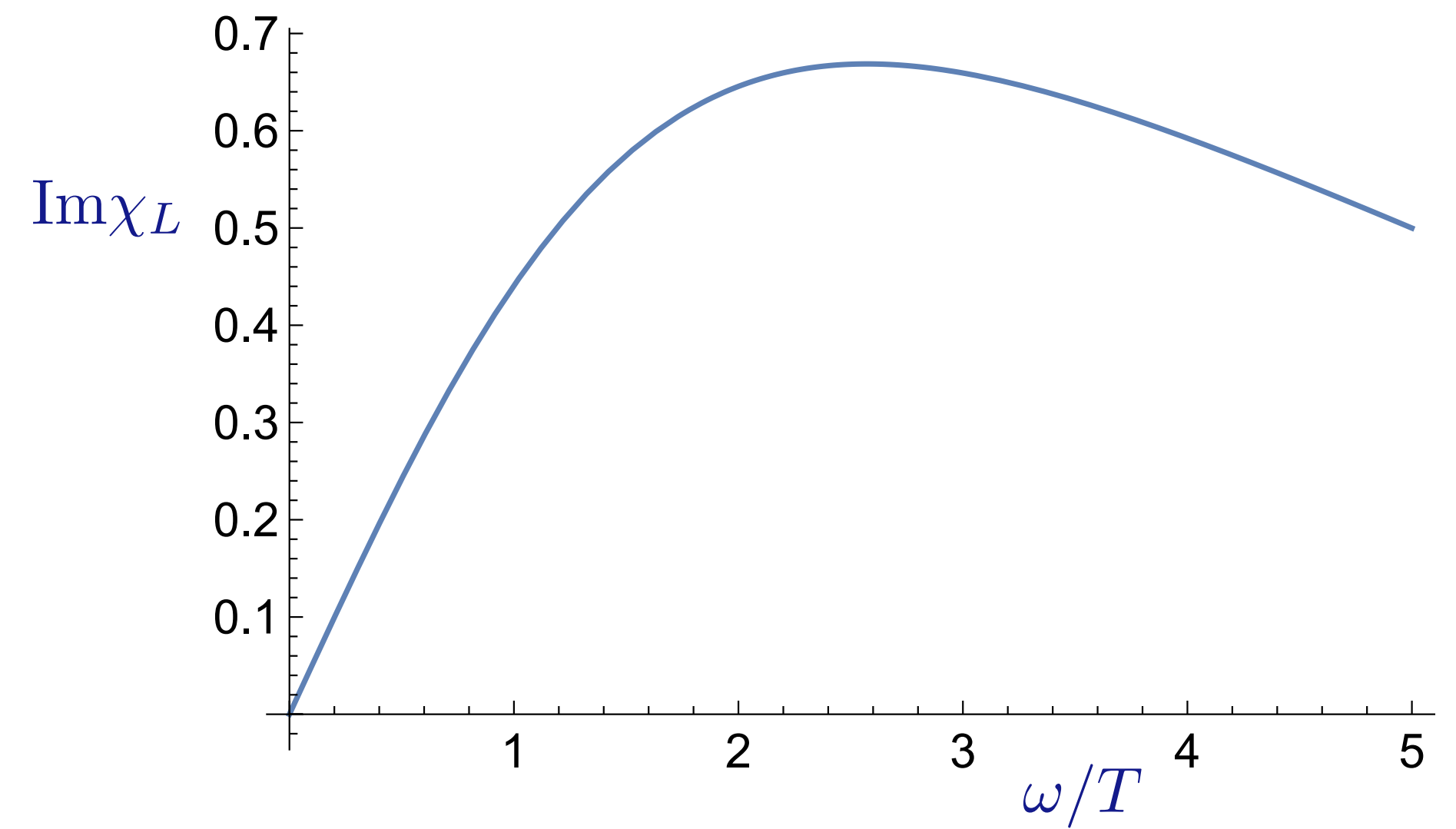
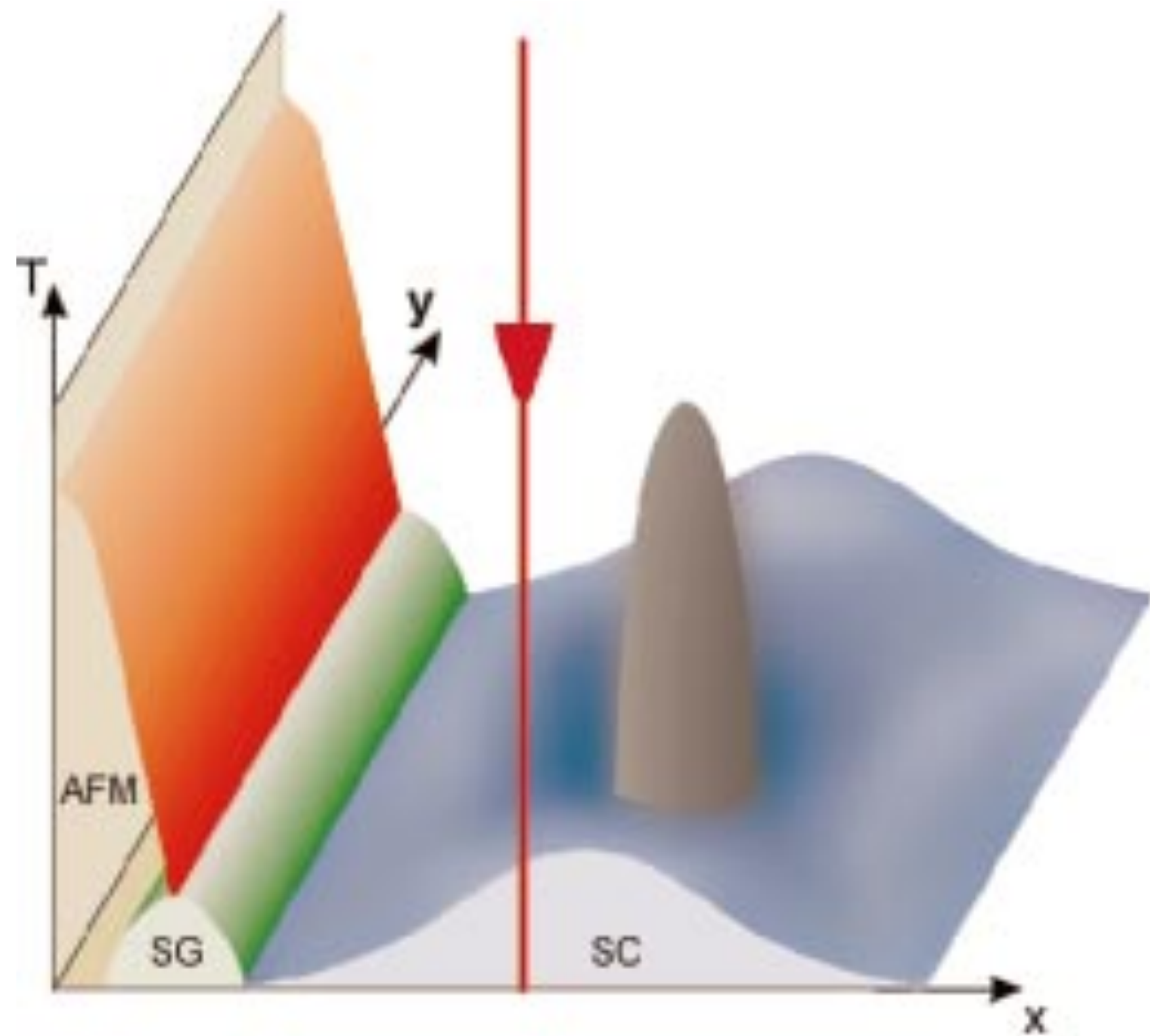
At  $T = 0$ ,

$$\text{Im}\chi_L(\omega) \sim \text{sgn}(\omega) \left[ 1 - \mathcal{C}\gamma|\omega| - \frac{7}{16}(\mathcal{C}\gamma)^2|\omega|^2 - \mathcal{C}'|\omega|^{2.77354\dots} + \frac{37}{48}(\mathcal{C}\gamma)^3|\omega|^3 - \dots \right]$$

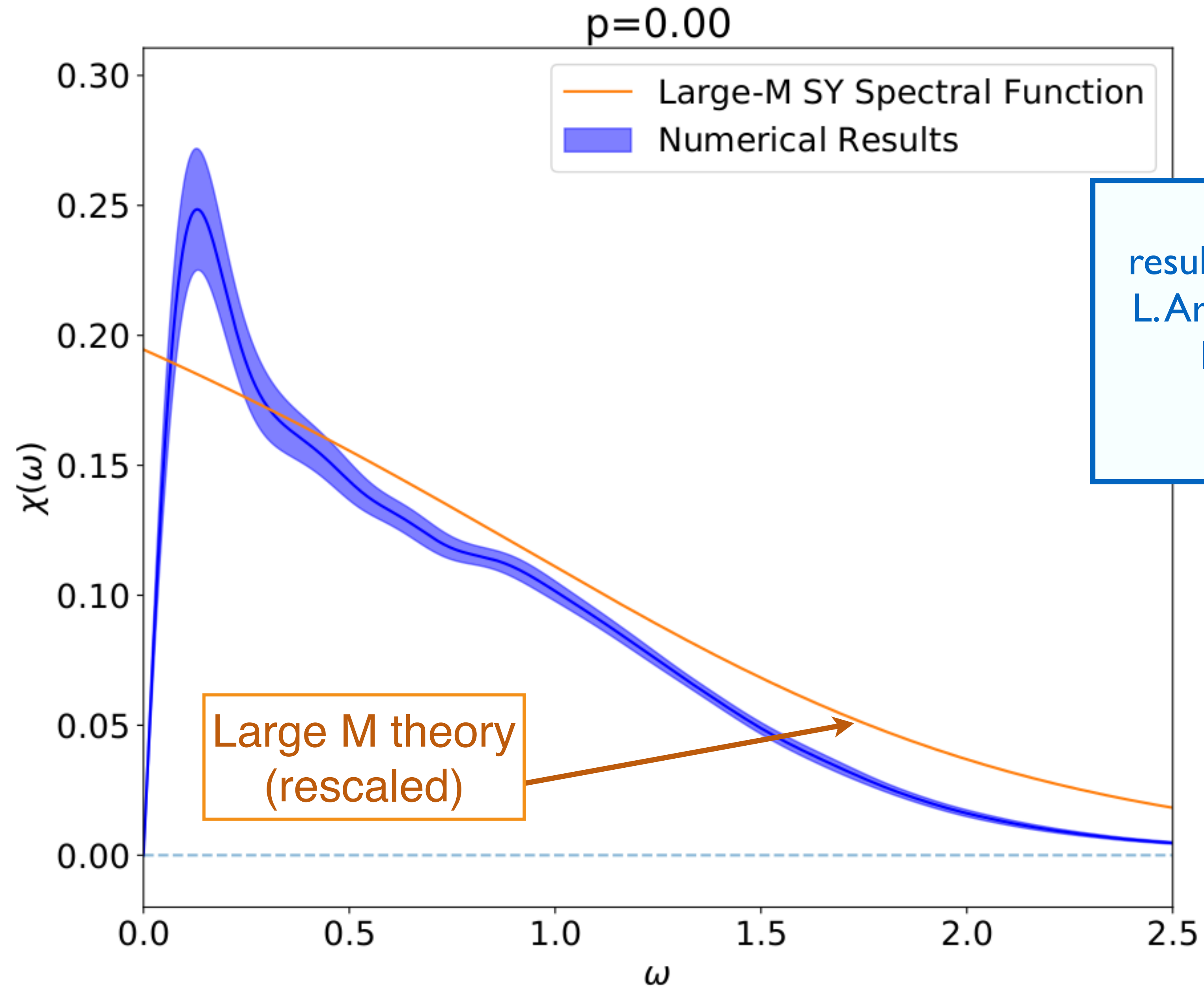
# Nearly Singular Magnetic Fluctuations in the Normal State of a High- $T_c$ Cuprate Superconductor

G. Aeppli, T. E. Mason,\* S. M. Hayden, H. A. Mook, J. Kulda

Science **278**, 1432 (1997)



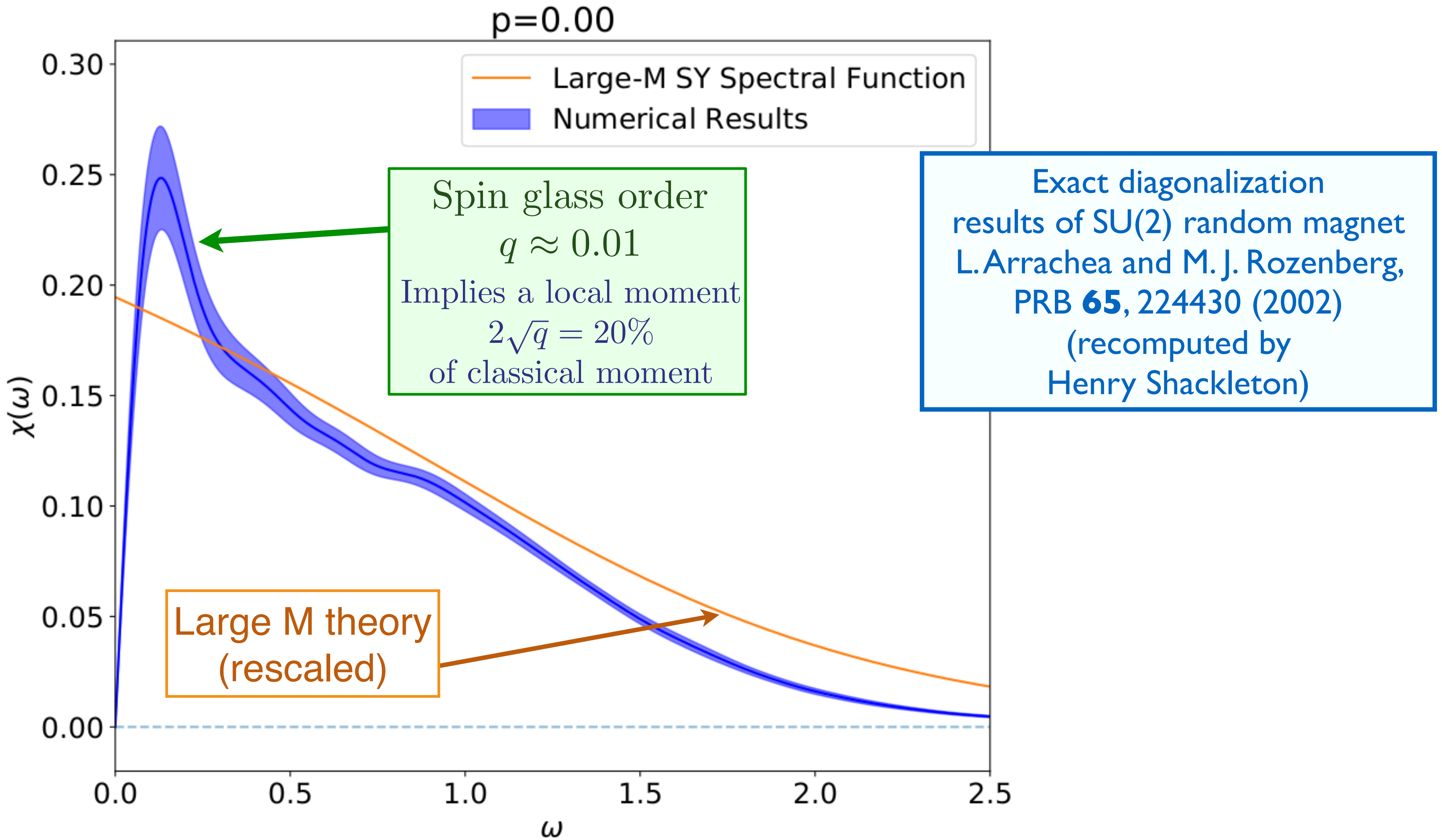
# Comparison with exact diagonalization on SU(2) random-J model



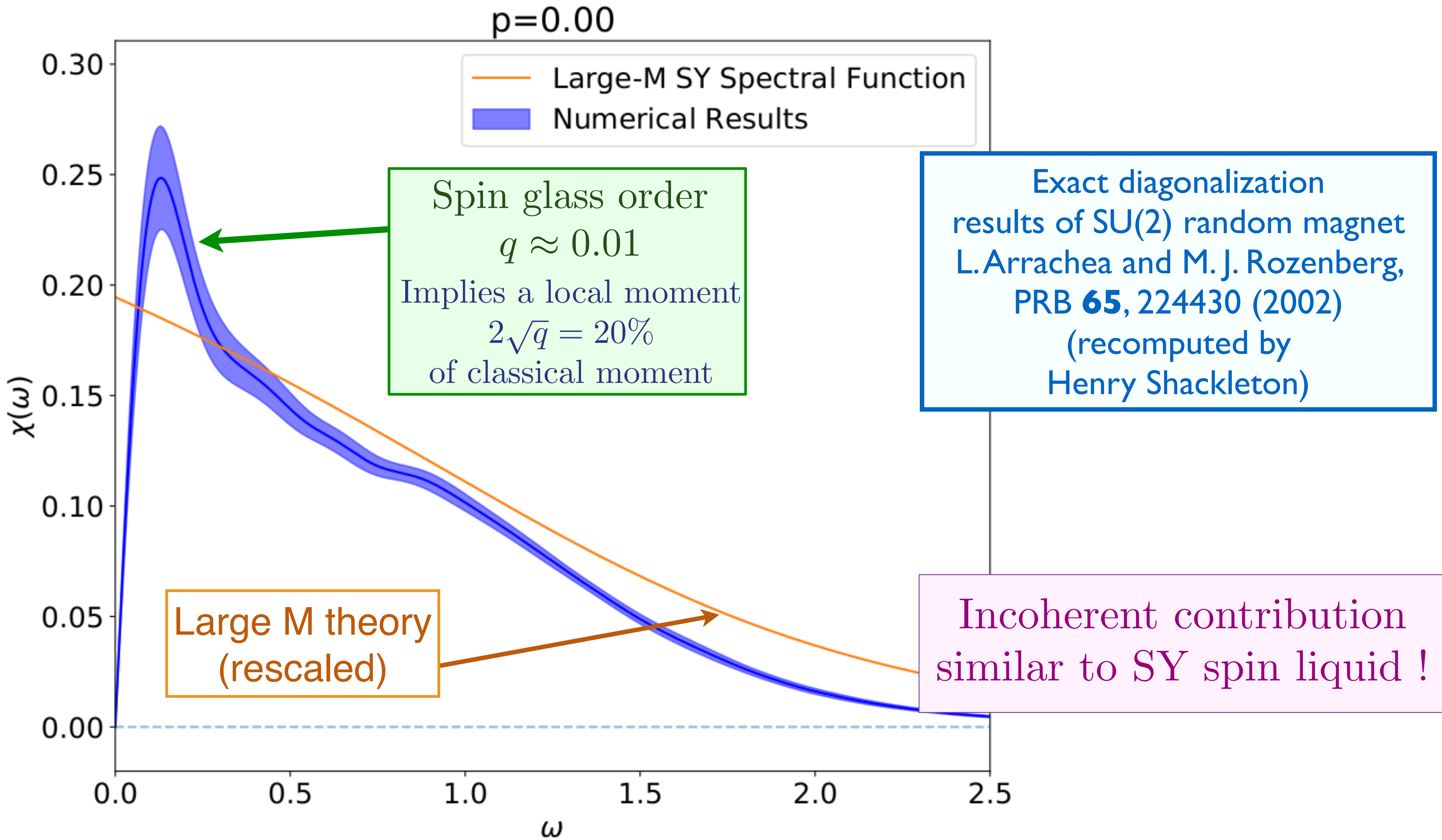
Exact diagonalization  
results of SU(2) random magnet  
L. Arrachea and M. J. Rozenberg,  
PRB **65**, 224430 (2002)  
(recomputed by  
Henry Shackleton)

Large M theory  
(rescaled)

# Comparison with exact diagonalization on SU(2) random-J model



# Comparison with exact diagonalization on SU(2) random-J model



1. Random  $J$  model (insulator)

*Operator spectrum and numerics*

2. Random  $t$ - $J$  model (metals)

*Deconfined criticality and numerics*

3. Random  $t$ - $J$ - $U$  model

# Random $t$ - $J$ model

$$H = -\frac{1}{\sqrt{N}} \sum_{i,j=1}^N t_{ij} c_{i\alpha}^\dagger c_{j\alpha} + \frac{1}{\sqrt{N}} \sum_{i<j=1}^N J_{ij} \vec{S}_i \cdot \vec{S}_j$$

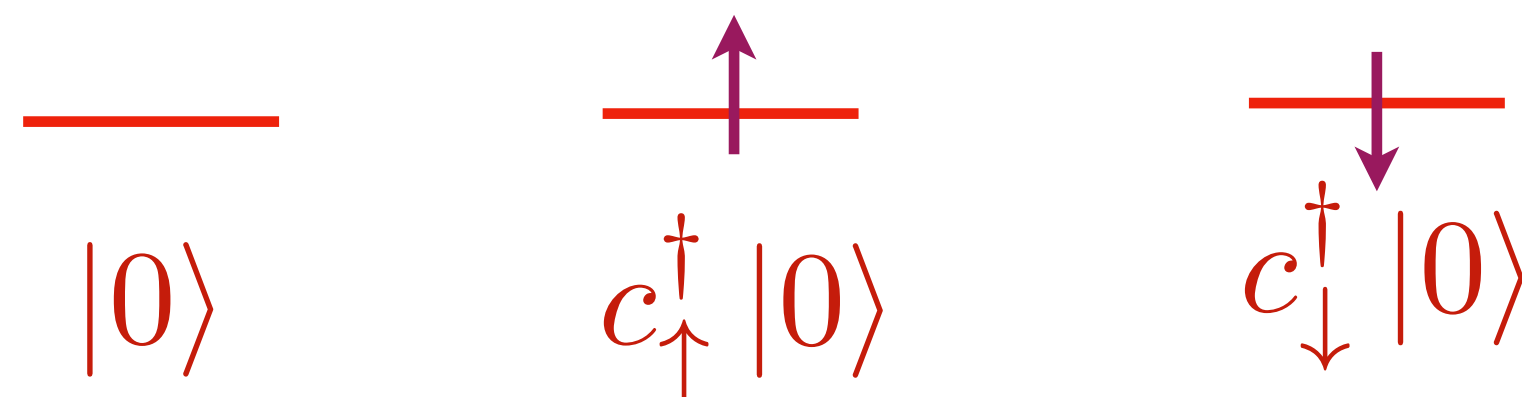
We consider the hole-doped case, with no double occupancy.

$$\alpha = \uparrow, \downarrow, \quad \{c_{i\alpha}, c_{j\beta}^\dagger\} = \delta_{ij} \delta_{\alpha\beta}, \quad \{c_{i\alpha}, c_{j\beta}\} = 0$$

$$\vec{S}_i = \frac{1}{2} c_{i\alpha}^\dagger \vec{\sigma}_{\alpha\beta} c_{i\beta}, \quad \sum_{\alpha} c_{i\alpha}^\dagger c_{i\alpha} \leq 1, \quad \frac{1}{N} \sum_{i\alpha} c_{i\alpha}^\dagger c_{i\alpha} = 1 - p$$

$$J_{ij} \text{ random, } \overline{J_{ij}} = 0, \quad \overline{J_{ij}^2} = J^2$$

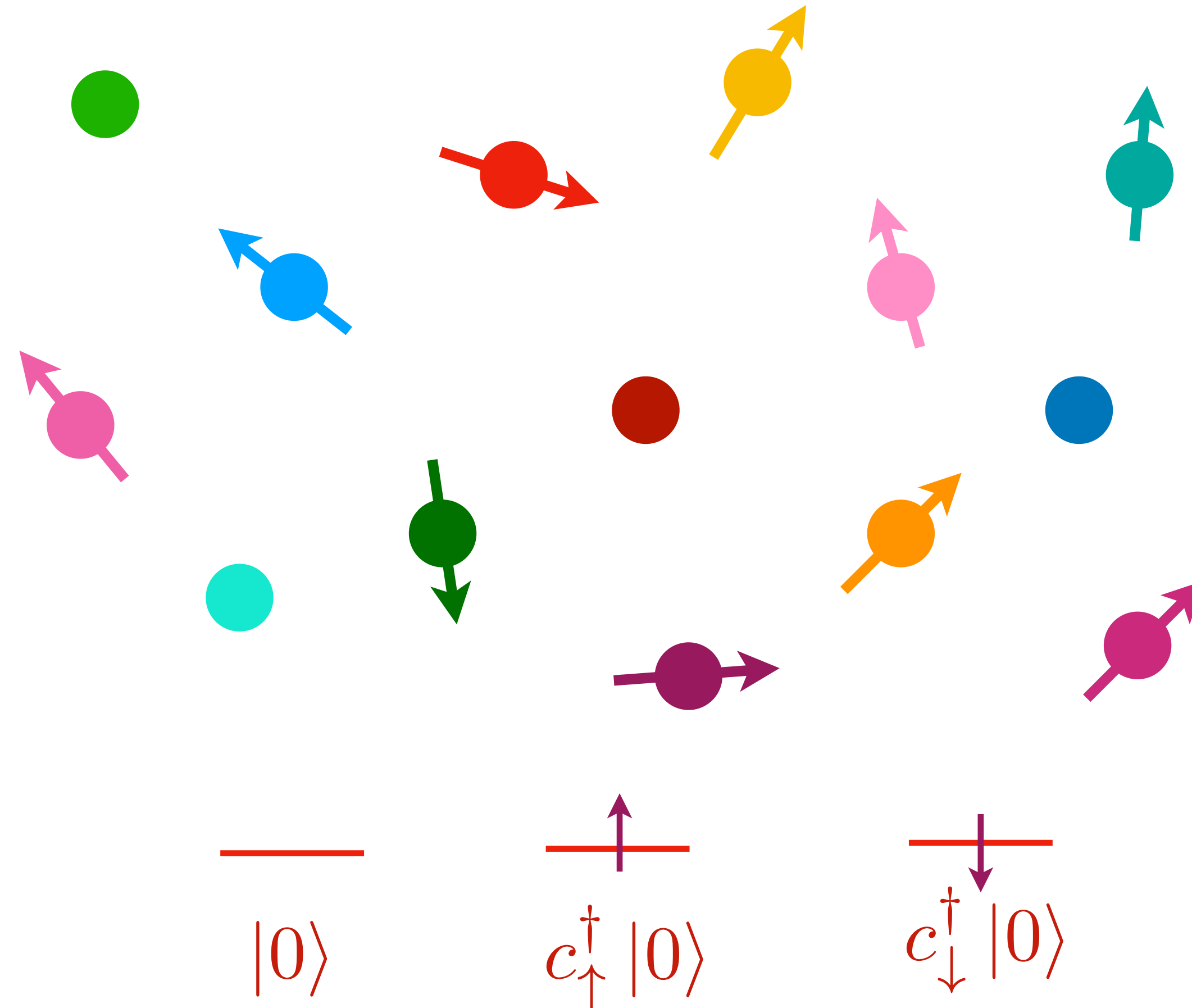
$$t_{ij} \text{ random, } \overline{t_{ij}} = 0, \quad \overline{t_{ij}^2} = t^2$$



# Random $t$ - $J$ model

$$H = -\frac{1}{\sqrt{N}} \sum_{i,j=1}^N t_{ij} c_{i\alpha}^\dagger c_{j\alpha} + \frac{1}{\sqrt{N}} \sum_{i<j=1}^N J_{ij} \vec{S}_i \cdot \vec{S}_j$$

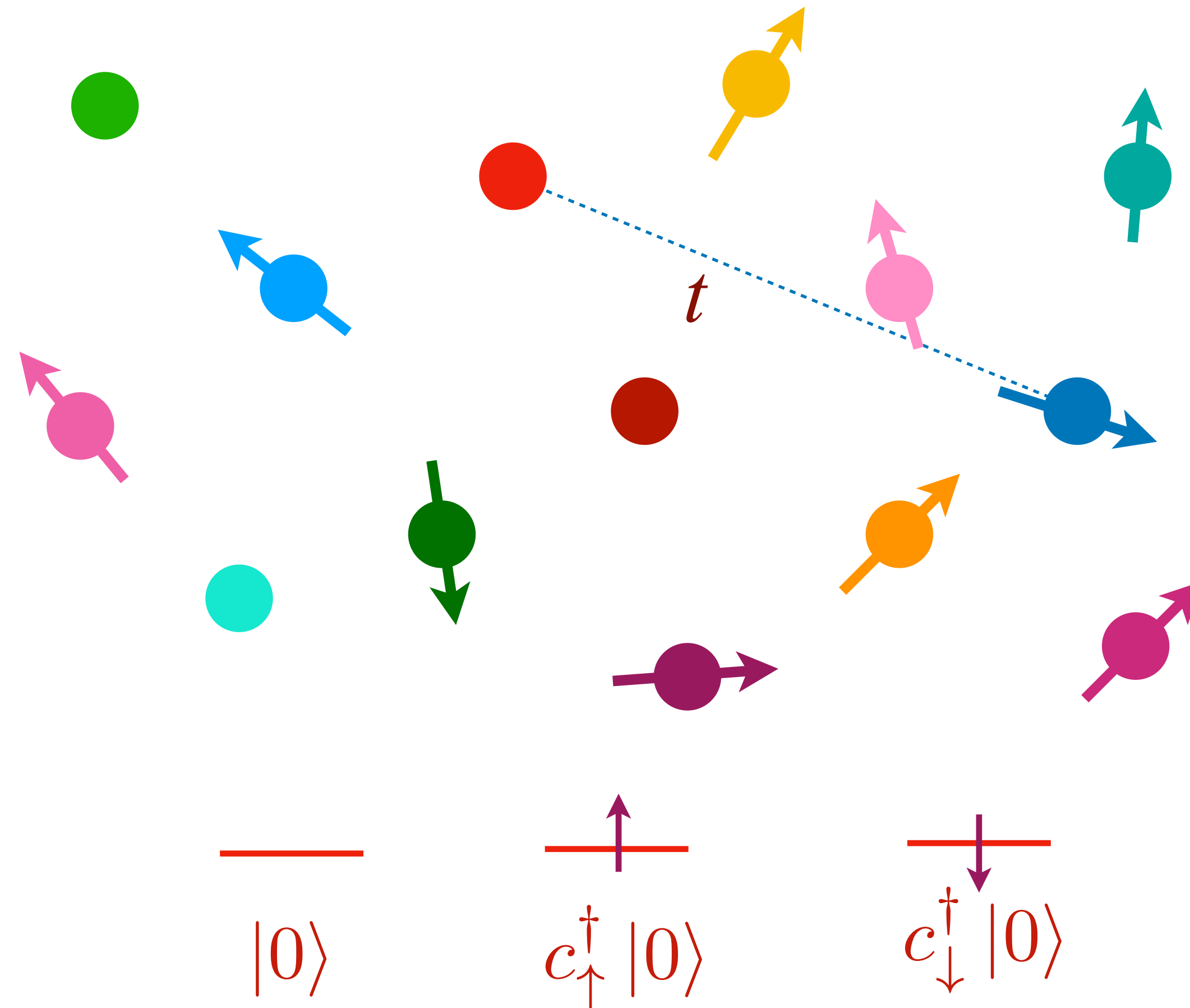
We consider the hole-doped case, with no double occupancy.



# Random $t$ - $J$ model

$$H = -\frac{1}{\sqrt{N}} \sum_{i,j=1}^N t_{ij} c_{i\alpha}^\dagger c_{j\alpha} + \frac{1}{\sqrt{N}} \sum_{i<j=1}^N J_{ij} \vec{S}_i \cdot \vec{S}_j$$

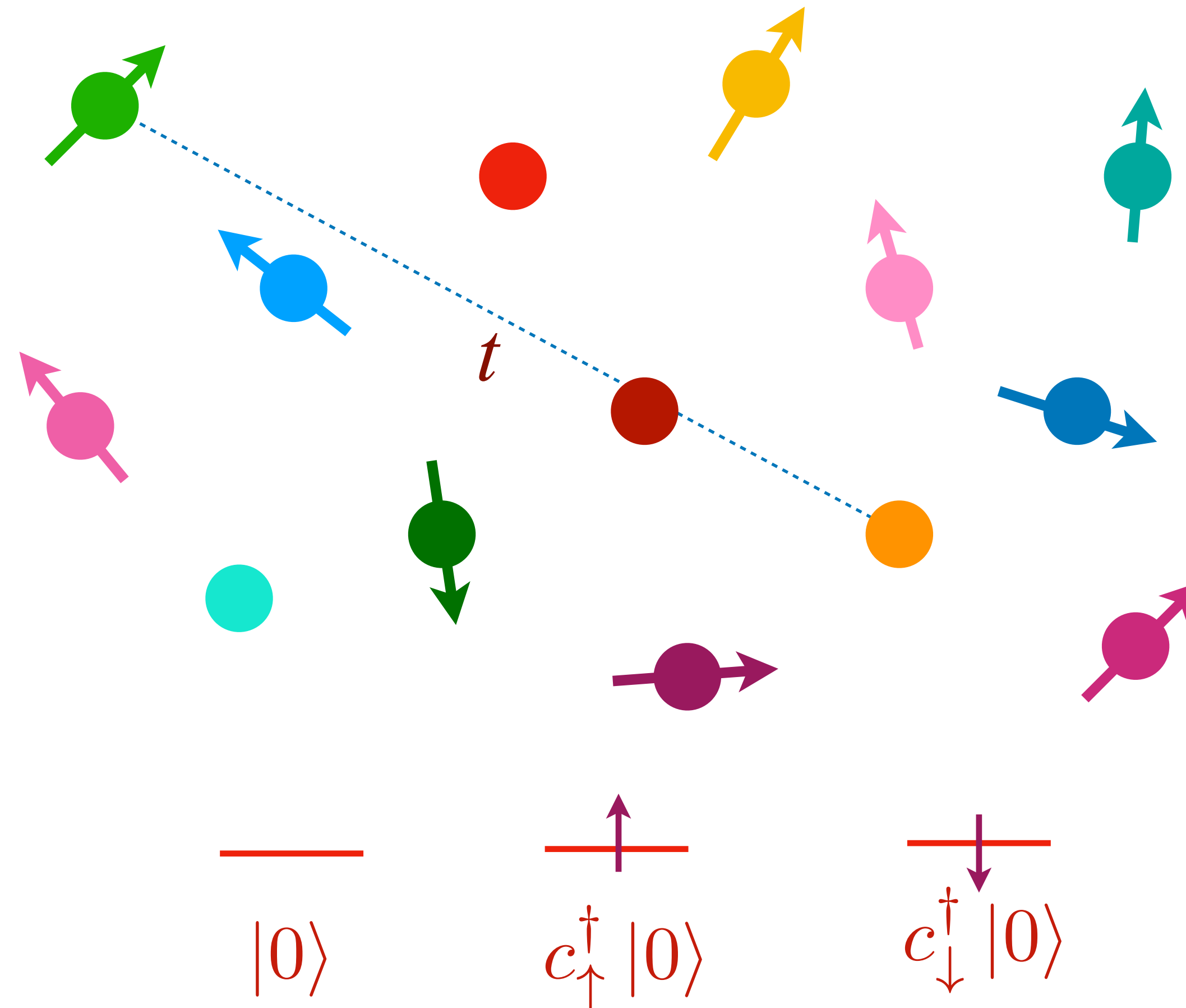
We consider the hole-doped case, with no double occupancy.



# Random $t$ - $J$ model

$$H = -\frac{1}{\sqrt{N}} \sum_{i,j=1}^N t_{ij} c_{i\alpha}^\dagger c_{j\alpha} + \frac{1}{\sqrt{N}} \sum_{i<j=1}^N J_{ij} \vec{S}_i \cdot \vec{S}_j$$

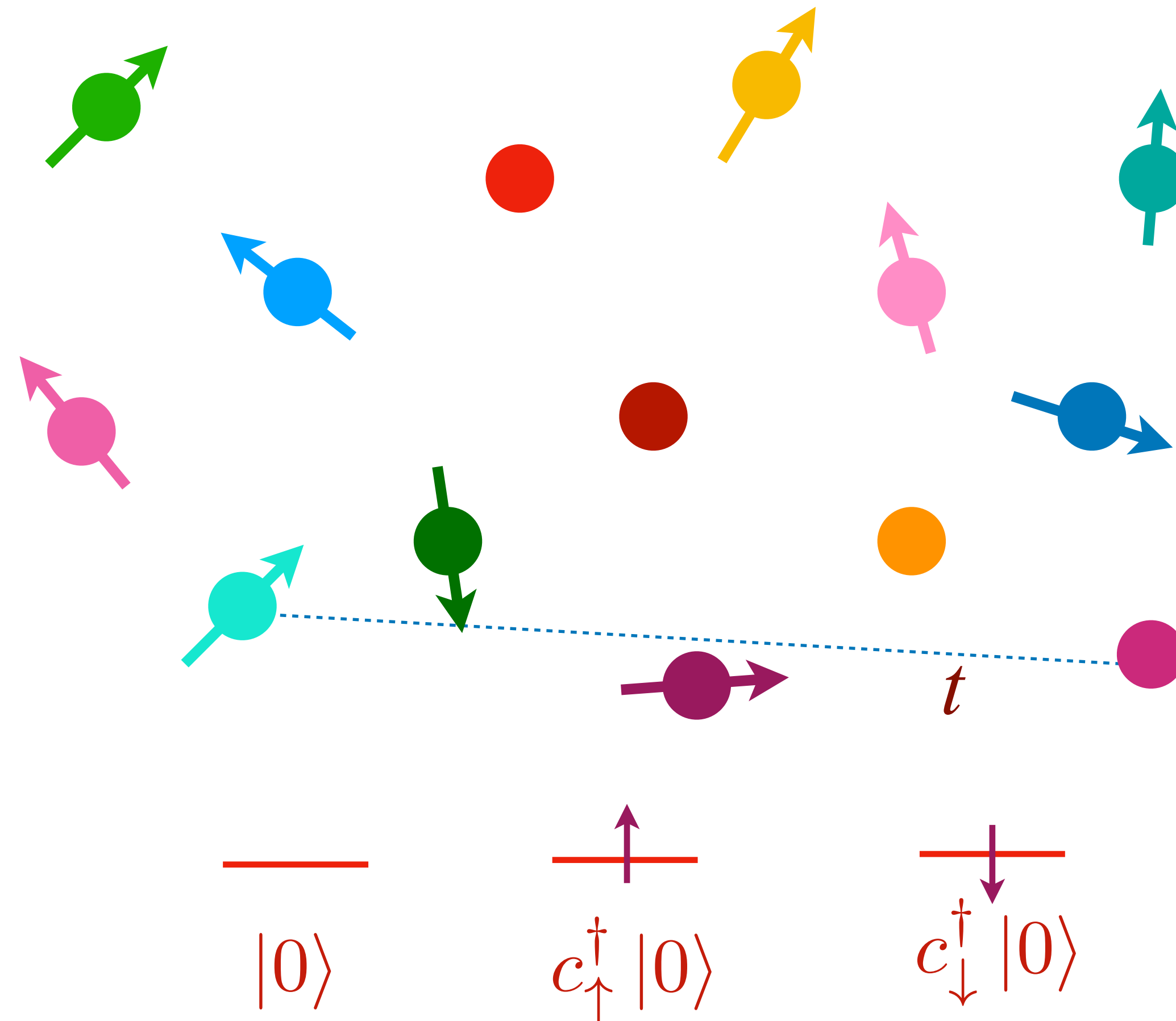
We consider the hole-doped case, with no double occupancy.



# Random $t$ - $J$ model

$$H = -\frac{1}{\sqrt{N}} \sum_{i,j=1}^N t_{ij} c_{i\alpha}^\dagger c_{j\alpha} + \frac{1}{\sqrt{N}} \sum_{i<j=1}^N J_{ij} \vec{S}_i \cdot \vec{S}_j$$

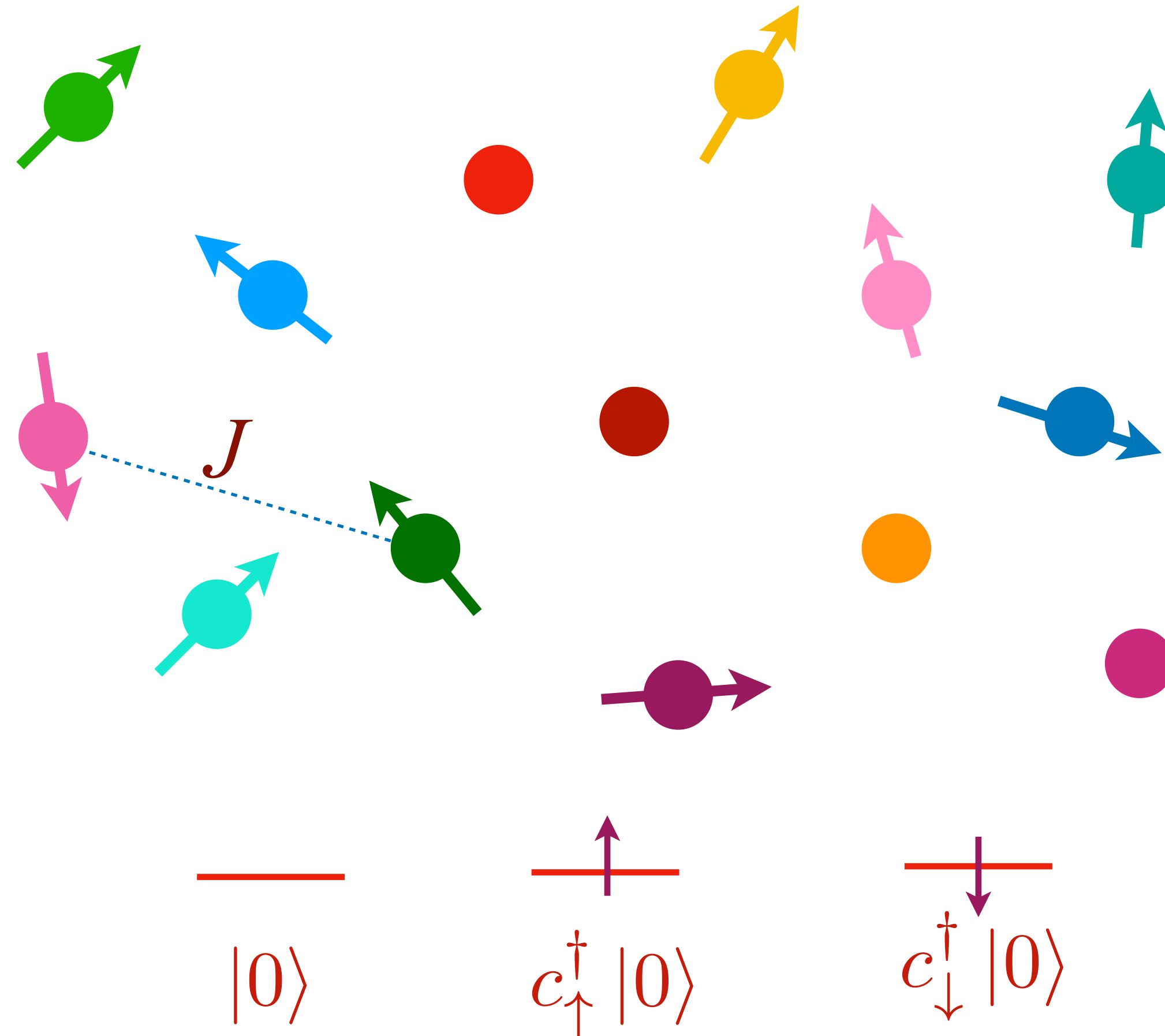
We consider the hole-doped case, with no double occupancy.



# Random $t$ - $J$ model

$$H = -\frac{1}{\sqrt{N}} \sum_{i,j=1}^N t_{ij} c_{i\alpha}^\dagger c_{j\alpha} + \frac{1}{\sqrt{N}} \sum_{i<j=1}^N J_{ij} \vec{S}_i \cdot \vec{S}_j$$

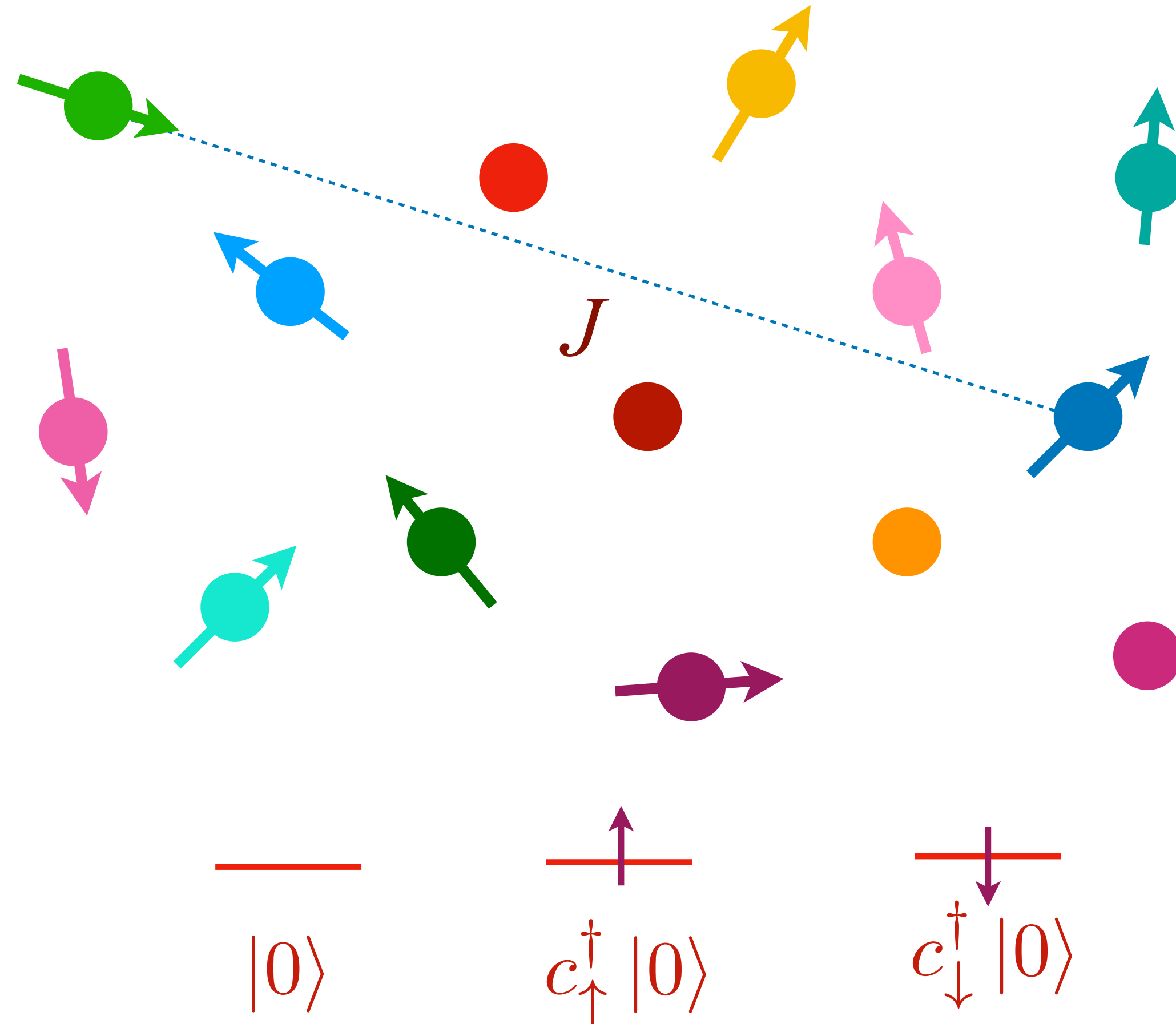
We consider the hole-doped case, with no double occupancy.



# Random $t$ - $J$ model

$$H = -\frac{1}{\sqrt{N}} \sum_{i,j=1}^N t_{ij} c_{i\alpha}^\dagger c_{j\alpha} + \frac{1}{\sqrt{N}} \sum_{i<j=1}^N J_{ij} \vec{S}_i \cdot \vec{S}_j$$

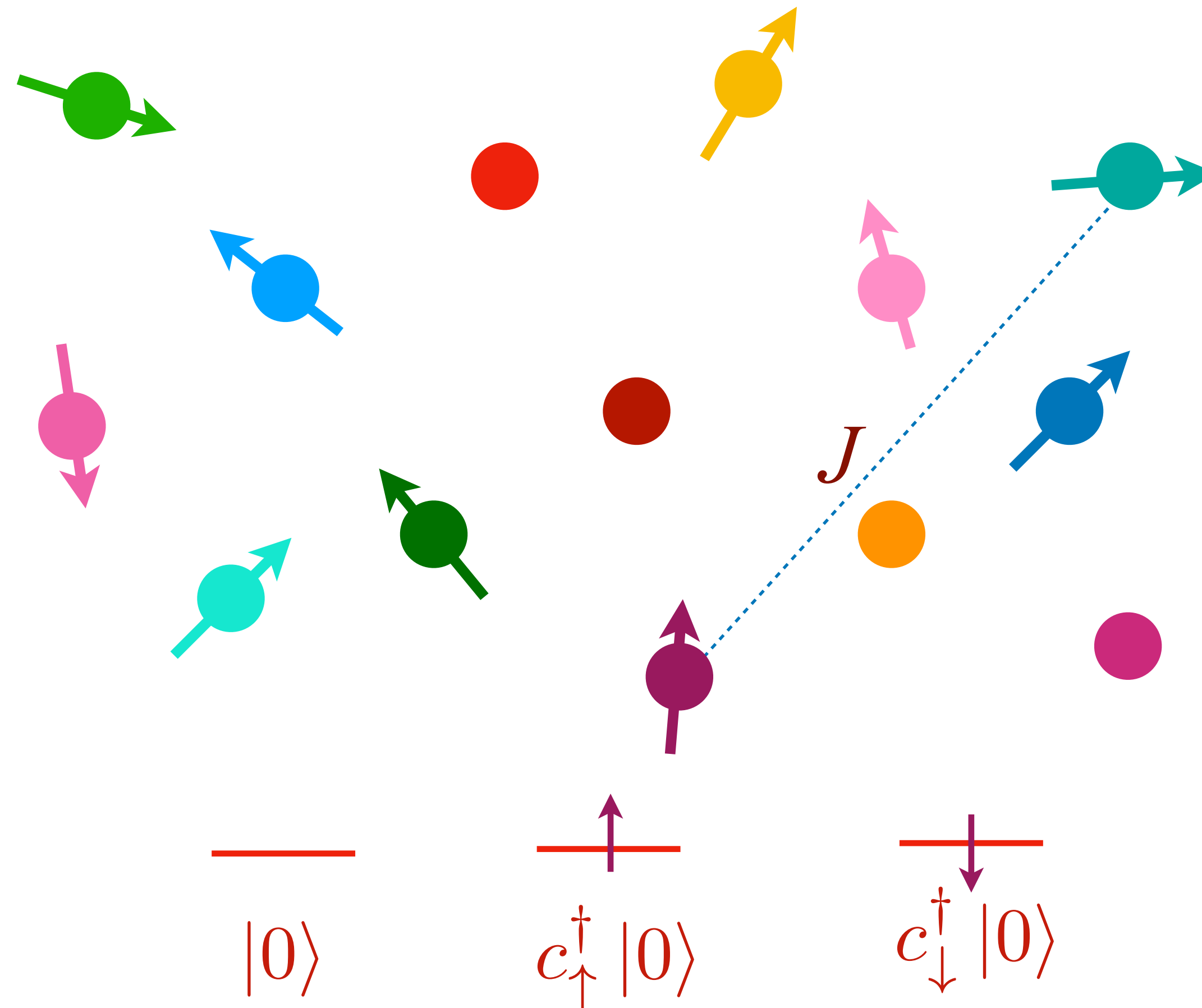
We consider the hole-doped case, with no double occupancy.



# Random $t$ - $J$ model

$$H = -\frac{1}{\sqrt{N}} \sum_{i,j=1}^N t_{ij} c_{i\alpha}^\dagger c_{j\alpha} + \frac{1}{\sqrt{N}} \sum_{i<j=1}^N J_{ij} \vec{S}_i \cdot \vec{S}_j$$

We consider the hole-doped case, with no double occupancy.



# Fractionalization in the $t$ - $J$ model

Large  $M$  limit of  $SU(M'|M)$  theory

Each site has 3 states which we map to the space of a boson  $b$  (the holon) and a fermion  $f_\alpha$  (the spinon):

$$\begin{aligned} |0\rangle &\Rightarrow b^\dagger |v\rangle & , & & c_\alpha^\dagger |0\rangle &\Rightarrow f_\alpha^\dagger |v\rangle \\ c_\alpha &= f_\alpha b^\dagger & , & & f_\alpha^\dagger f_\alpha + b^\dagger b &= 1 \end{aligned}$$

To obtain a large  $M$  limit, let  $\alpha = 1 \dots M$ , endow the boson with an ‘orbital’ index  $a = 1 \dots M'$  and send  $M \rightarrow \infty$  at fixed  $k = M'/M$ . Then

$$c_{a\alpha} = f_\alpha b_a^\dagger \quad , \quad f_\alpha^\dagger f_\alpha + b_a^\dagger b_a = \kappa M$$

# Fractionalization in the $t$ - $J$ model

Large  $M$  limit of  $SU(M'|M)$  theory

Assuming the bosons are not condensed, we obtain SYK-like equations for the boson and fermion Green's functions:

$$\begin{aligned} G_b(i\omega_n) &= \frac{1}{i\omega_n + \mu_b - \Sigma_b(i\omega_n)} \\ \Sigma_b(\tau) &= -t^2 G_f(\tau) G_f(-\tau) G_b(\tau) \\ G_f(i\omega_n) &= \frac{1}{i\omega_n + \mu_f - \Sigma_f(i\omega_n)} \\ \Sigma_f(\tau) &= -J^2 G_f^2(\tau) G_f(-\tau) + k t^2 G_f(\tau) G_b(\tau) G_b(-\tau) \end{aligned}$$

Here  $\mu_f$  and  $\mu_b$  are chemical potentials chosen to satisfy

$$\langle f^\dagger f \rangle = \kappa - kp \quad , \quad \langle b^\dagger b \rangle = p .$$

# Fractionalization in the $t$ - $J$ model

Large  $M$  limit of  $SU(M'|M)$  theory

These equations have critical solutions with

$$G_f(z) = C_f \frac{e^{-i(\pi\Delta_f + \theta_f)}}{z^{1-2\Delta_f}}, \quad G_b(z) = C_b \frac{e^{-i(\pi\Delta_b + \theta_b)}}{z^{1-2\Delta_b}}, \quad \text{Im}(z) > 0$$

$$\Delta_f + \Delta_b = \frac{1}{2}$$

$$\frac{\theta_f}{\pi} + \left( \frac{1}{2} - \Delta_f \right) \frac{\sin(2\theta_f)}{\sin(2\pi\Delta_f)} = kp$$

$$\frac{\theta_b}{\pi} + \left( \frac{1}{2} - \Delta_b \right) \frac{\sin(2\theta_b)}{\sin(2\pi\Delta_b)} = \kappa + p.$$

The last two are analogs of ‘Luttinger’ relations

## Fractionalization in the $t$ - $J$ model

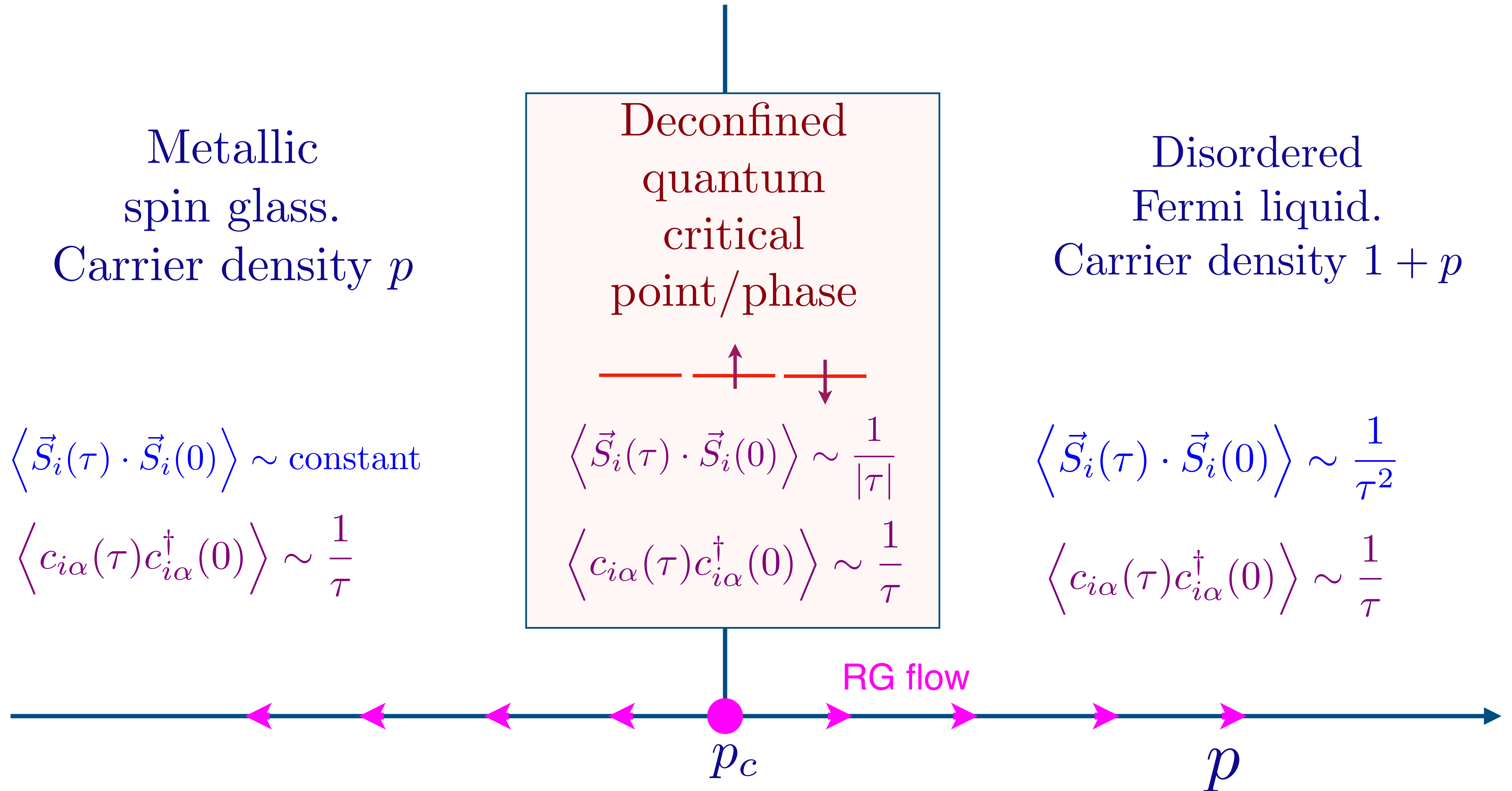
Large  $M$  limit of  $SU(M'|M)$  theory

The critical solution which is self-consistent in both the  $t$  and  $J$  terms has  $\Delta_b = \Delta_f = 1/4$ , implying

$$\langle c_\alpha(\tau)c_\alpha^\dagger(0) \rangle \sim \begin{cases} \frac{A_+}{|\tau|} & , \quad \tau > 0 \\ -\frac{A_-}{|\tau|} & , \quad \tau < 0 \end{cases} , \quad \langle \vec{S}(\tau) \cdot \vec{S}(0) \rangle \sim \frac{1}{|\tau|} .$$

RG computations show that these results for the exponents of gauge-invariant operators are expected to be exact beyond the large  $M$  limit.

# Proposed phase diagram of random $t$ - $J$ model



At the critical point/phase of the  $t$ - $J$  model, the Fermi liquid-like behavior of the electron Green's function

$$\left\langle c_{i\alpha}(\tau) c_{i\alpha}^\dagger(0) \right\rangle \sim \frac{1}{\tau}$$

leads to a non-zero *residual resistivity*,  $\rho(0) \neq 0$ .

However, the critical state is *not* a Fermi liquid, as indicated by the slow decay of the spin correlations

$$\left\langle \vec{S}_i(\tau) \cdot \vec{S}_i(0) \right\rangle \sim \frac{1}{|\tau|}$$

Moreover, in a Fermi liquid, we expect  $\rho(T) - \rho(0) \sim T^2$ , which also does not hold here.

# Time reparameterization soft mode

Corrections to the critical **spinon** Green's function arising from the time reparameterization soft mode take the form

$$\langle f_\alpha(\tau) f_\alpha^\dagger(0) \rangle \sim \left[ \frac{\pi T}{\sin(\pi T \tau)} \right]^{1/2} (1 + \mathcal{C}_f \gamma \Phi_{\text{non-conformal}}(T\tau))$$

where  $\Phi_{\text{non-conformal}}(T\tau)$  is a computable (in the large  $M$  limit) scaling function,  $\gamma T$  is the specific heat per spin component, and  $\mathcal{C}_f$  is a UV-insensitive number

# Time reparameterization soft mode

Corrections to the critical **electron** Green's function arising from the time reparameterization soft mode take the form

$$\langle c_\alpha(\tau) c_\alpha^\dagger(0) \rangle \sim \left[ \frac{\pi T}{\sin(\pi T \tau)} \right] (1 + \mathcal{C}_c \gamma \Phi_{\text{non-conformal}}(T\tau))$$

where  $\Phi_{\text{non-conformal}}(T\tau)$  is a computable (in the large  $M$  limit) scaling function,  $\gamma T$  is the specific heat per spin component, and  $\mathcal{C}_c$  is a UV-insensitive number

# Time reparameterization soft mode

Computing the resistivity from this Green's function via the Kubo formula, we find

$$\rho(T) = \rho(0) (1 + \mathcal{C}_\rho \gamma T + \dots)$$

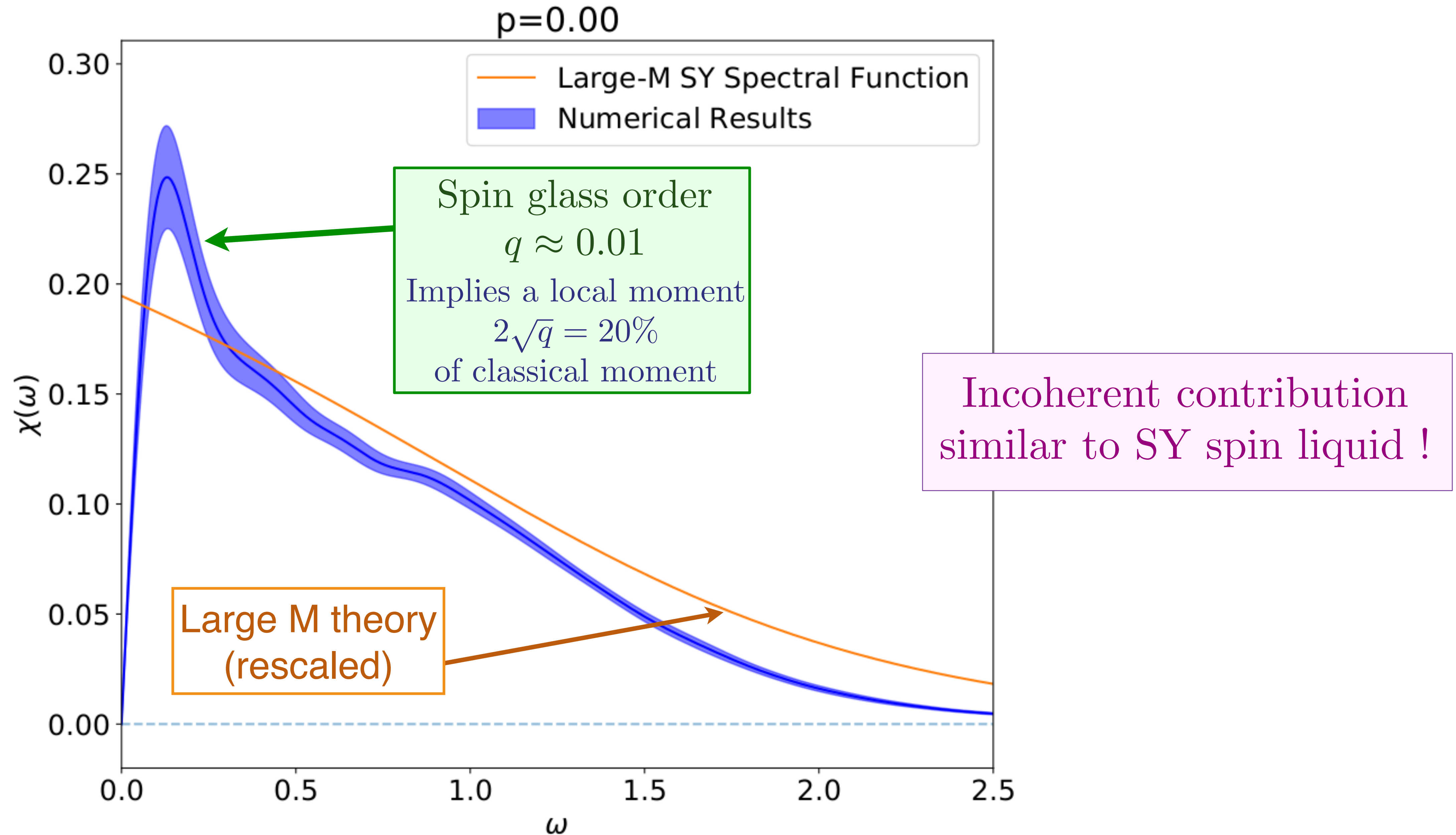
# Time reparameterization soft mode

Computing the resistivity from this Green's function via the Kubo formula, we find

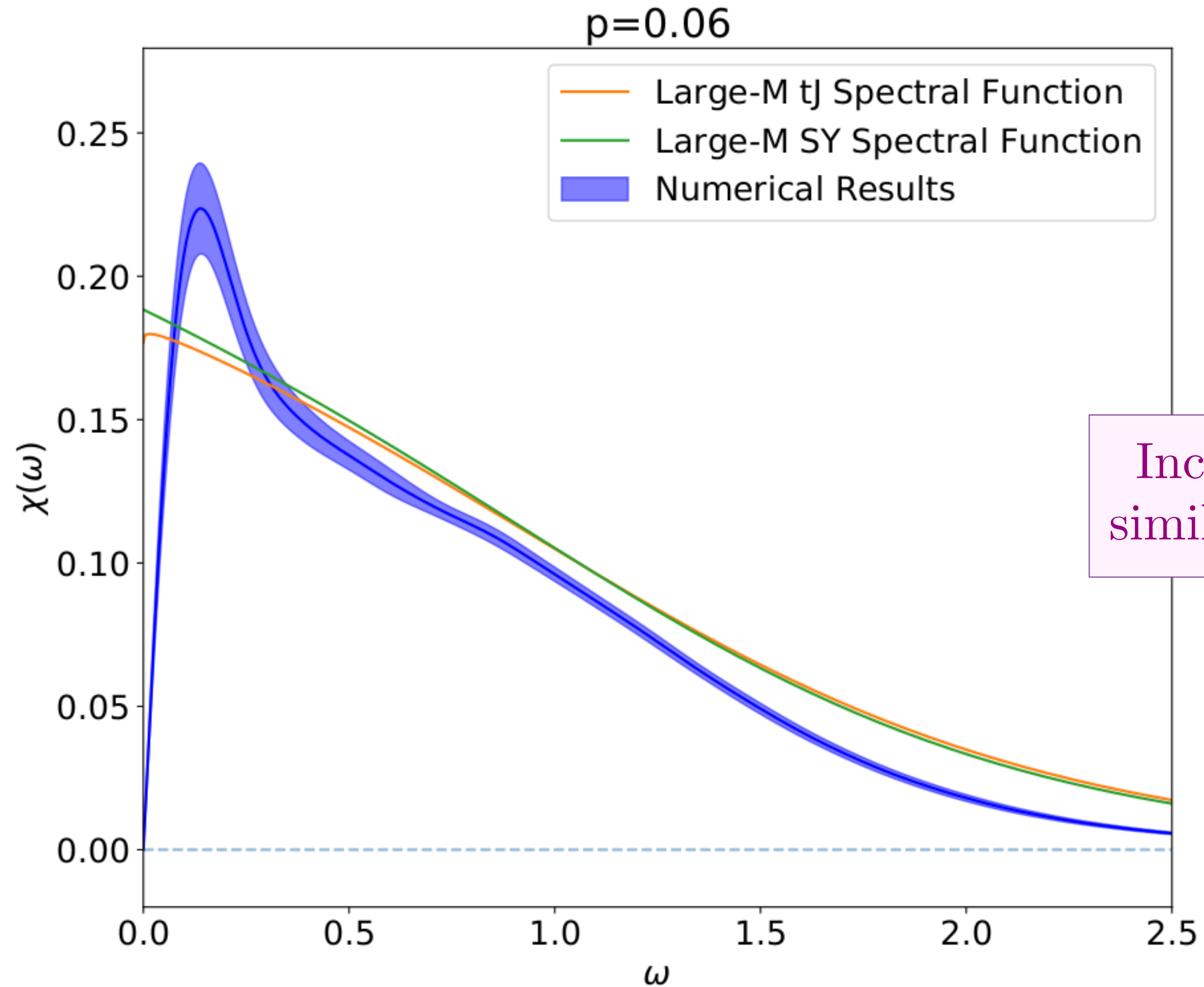
$$\rho(T) = \rho(0) (1 + \mathcal{C}_\rho \gamma T + \dots)$$

In general, an operator with scaling dimension  $h$ , yield a resistivity  $\rho(T) \sim T^{h-1}$ . In the large  $M$  solution of the  $t$ - $J$  model, we do find an operator with  $1 < h < 2$ , but with a smaller prefactor.

# Comparison with exact diagonalization on SU(2) random-t-J model

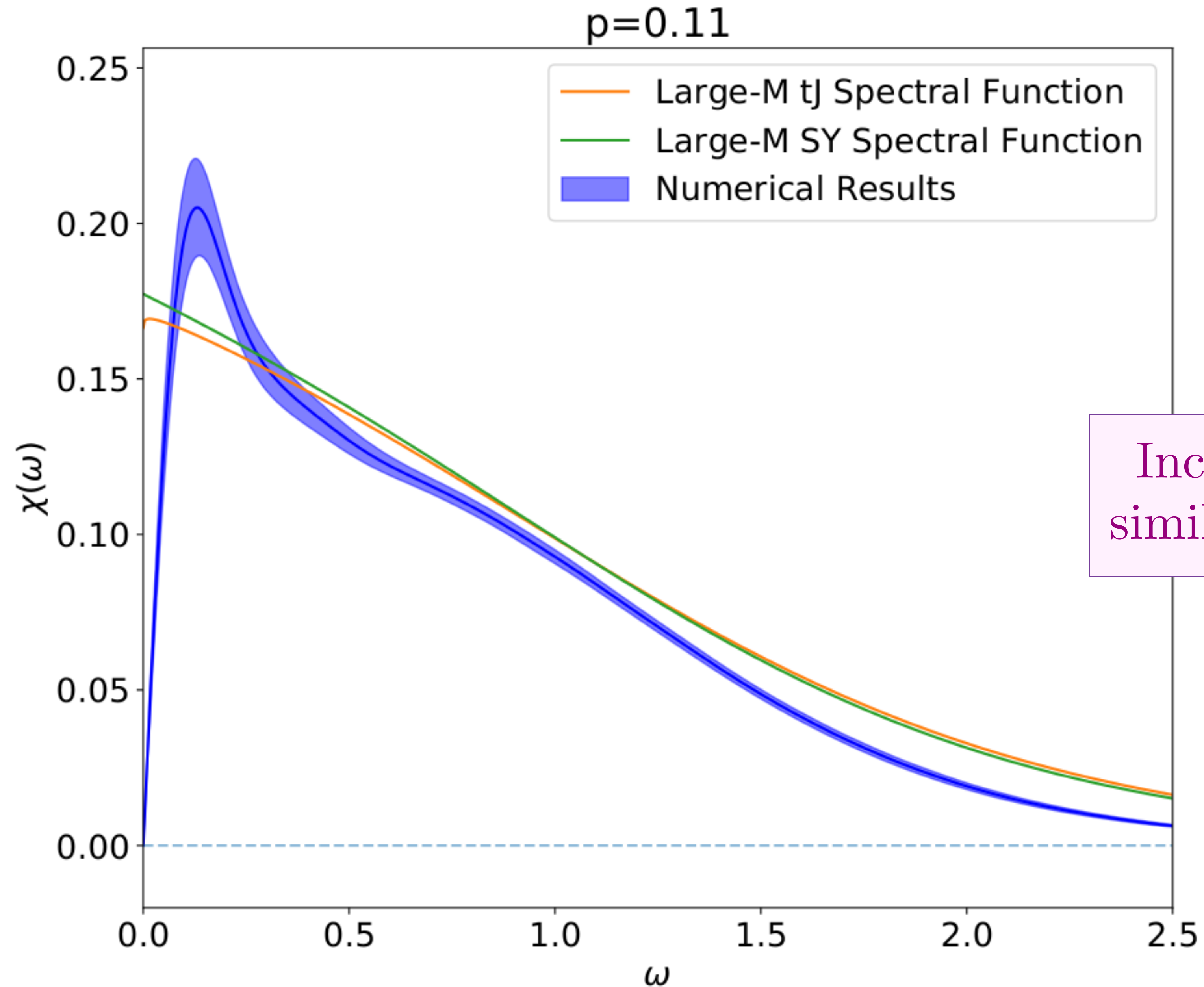


# Comparison with exact diagonalization on SU(2) random-t-J model



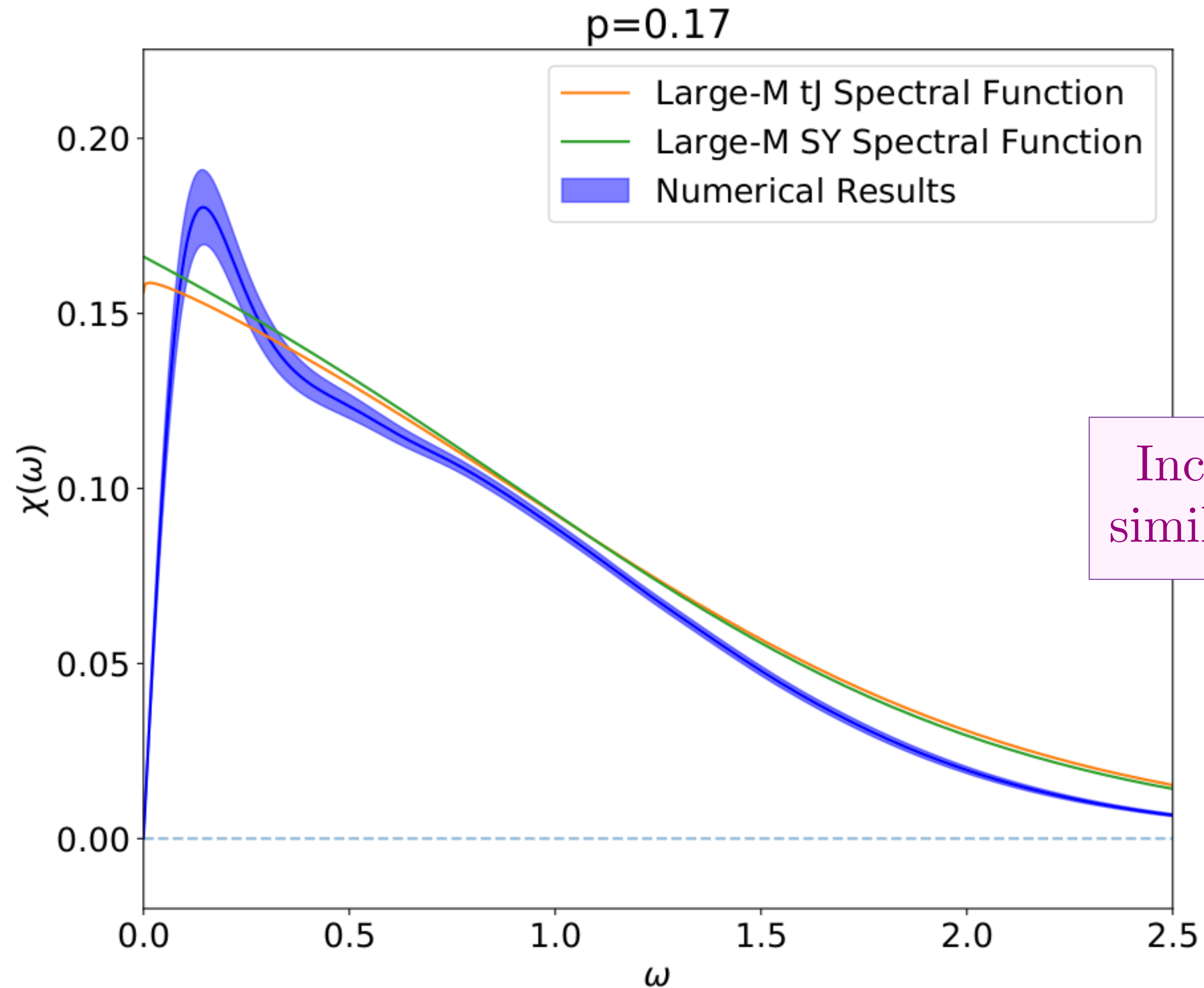
Incoherent contribution  
similar to SY spin liquid !

# Comparison with exact diagonalization on SU(2) random-t-J model



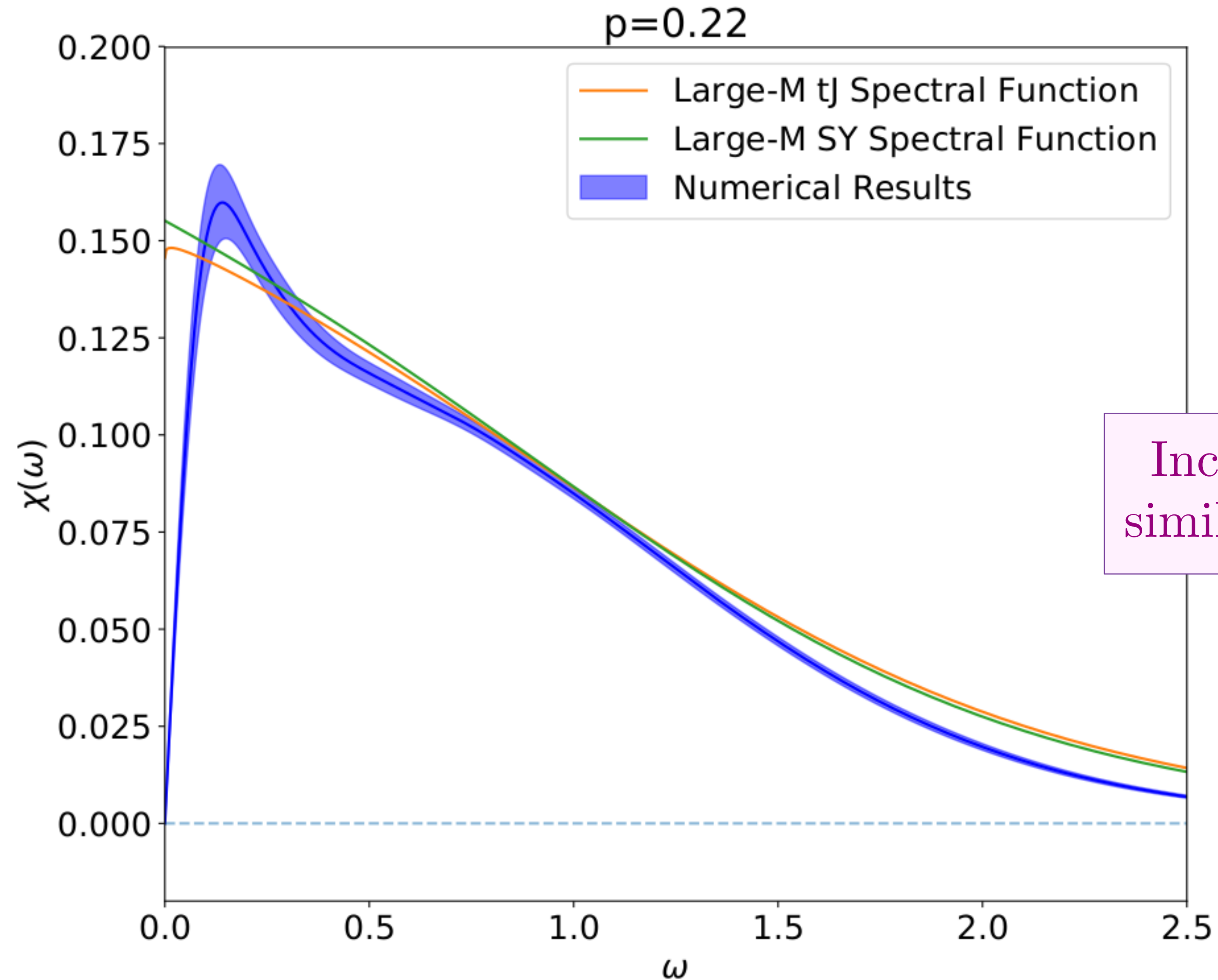
Incoherent contribution similar to SY spin liquid !

# Comparison with exact diagonalization on SU(2) random-t-J model



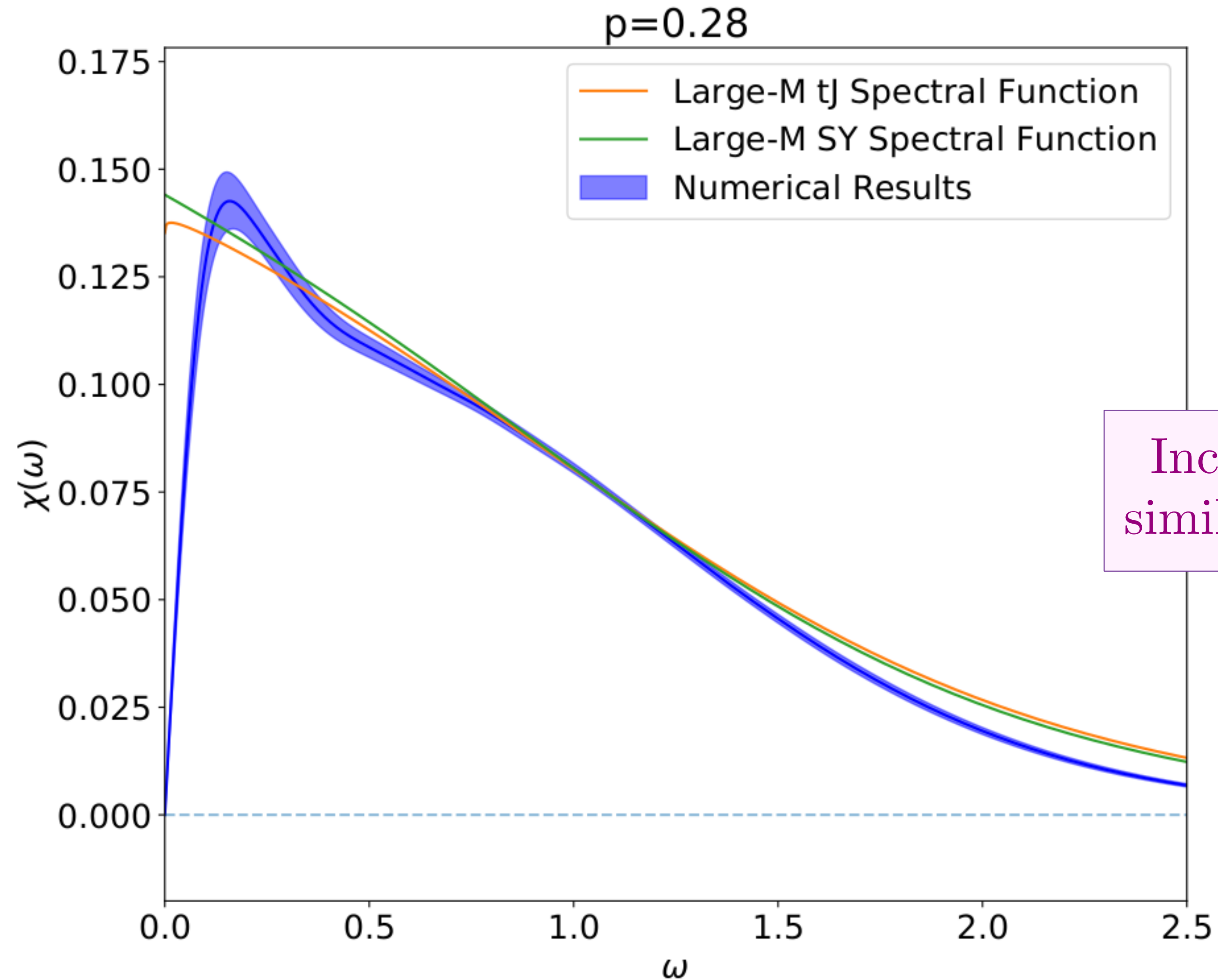
Incoherent contribution similar to SY spin liquid !

# Comparison with exact diagonalization on SU(2) random-t-J model



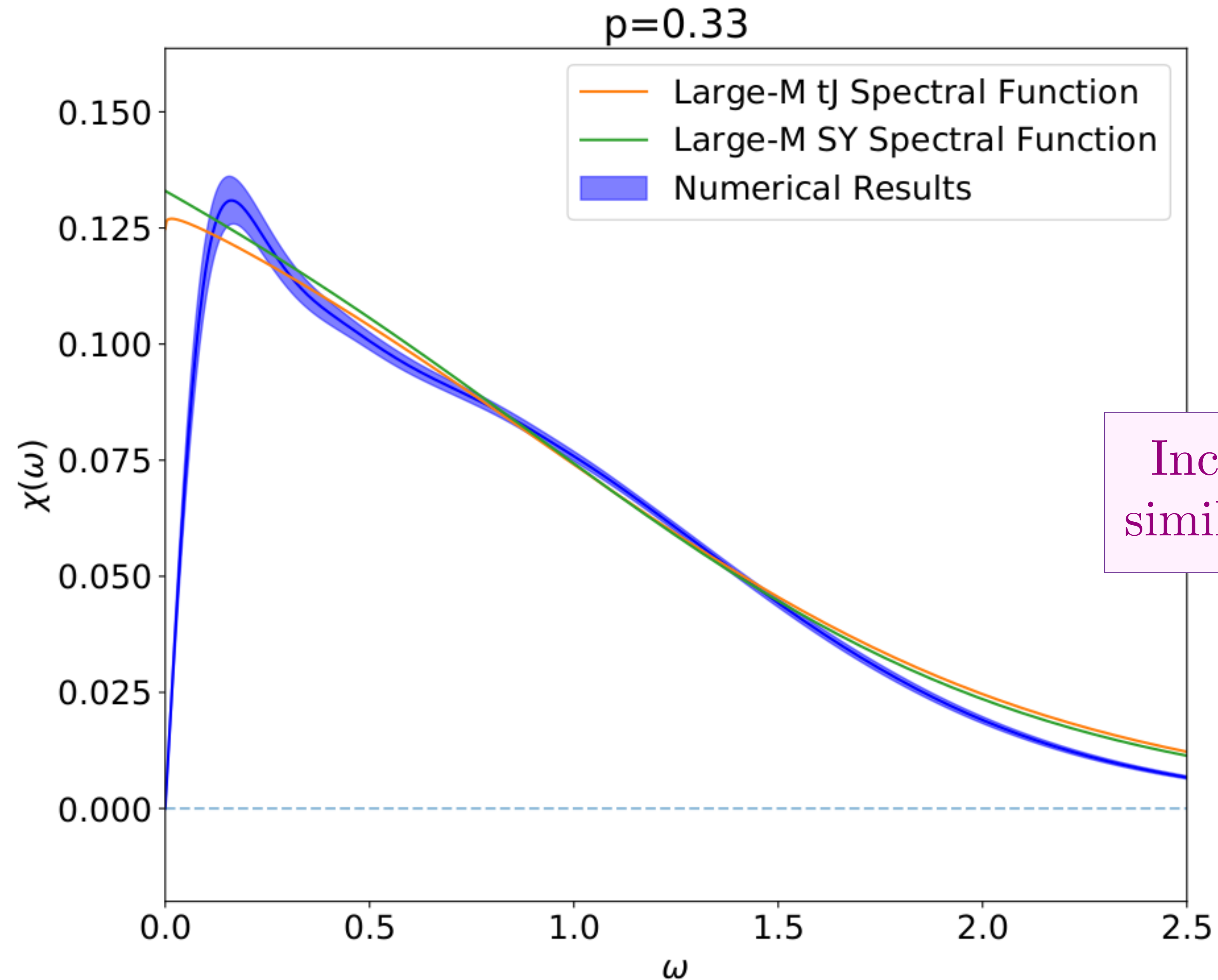
Incoherent contribution similar to SY spin liquid !

# Comparison with exact diagonalization on SU(2) random-t-J model



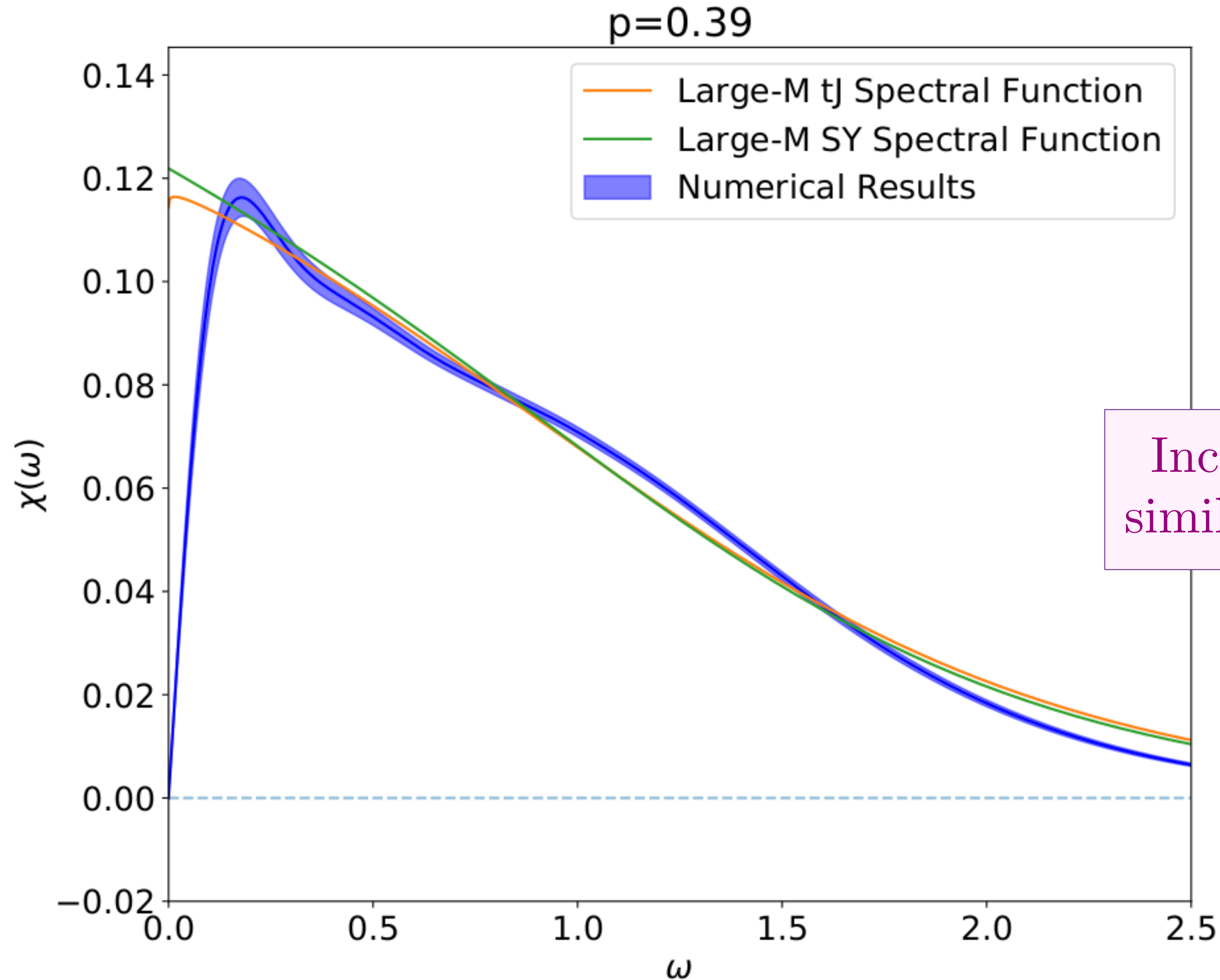
Incoherent contribution similar to SY spin liquid !

# Comparison with exact diagonalization on SU(2) random-t-J model

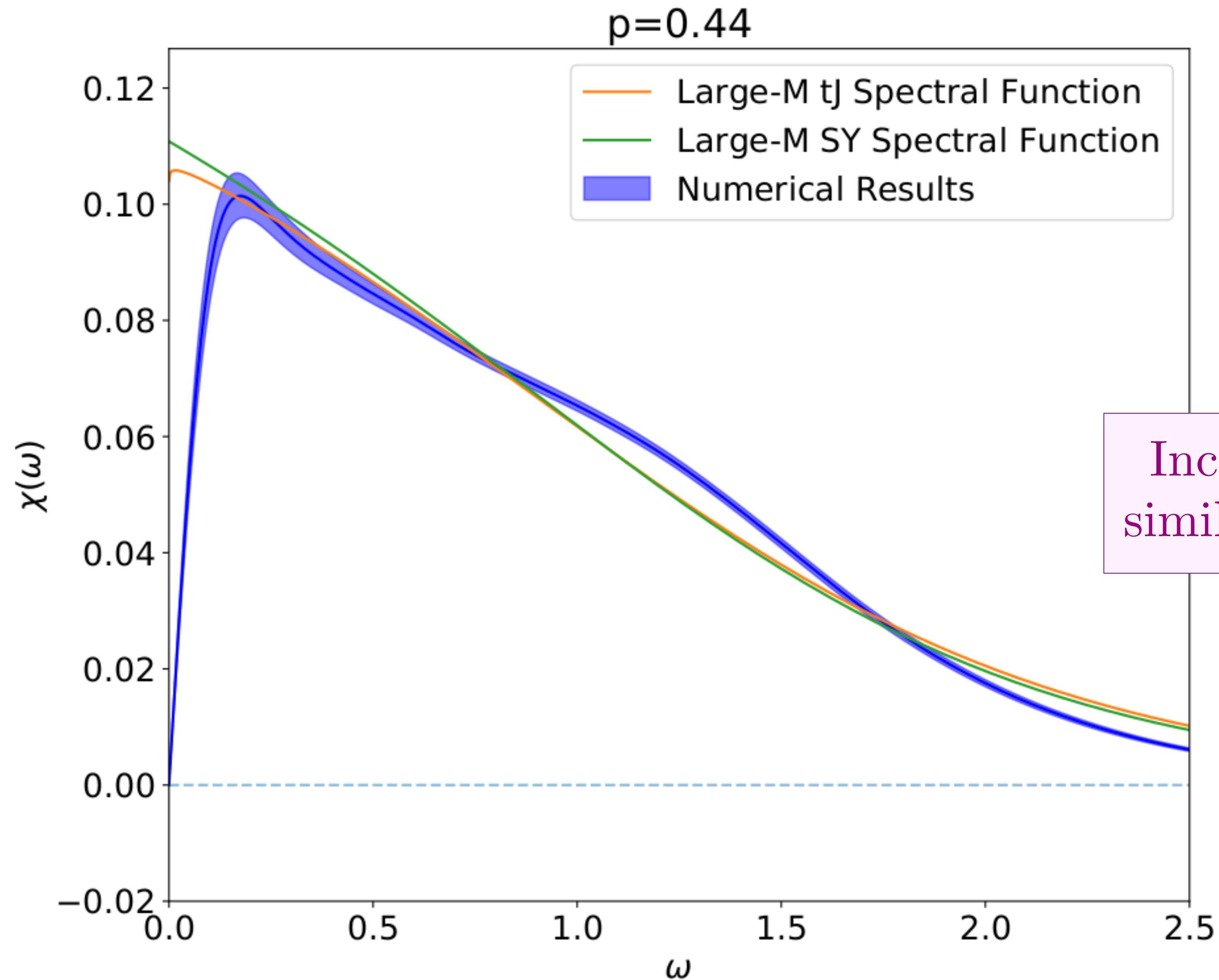


Incoherent contribution similar to SY spin liquid !

# Comparison with exact diagonalization on SU(2) random-t-J model

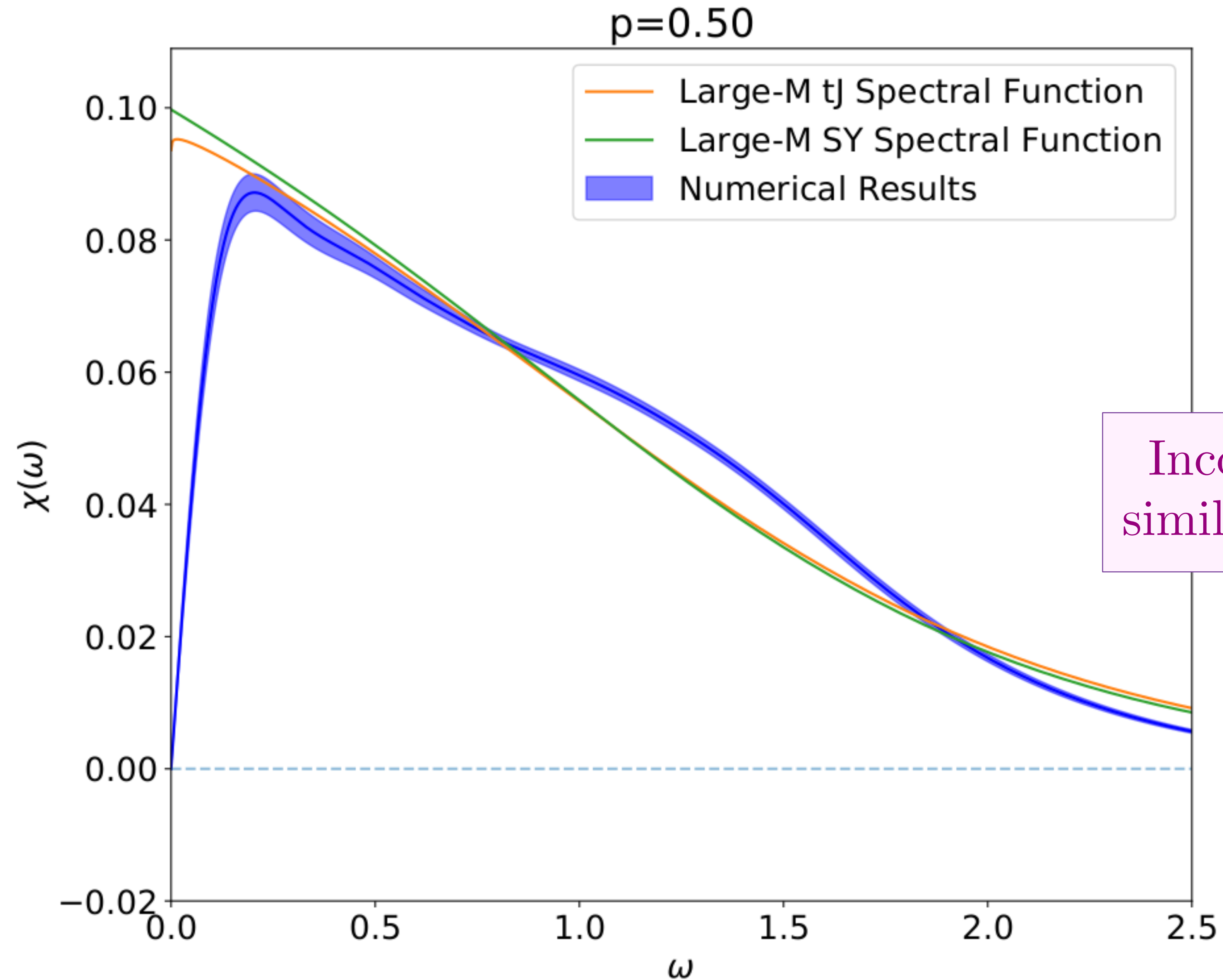


# Comparison with exact diagonalization on SU(2) random-t-J model



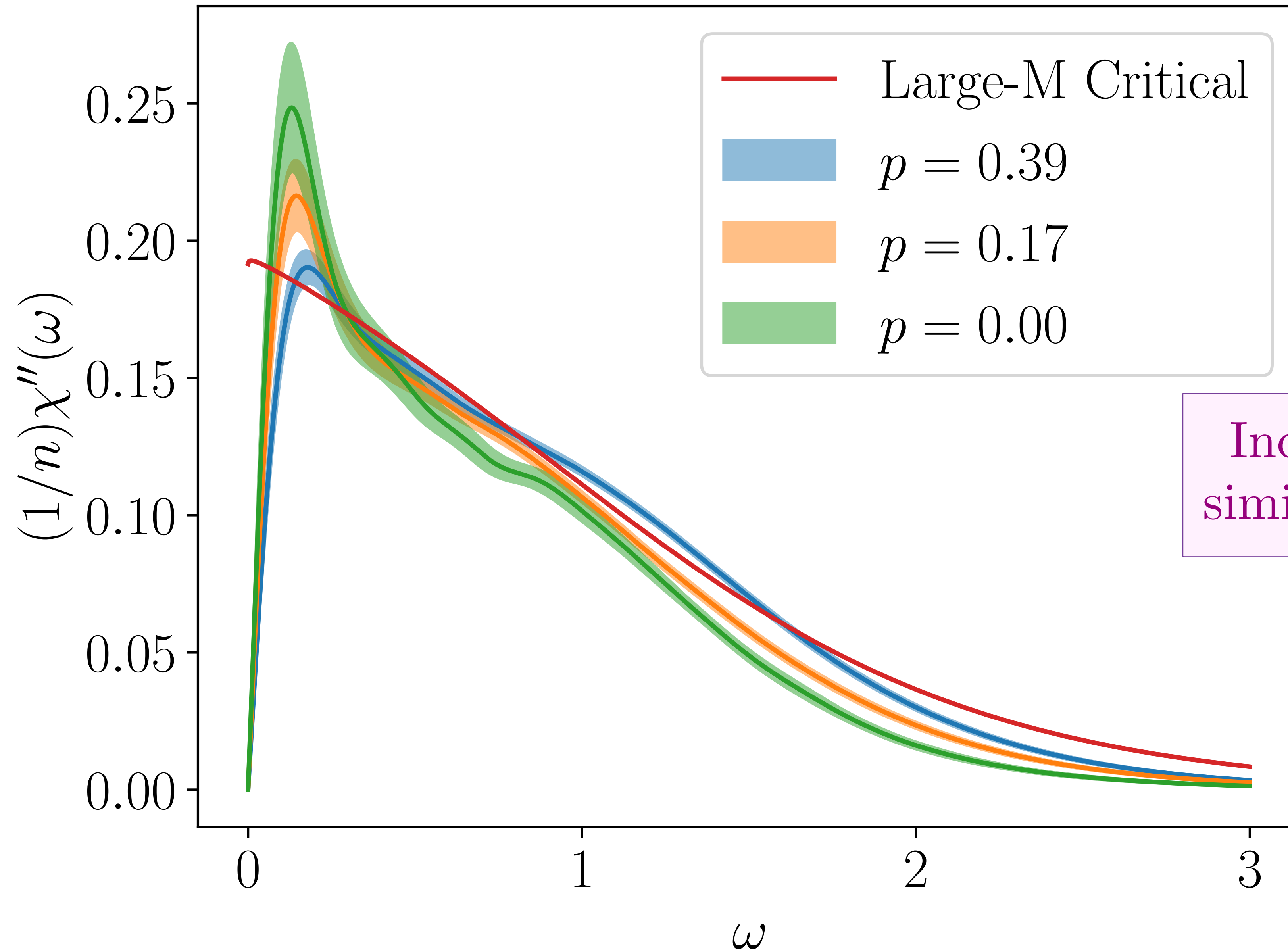
Incoherent contribution similar to SY spin liquid !

# Comparison with exact diagonalization on SU(2) random-t-J model



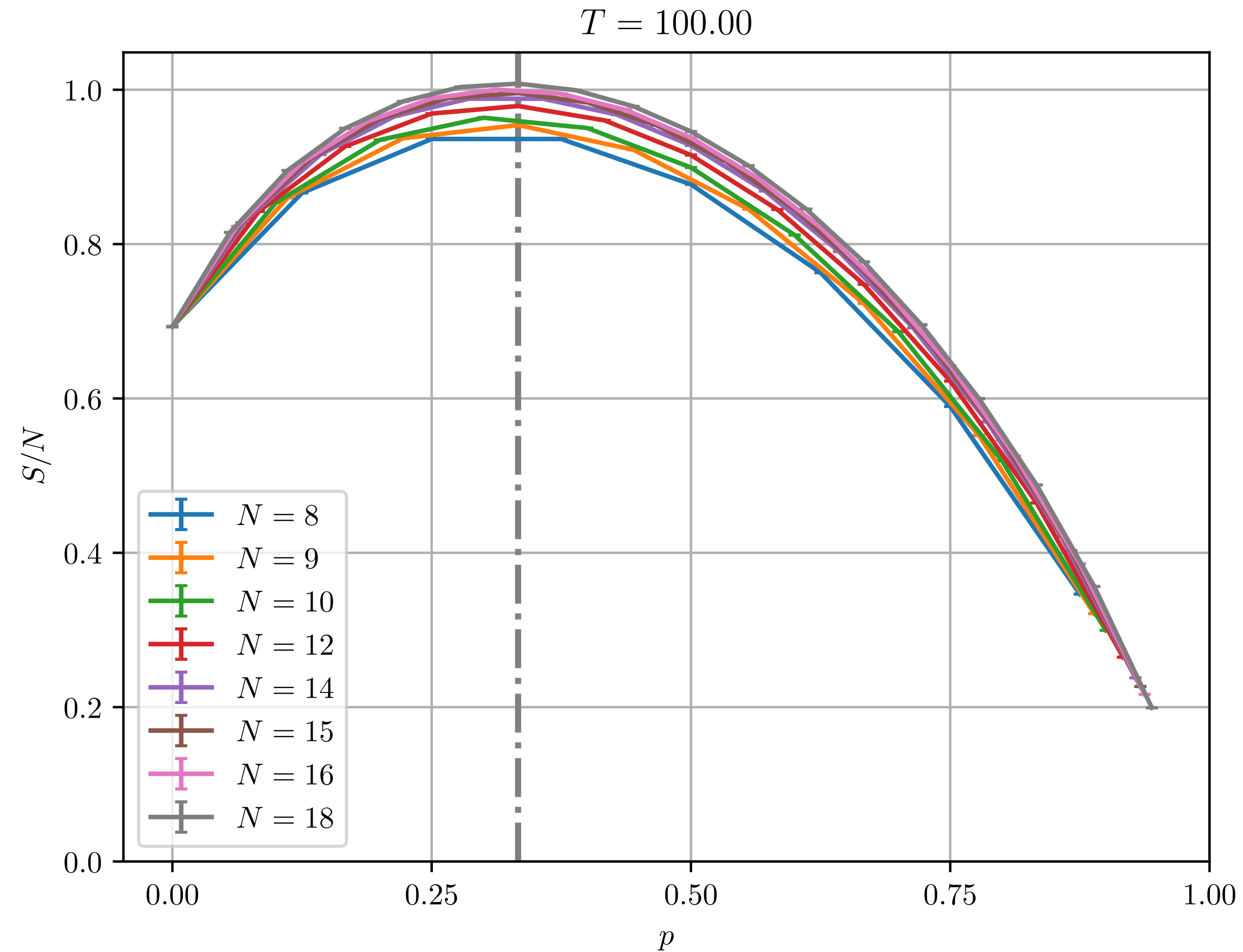
Incoherent contribution similar to SY spin liquid !

# Comparison with exact diagonalization on SU(2) random-t-J model



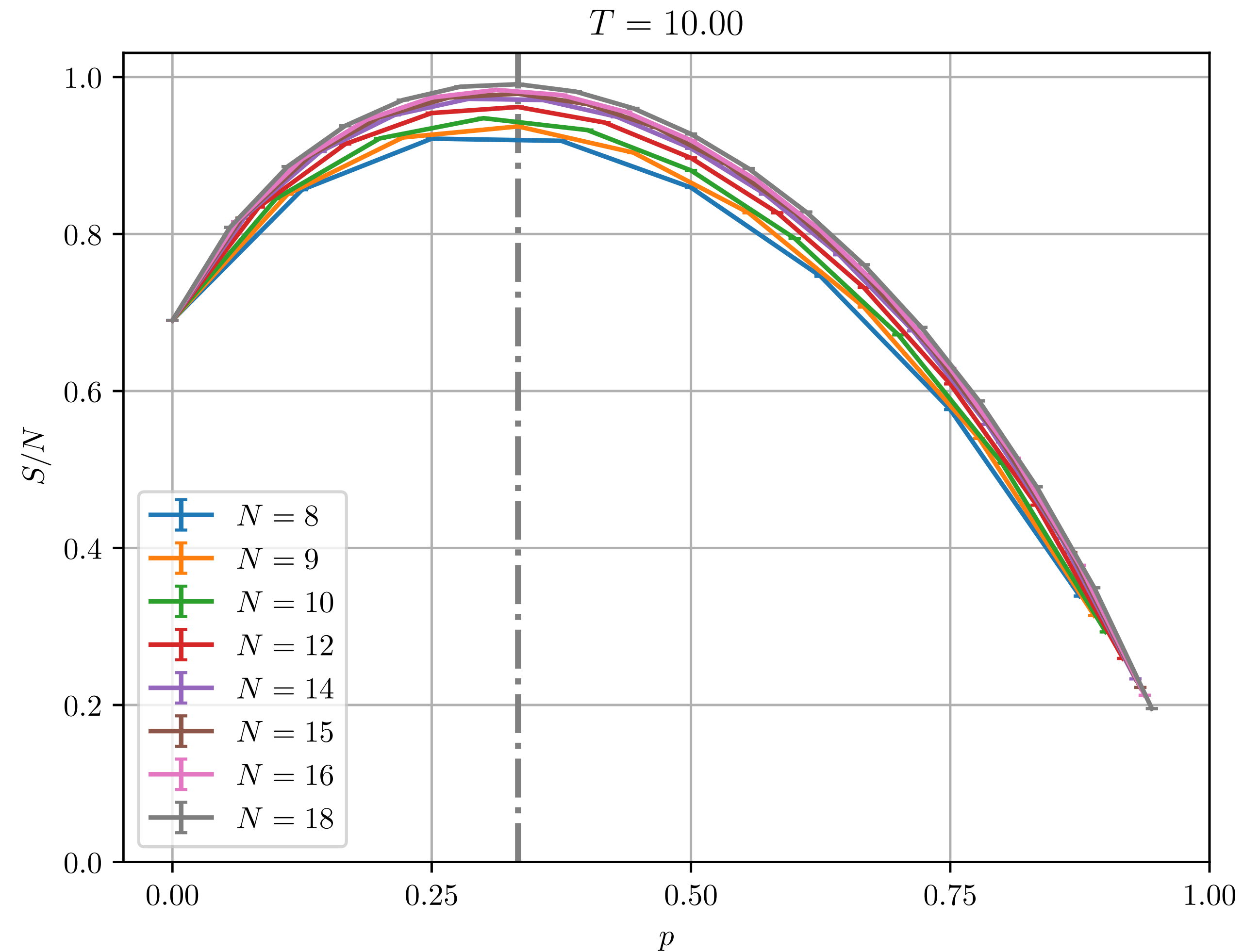
Incoherent contribution  
similar to SY spin liquid !

Entropy at  $T \gg 1$  determined by  $\dim(\mathcal{H})$



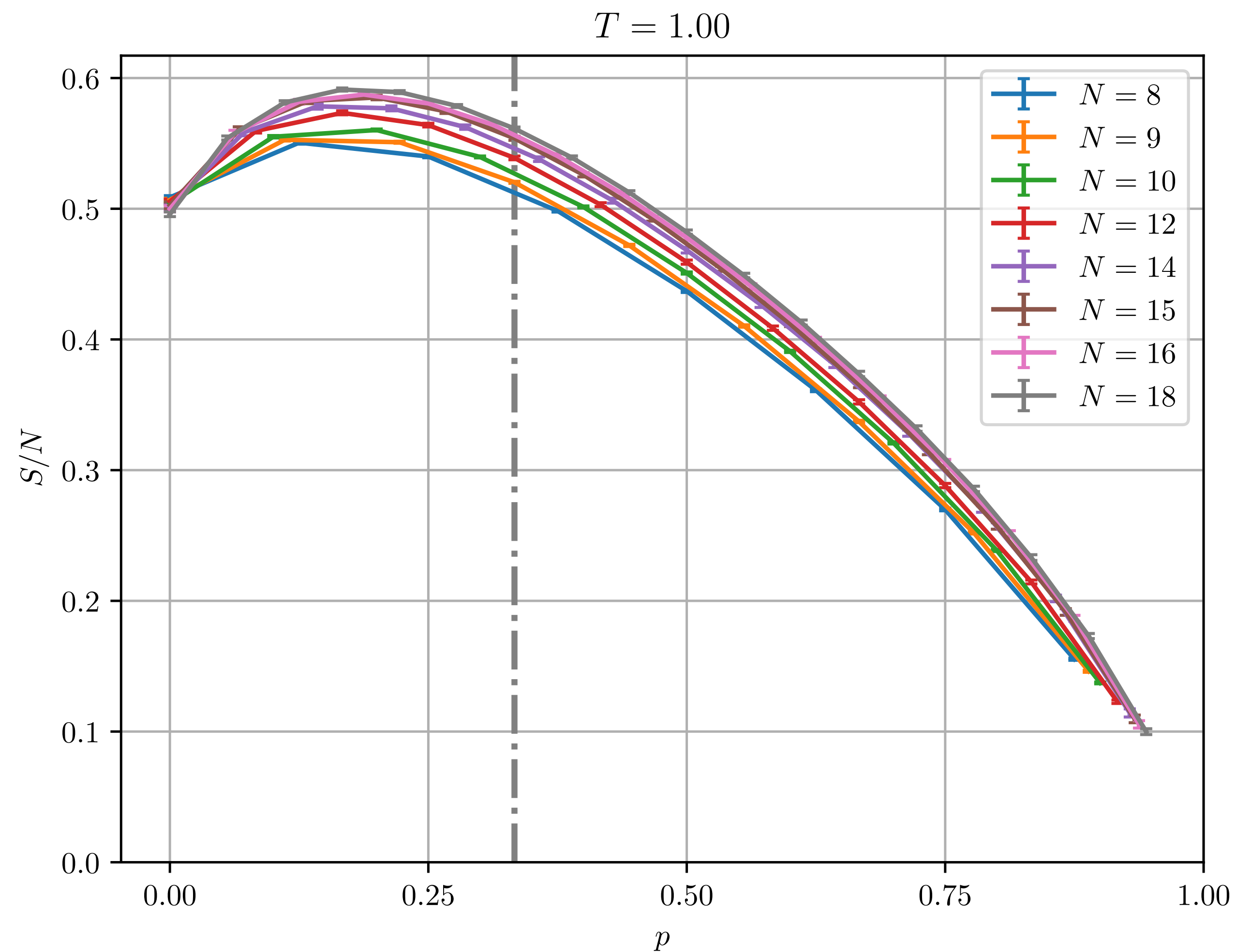
Thermodynamics from exact diagonalization of SU(2) random-t-J model

# Maximum entropy shifts at lower temperature



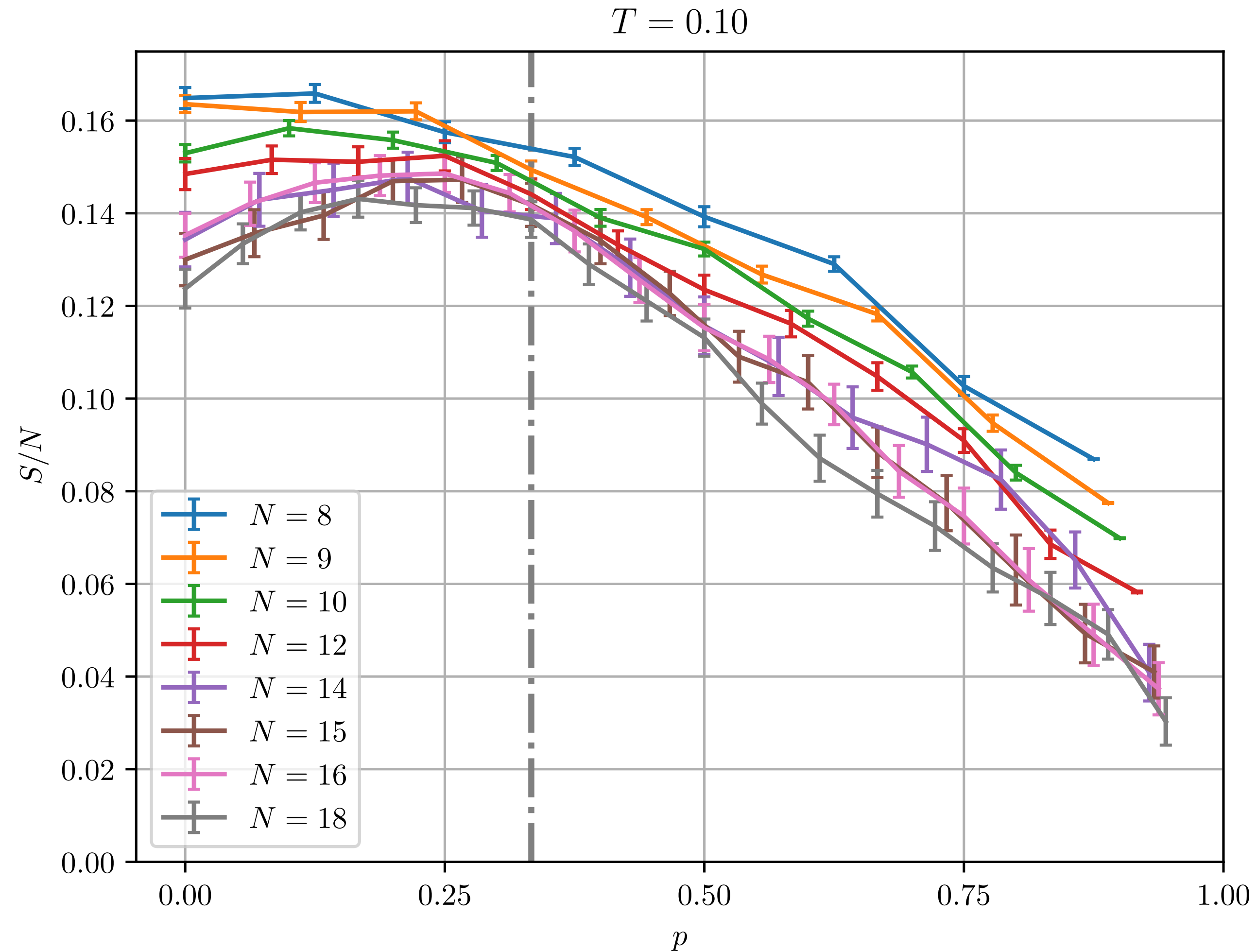
Thermodynamics from exact diagonalization of SU(2) random-t-J model

# Maximum entropy shifts at lower temperature



Thermodynamics from exact diagonalization of SU(2) random-t-J model

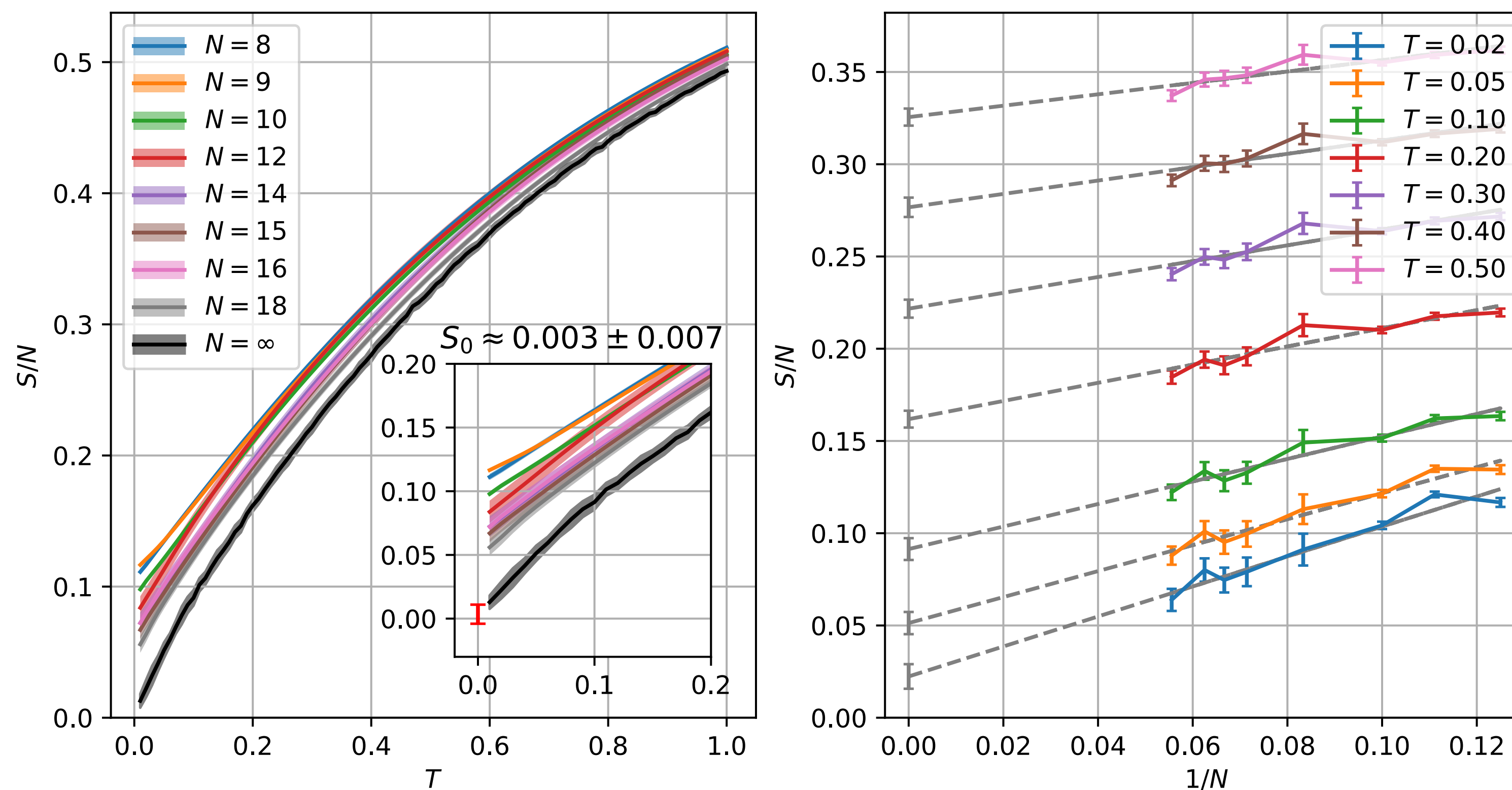
# Maximum entropy shifts at lower temperature



Thermodynamics from exact diagonalization of SU(2) random-t-J model

# Large-N extrapolation of entropy density

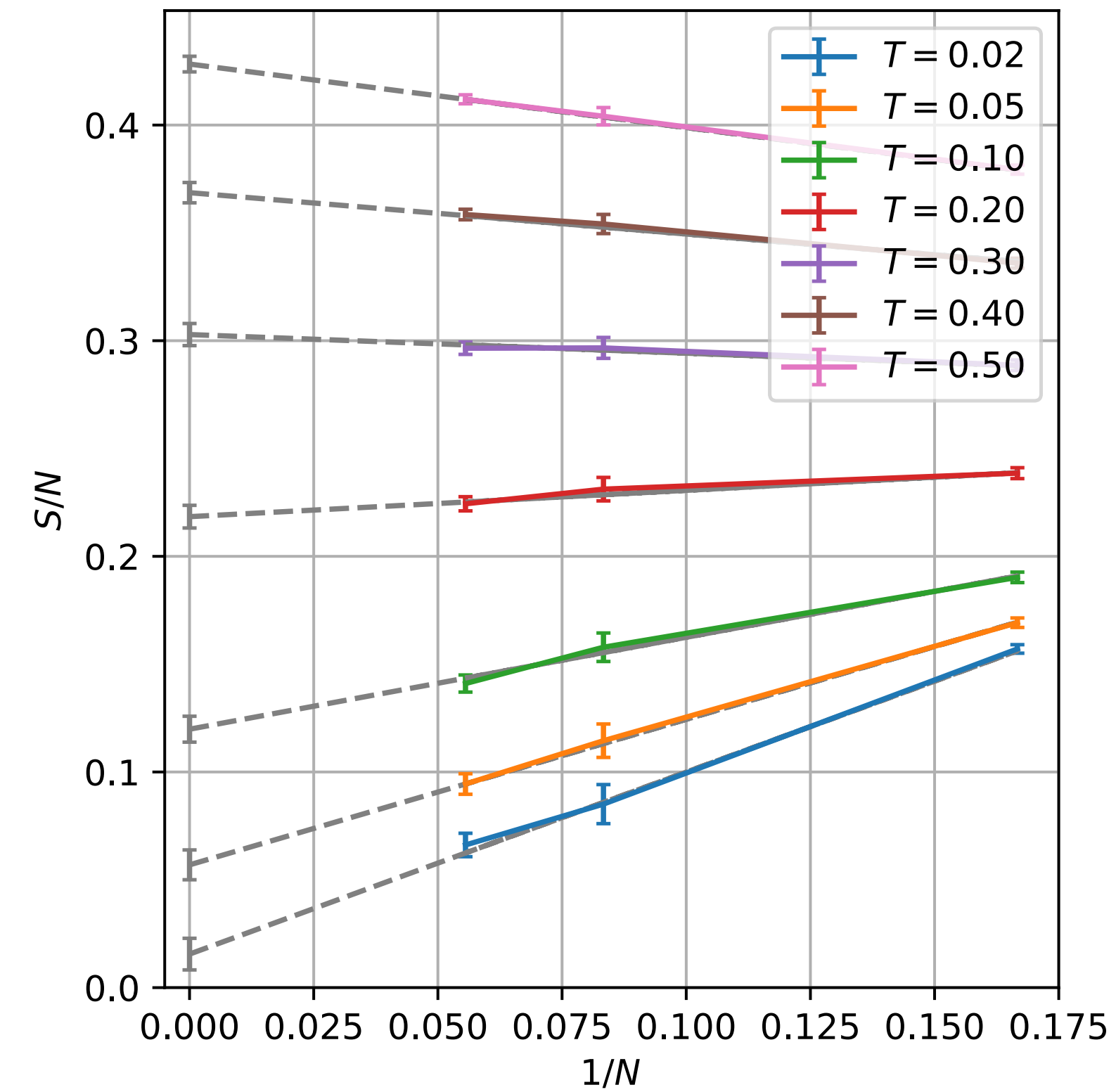
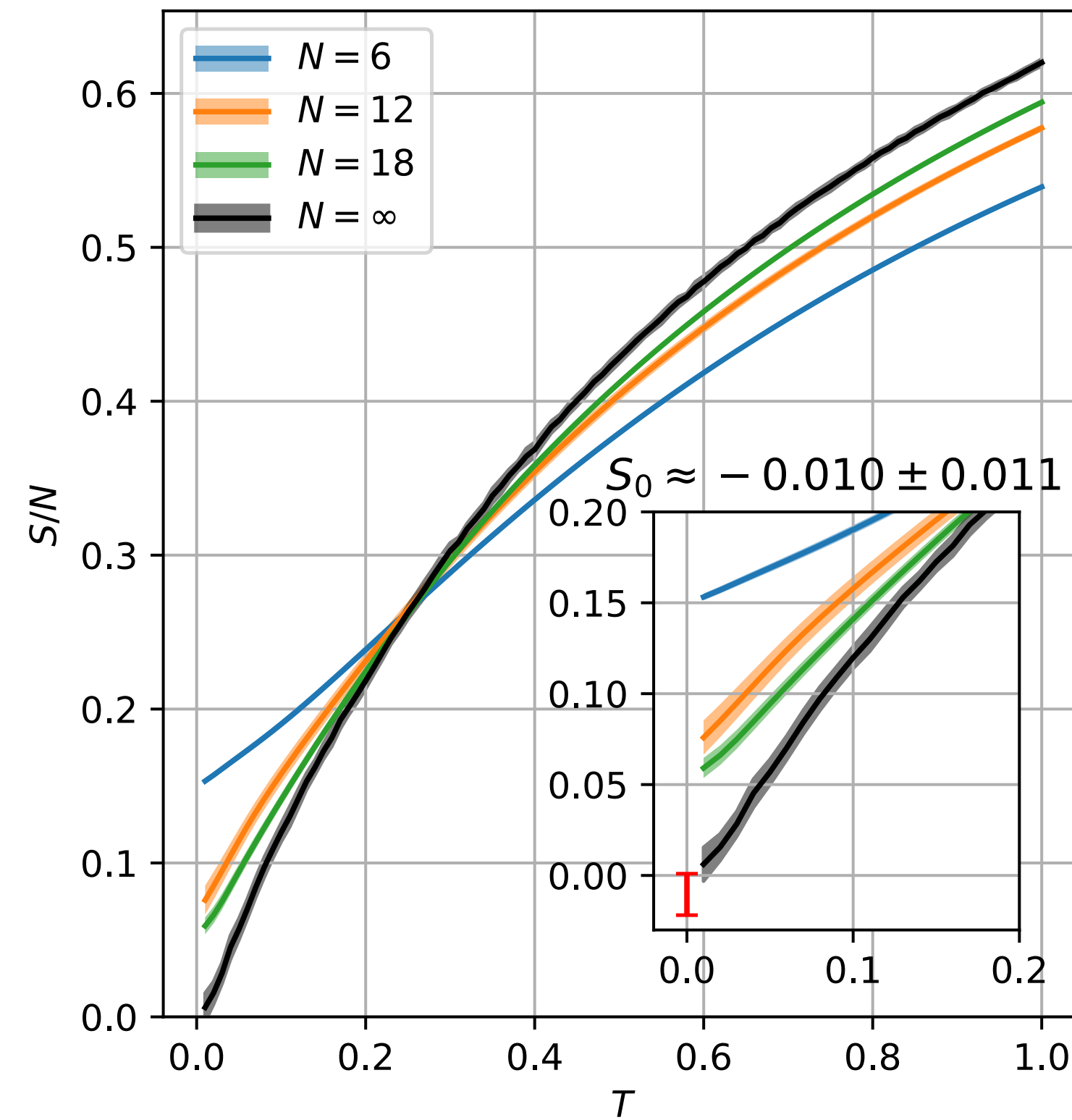
Entropy,  $p = 0$



**Thermodynamics from exact diagonalization of SU(2) random-t-J model**

# Large-N extrapolation of entropy density

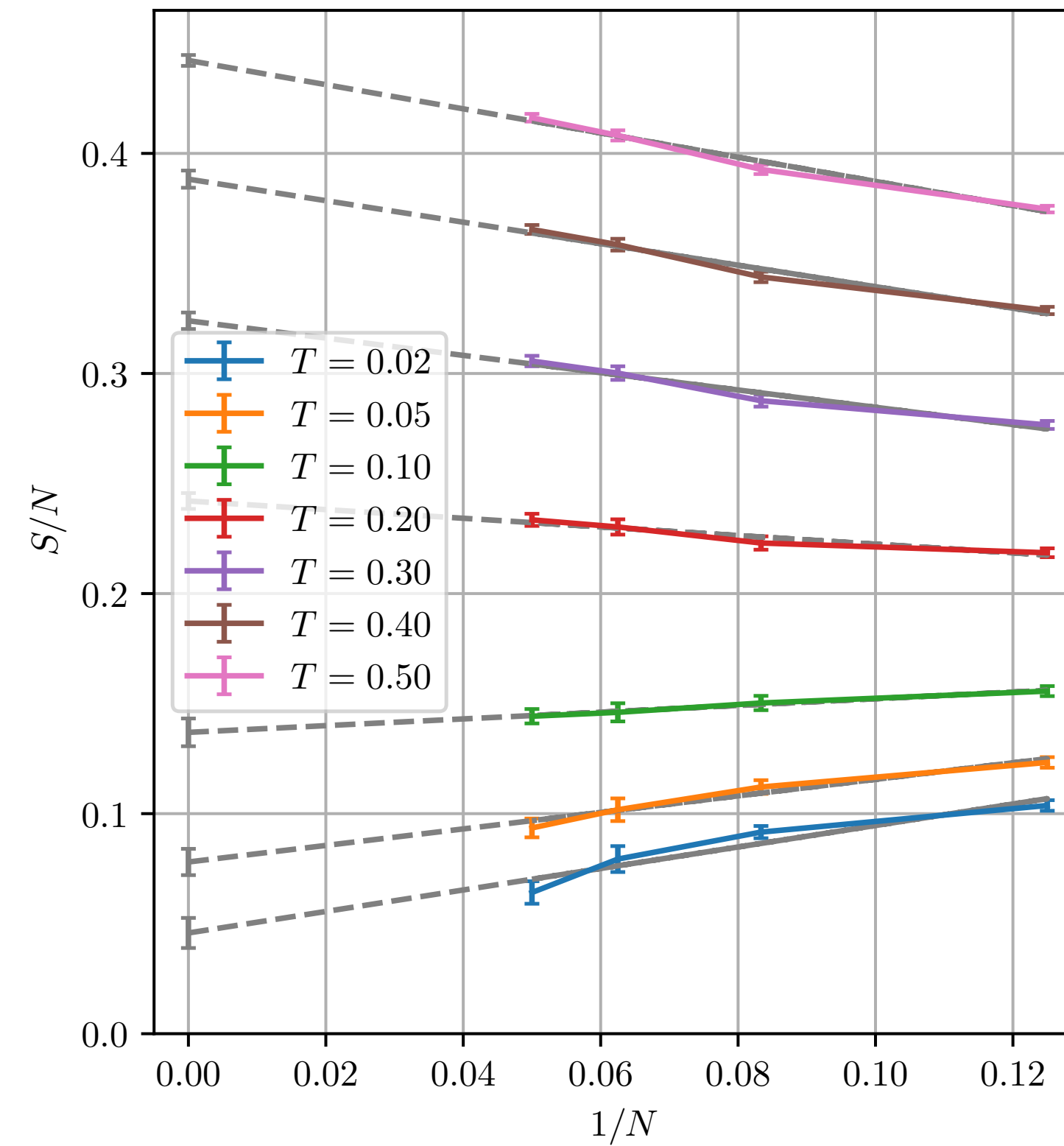
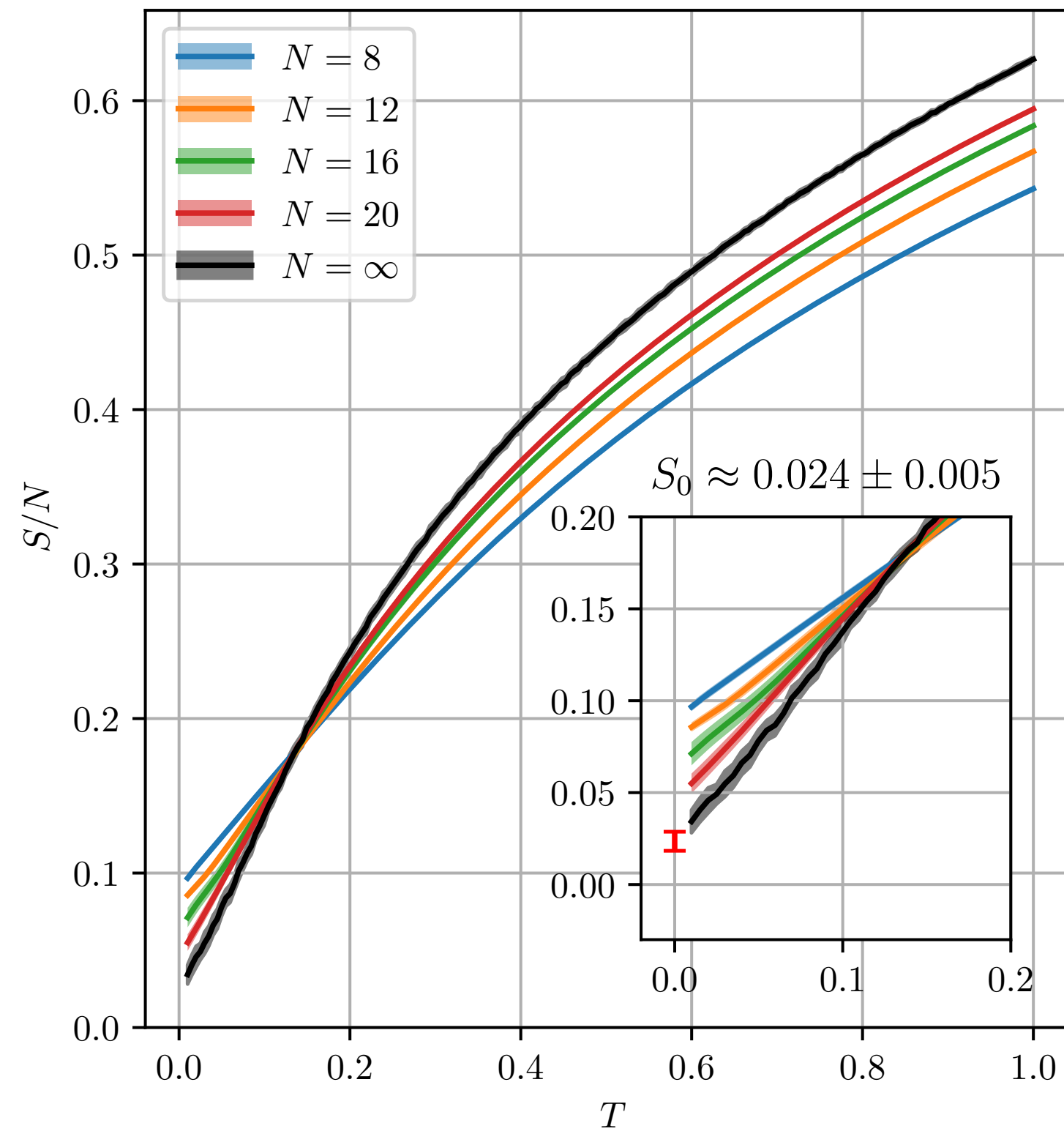
Entropy,  $\rho = 1/6$



Thermodynamics from exact diagonalization of SU(2) random-t-J model

# Large-N extrapolation of entropy density

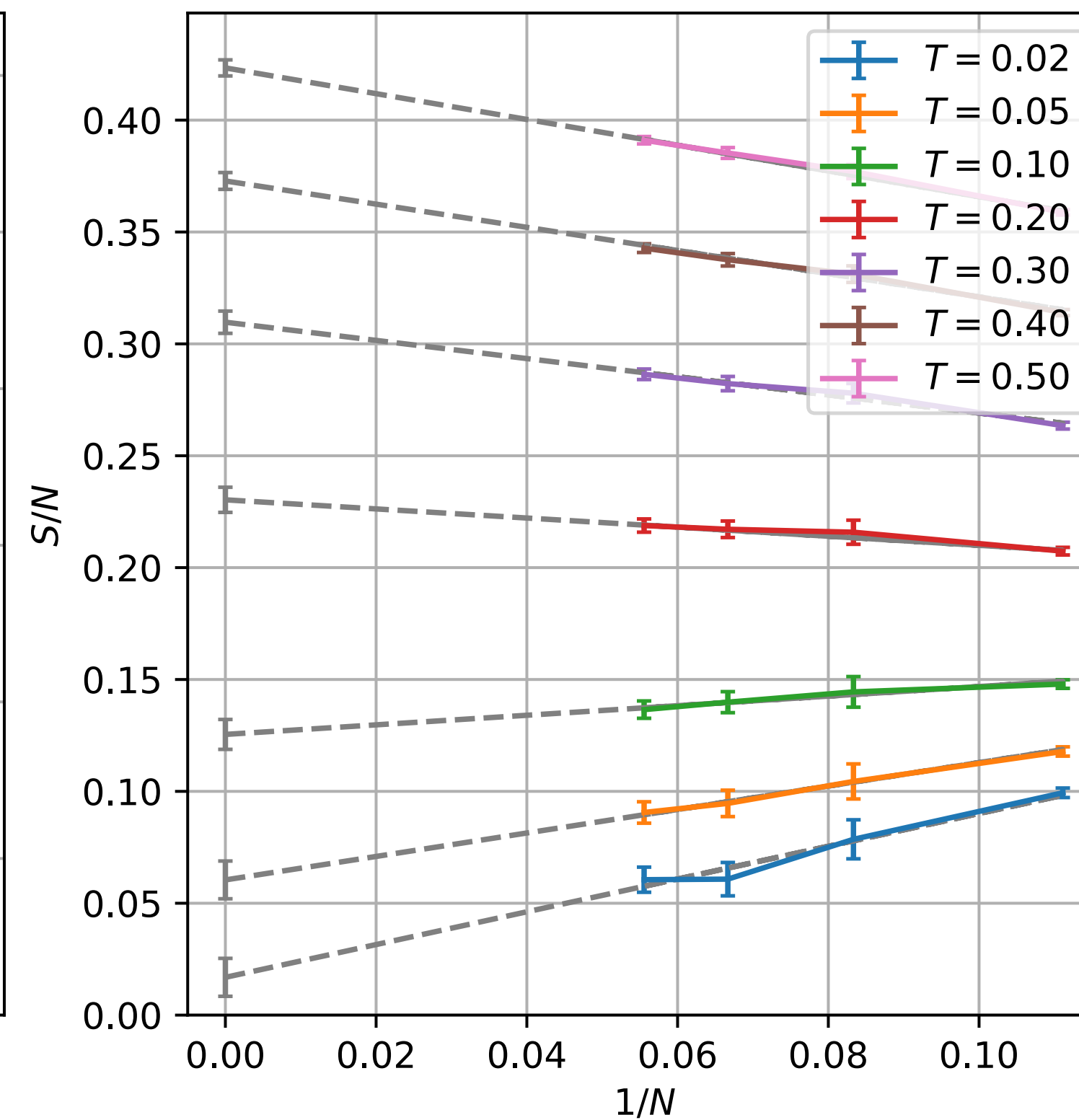
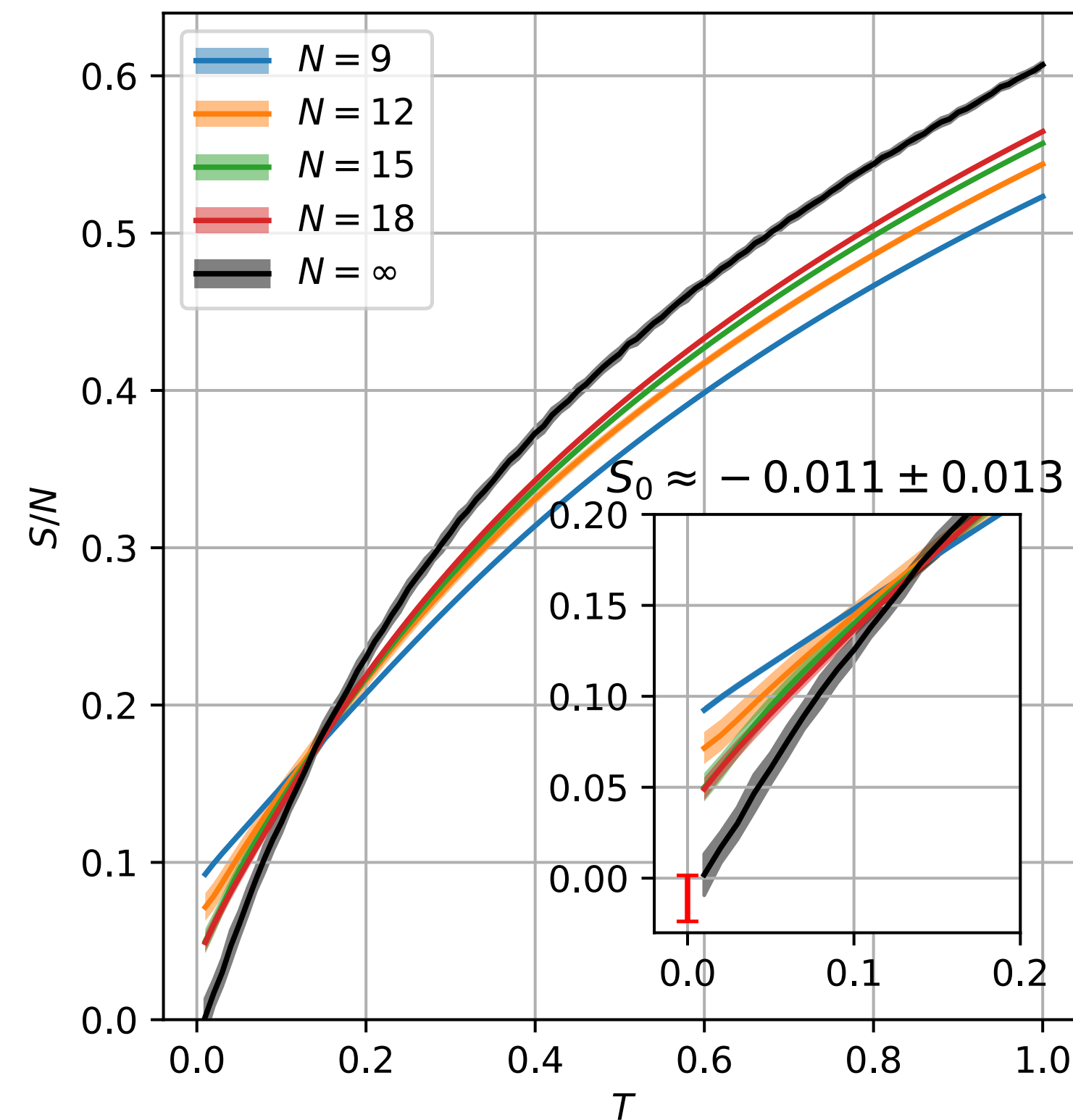
$$p = 1/4$$



**Thermodynamics from exact diagonalization of SU(2) random-t-J model**

# Large-N extrapolation of entropy density

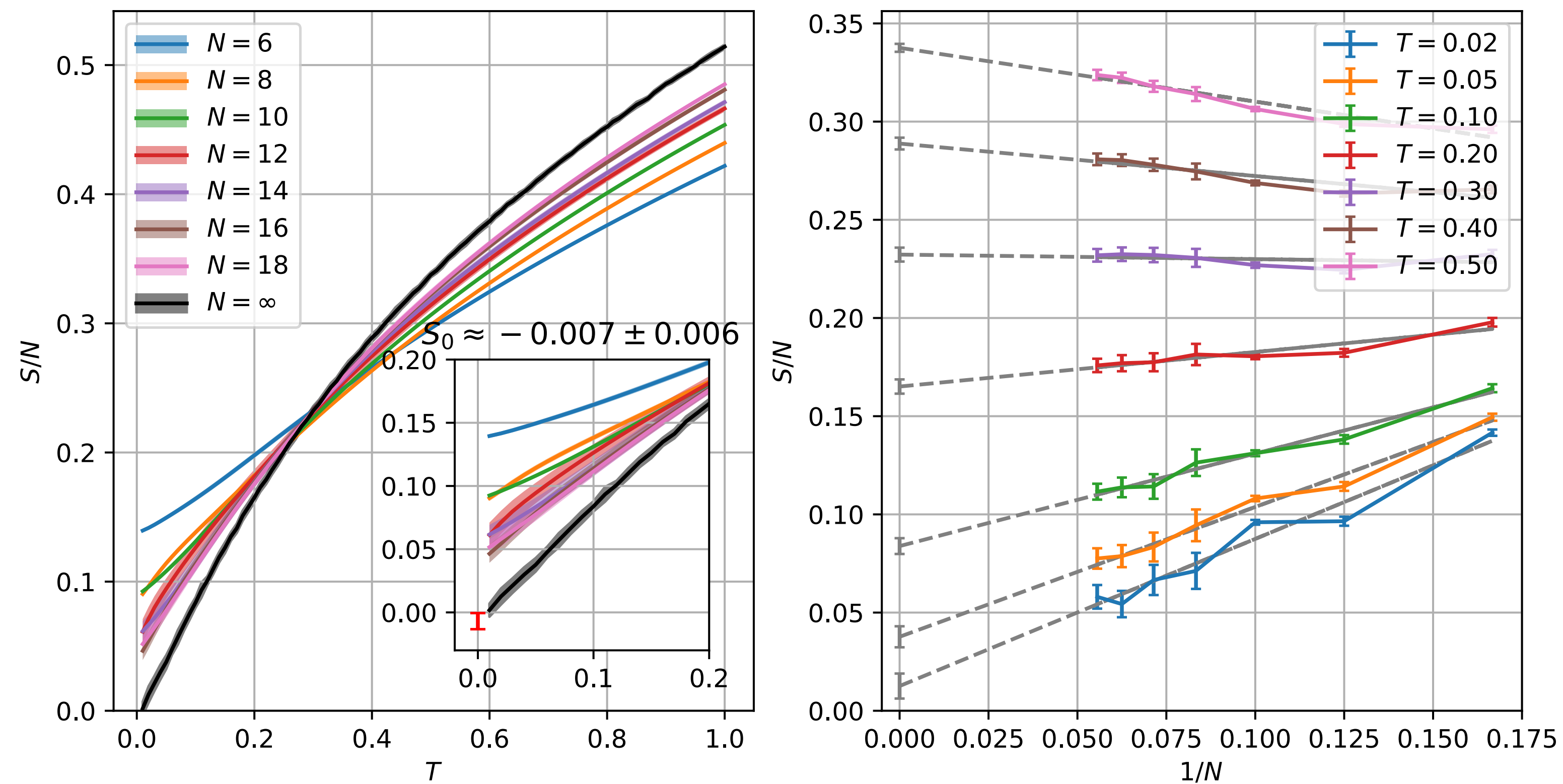
Entropy,  $\rho = 1/3$



Thermodynamics from exact diagonalization of SU(2) random-t-J model

# Large-N extrapolation of entropy density

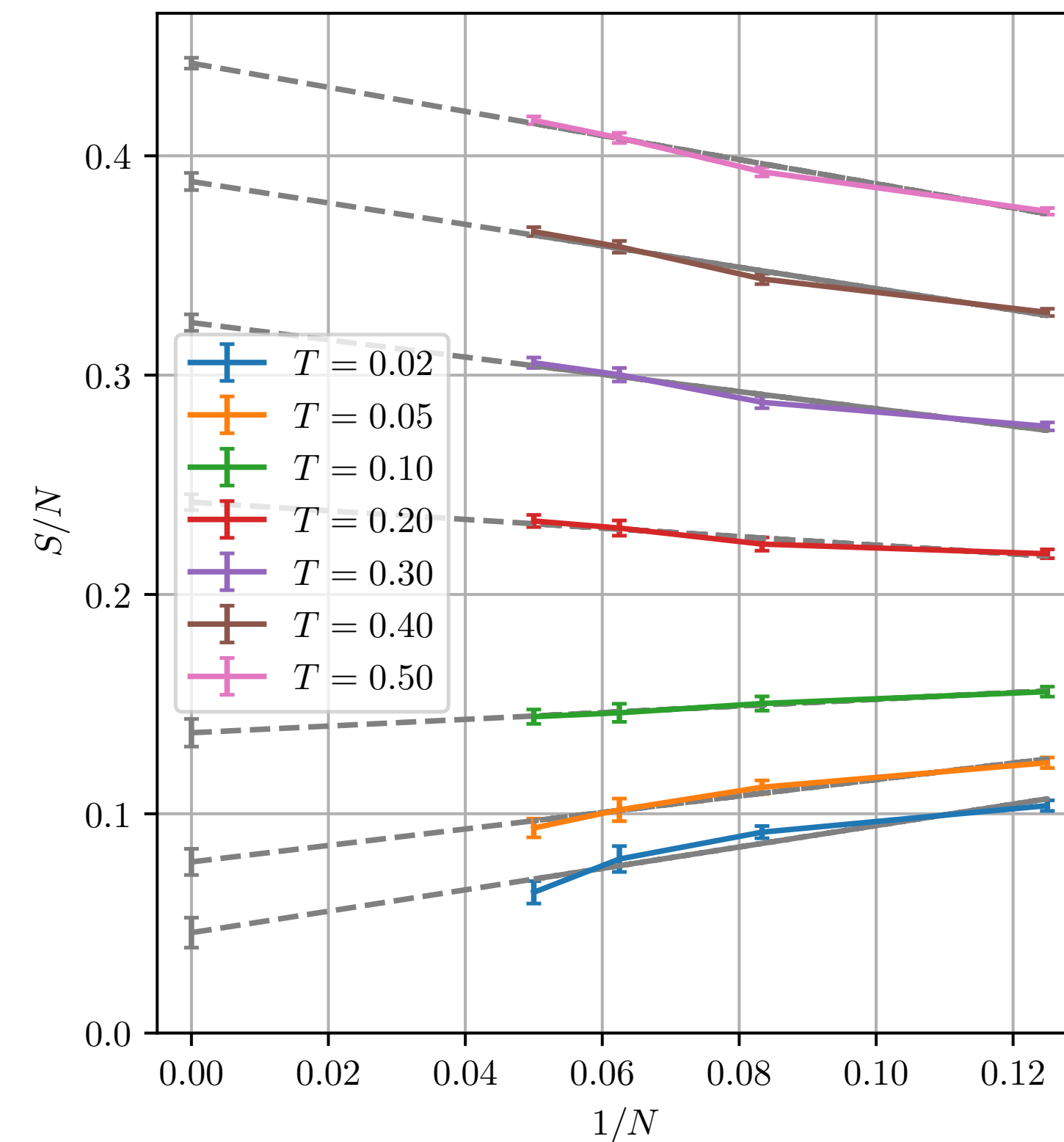
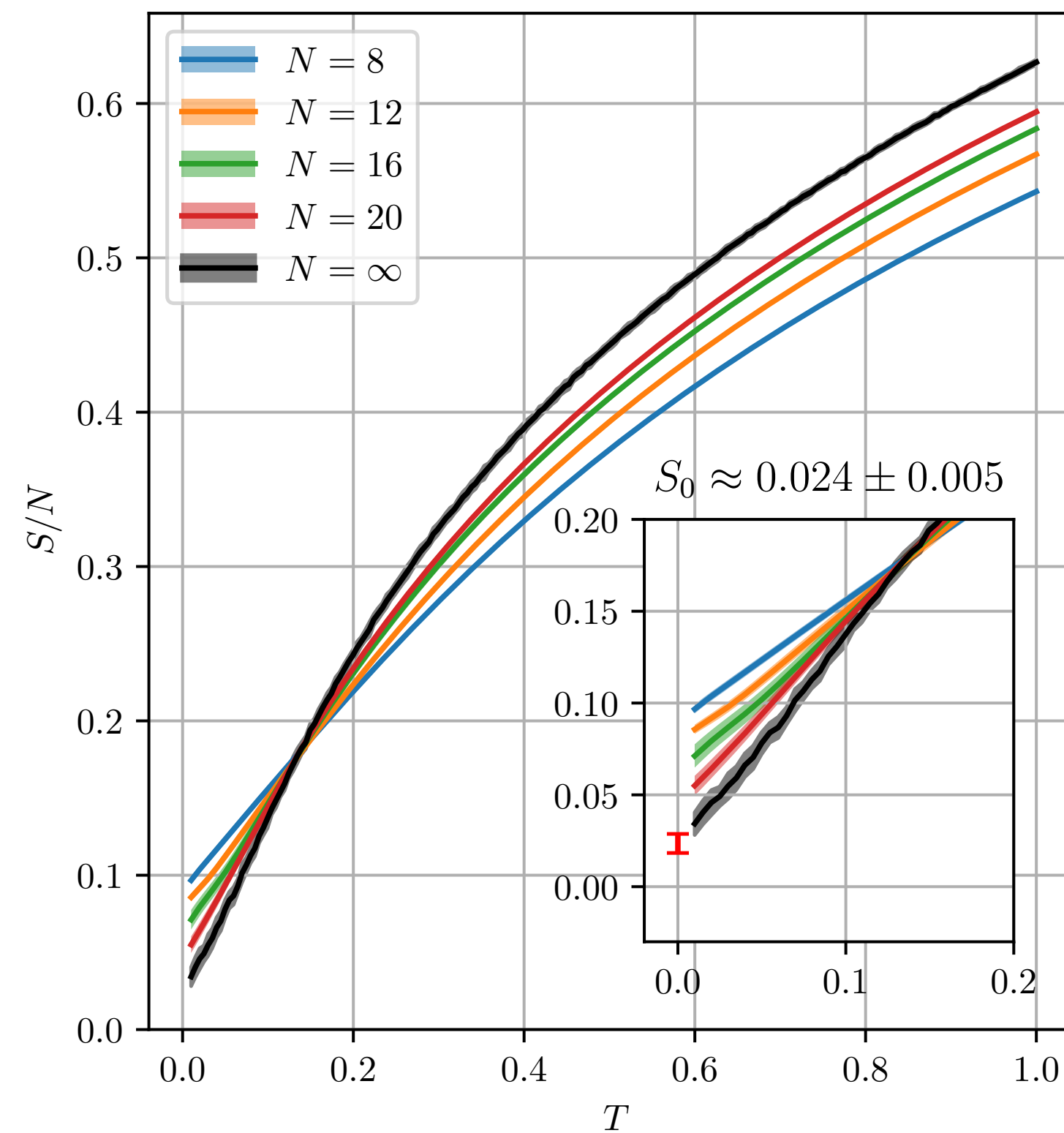
Entropy,  $\rho = 1/2$



**Thermodynamics from exact diagonalization of SU(2) random-t-J model**

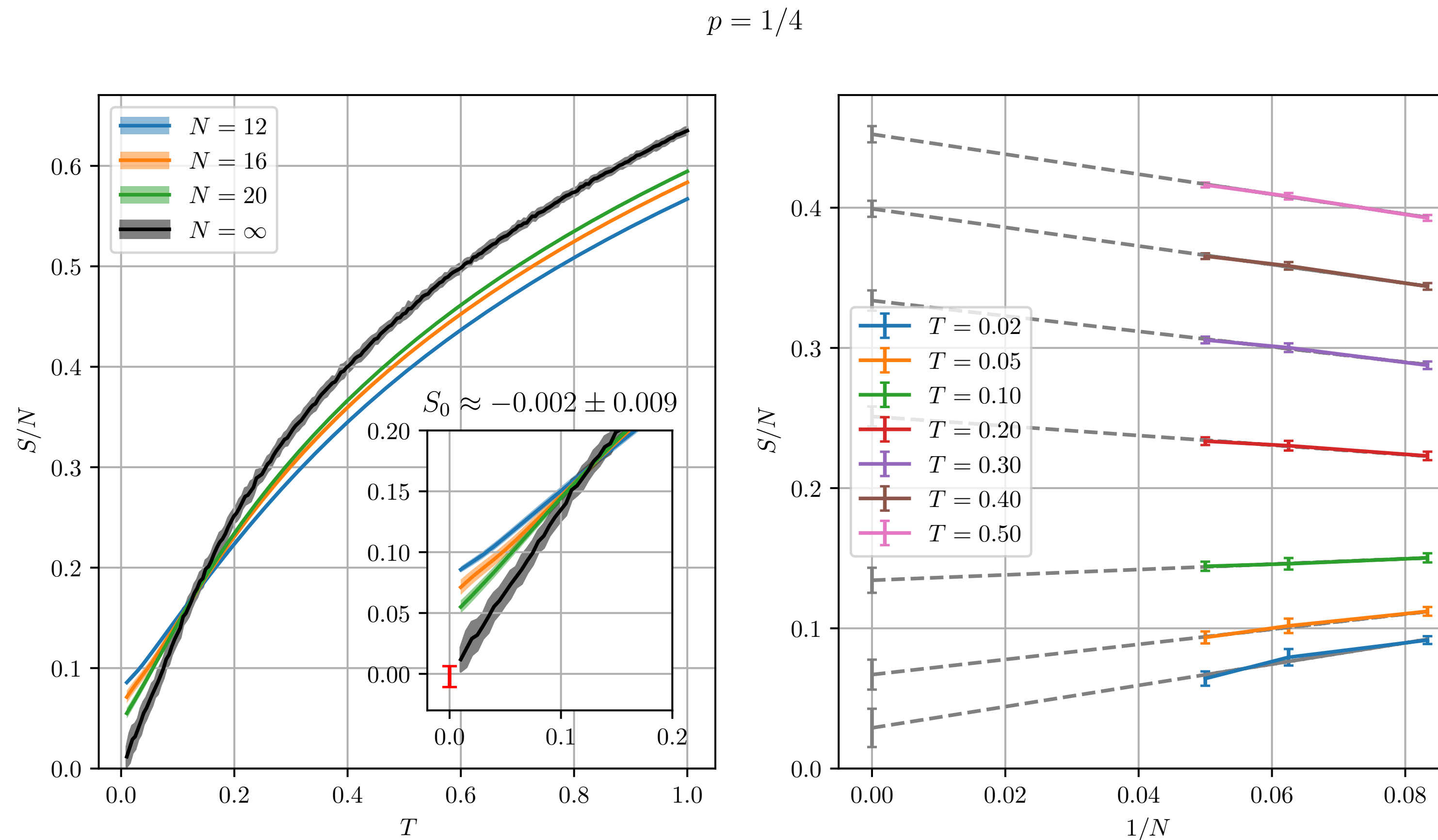
# Non-zero $s_0$ at $p = 1/4$ is extrapolation-dependent

$p = 1/4$



Thermodynamics from exact diagonalization of SU(2) random-t-J model

# Non-zero $s_0$ at $p = 1/4$ is extrapolation-dependent



Thermodynamics from exact diagonalization of SU(2) random-t-J model

1. Random  $J$  model (insulator)

*Operator spectrum and numerics*

2. Random  $t$ - $J$  model (metals)

*Deconfined criticality and numerics*

3. Random  $t$ - $J$ - $U$  model

## Random $t$ - $J$ - $U_H$ model

$$H = -\frac{1}{\sqrt{N}} \sum_{i,j=1}^N t_{ij} c_{i\alpha}^\dagger c_{j\alpha} + \frac{1}{\sqrt{N}} \sum_{i<j=1}^N J_{ij} \vec{S}_i \cdot \vec{S}_j + U_H \sum_{i=1}^N n_{i\uparrow} n_{i\downarrow}$$

$$\alpha = \uparrow, \downarrow, \quad \vec{S}_i = \frac{1}{2} c_{i\alpha}^\dagger \vec{\sigma}_{\alpha\beta} c_{i\beta}, \quad n_{i\alpha} = c_{i\alpha}^\dagger c_{i\alpha},$$

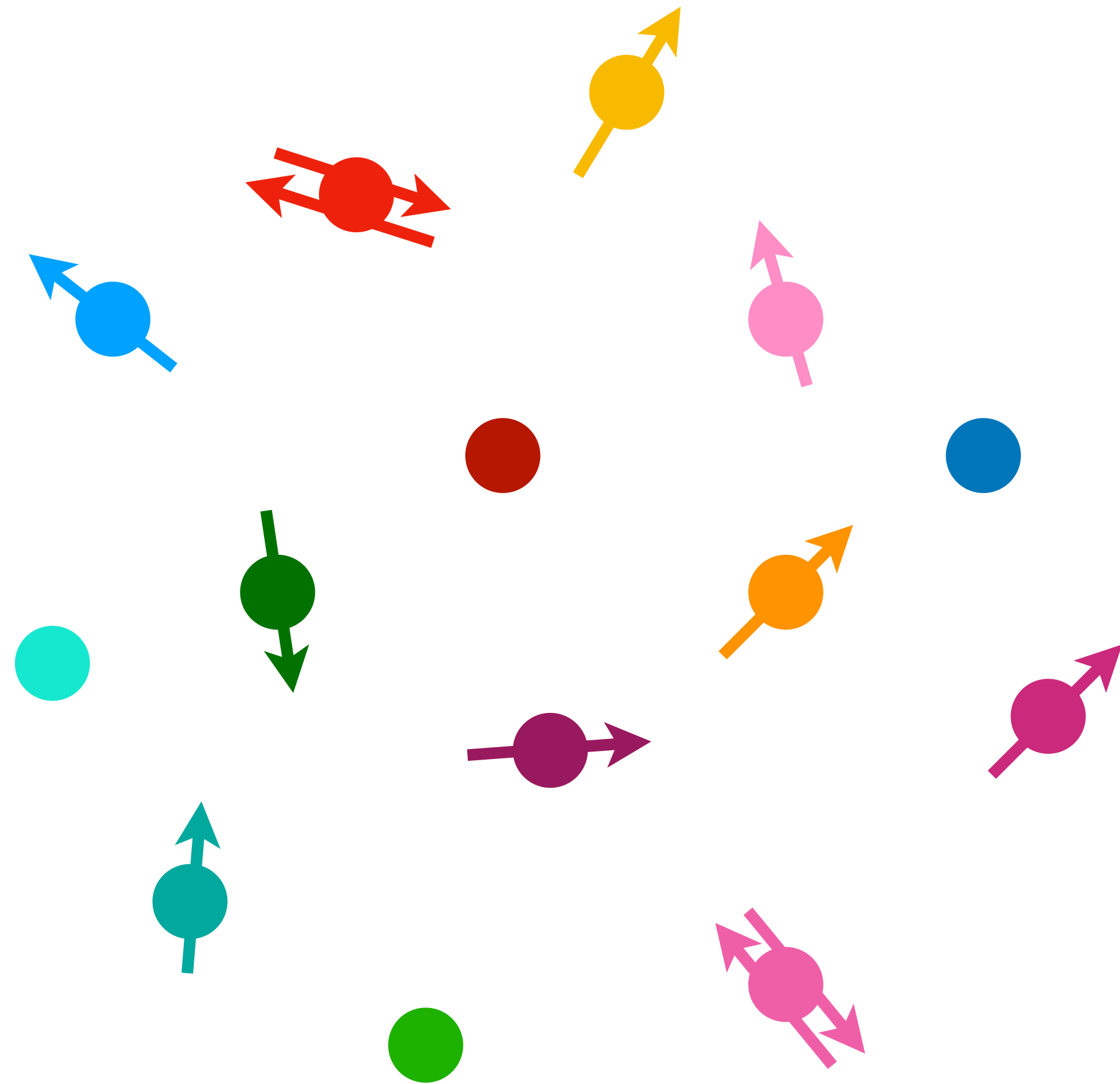
$$J_{ij} \text{ random, } \overline{J_{ij}} = 0, \overline{J_{ij}^2} = J^2$$

$$t_{ij} \text{ random, } \overline{t_{ij}} = 0, \overline{t_{ij}^2} = t^2$$

$$U_H > 0 \text{ non-random}$$

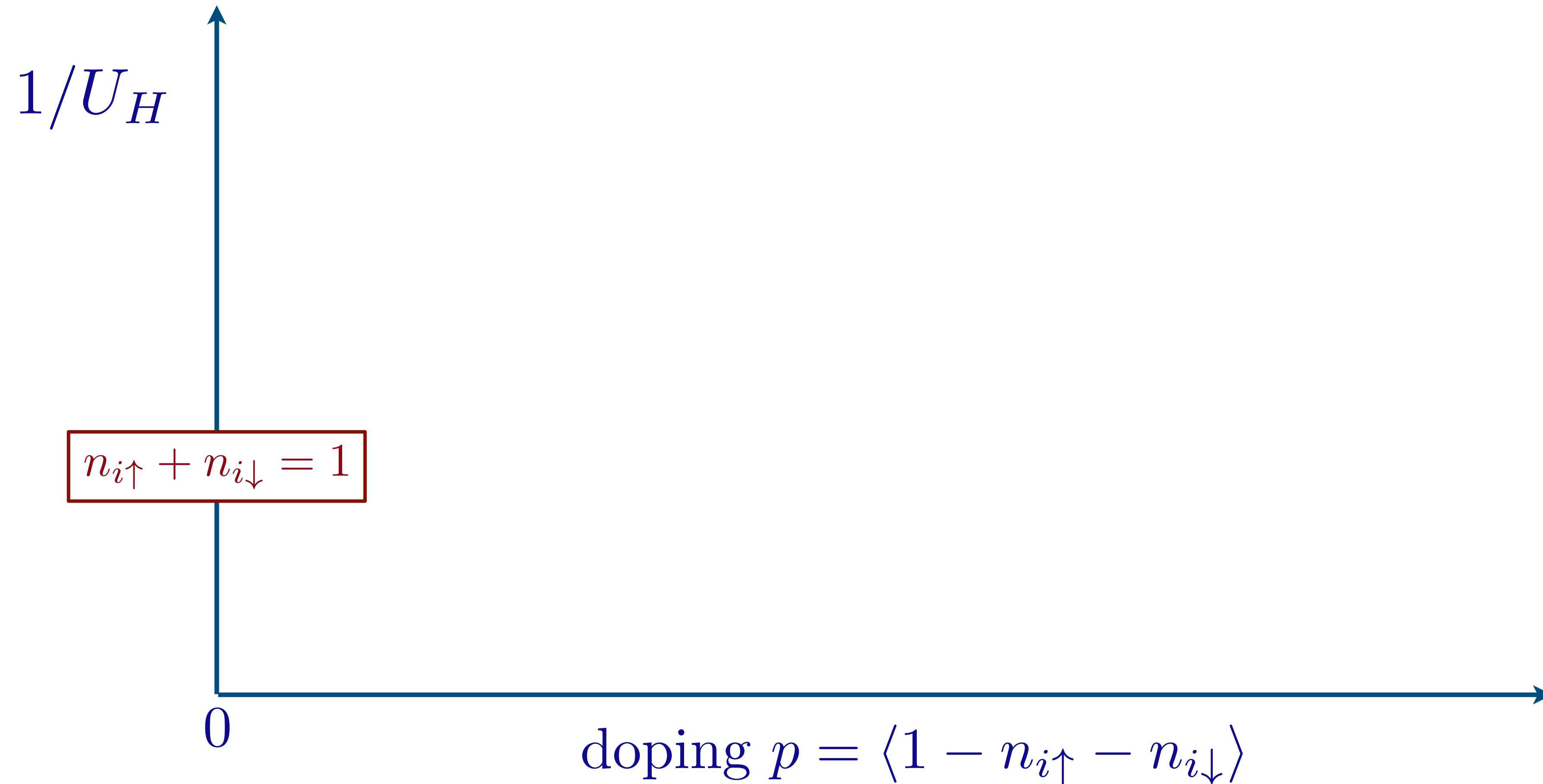
# Random $t$ - $J$ - $U_H$ model

$$H = -\frac{1}{\sqrt{N}} \sum_{i,j=1}^N t_{ij} c_{i\alpha}^\dagger c_{j\alpha} + \frac{1}{\sqrt{N}} \sum_{i<j=1}^N J_{ij} \vec{S}_i \cdot \vec{S}_j + U_H \sum_{i=1}^N n_{i\uparrow} n_{i\downarrow}$$



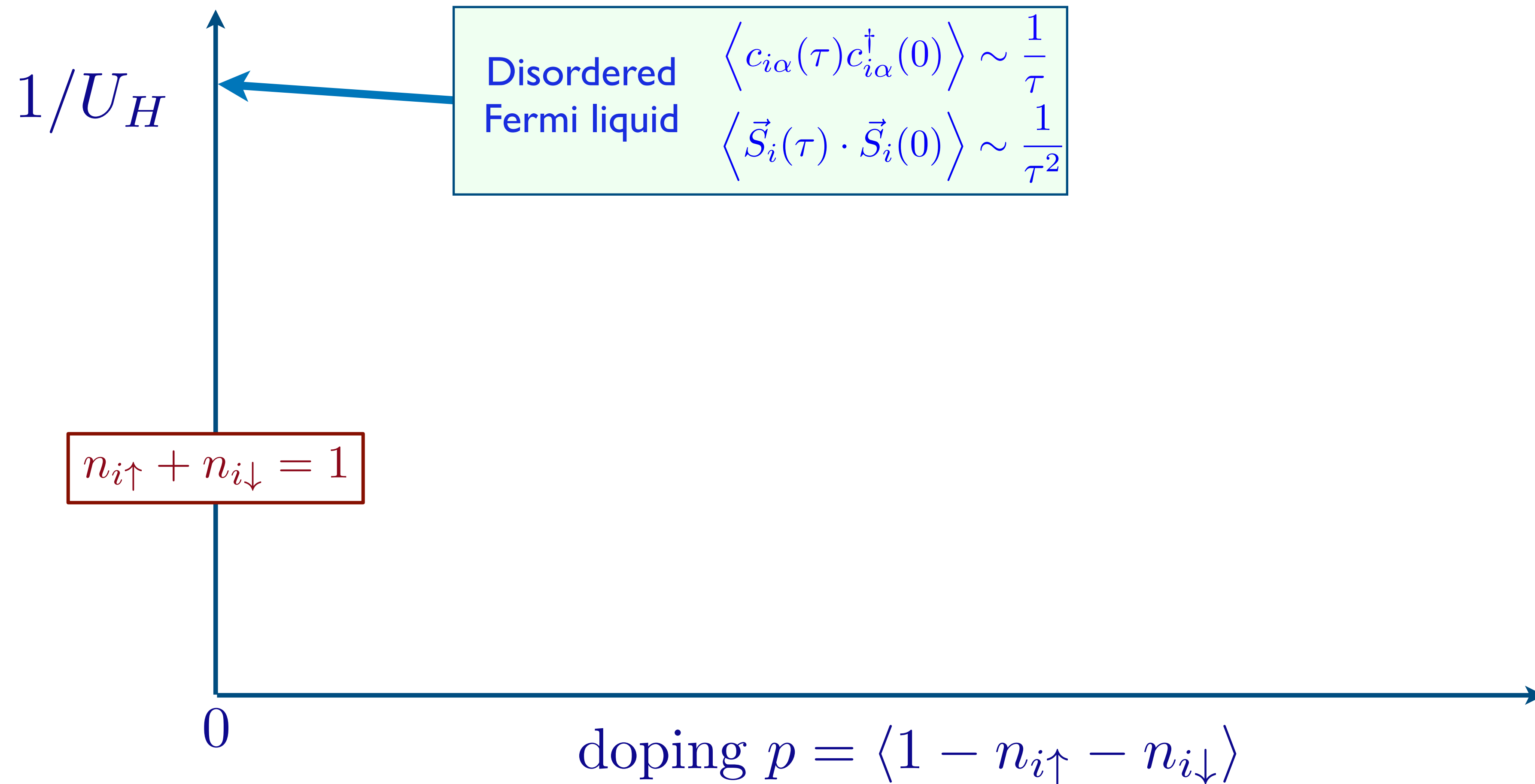
# Random $t$ - $J$ - $U_H$ model

$$H = -\frac{1}{\sqrt{N}} \sum_{i,j=1}^N t_{ij} c_{i\alpha}^\dagger c_{j\alpha} + \frac{1}{\sqrt{N}} \sum_{i<j=1}^N J_{ij} \vec{S}_i \cdot \vec{S}_j + U_H \sum_{i=1}^N n_{i\uparrow} n_{i\downarrow}$$



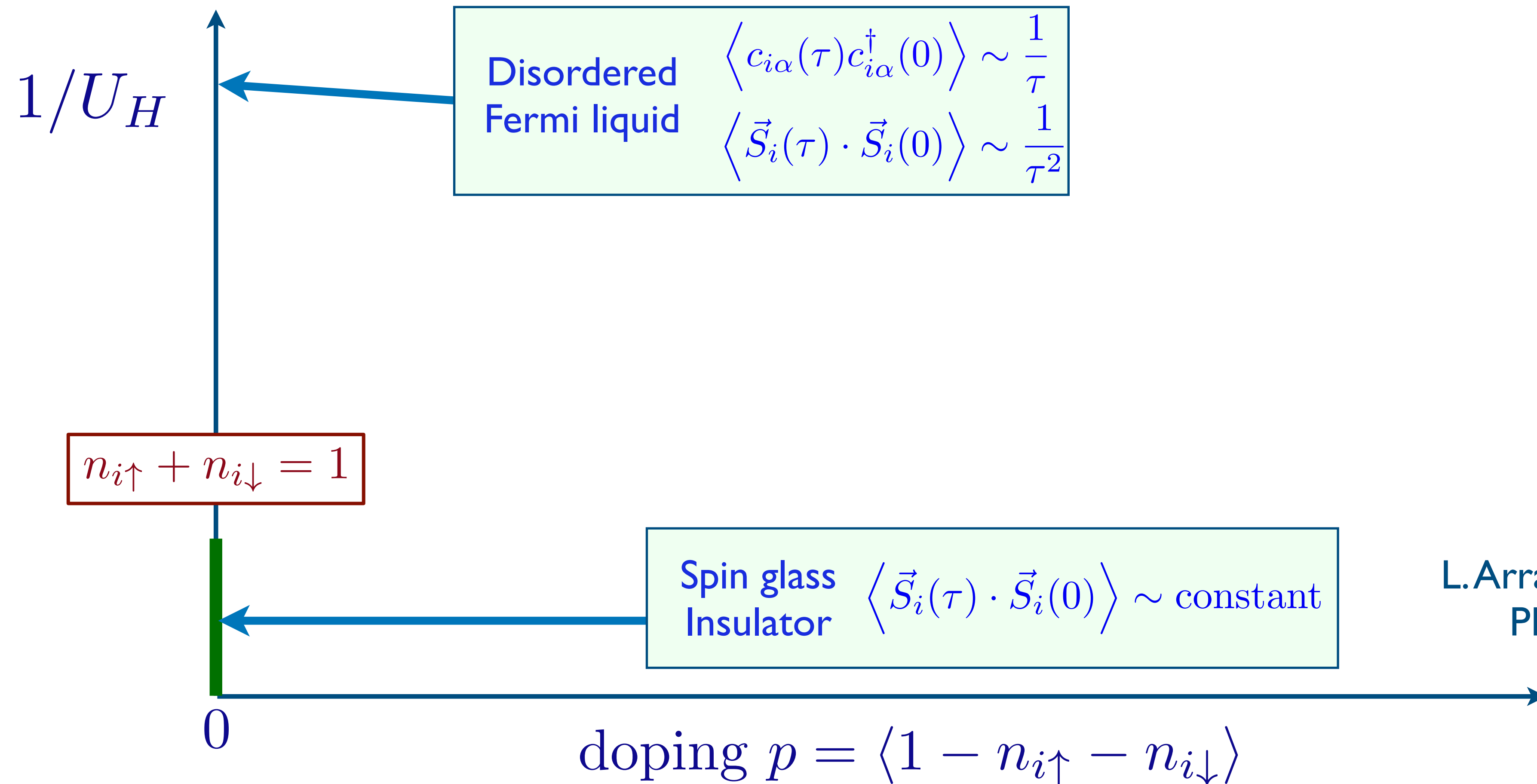
# Random $t$ - $J$ - $U_H$ model

$$H = -\frac{1}{\sqrt{N}} \sum_{i,j=1}^N t_{ij} c_{i\alpha}^\dagger c_{j\alpha} + \frac{1}{\sqrt{N}} \sum_{i<j=1}^N J_{ij} \vec{S}_i \cdot \vec{S}_j + U_H \sum_{i=1}^N n_{i\uparrow} n_{i\downarrow}$$



# Random $t$ - $J$ - $U_H$ model

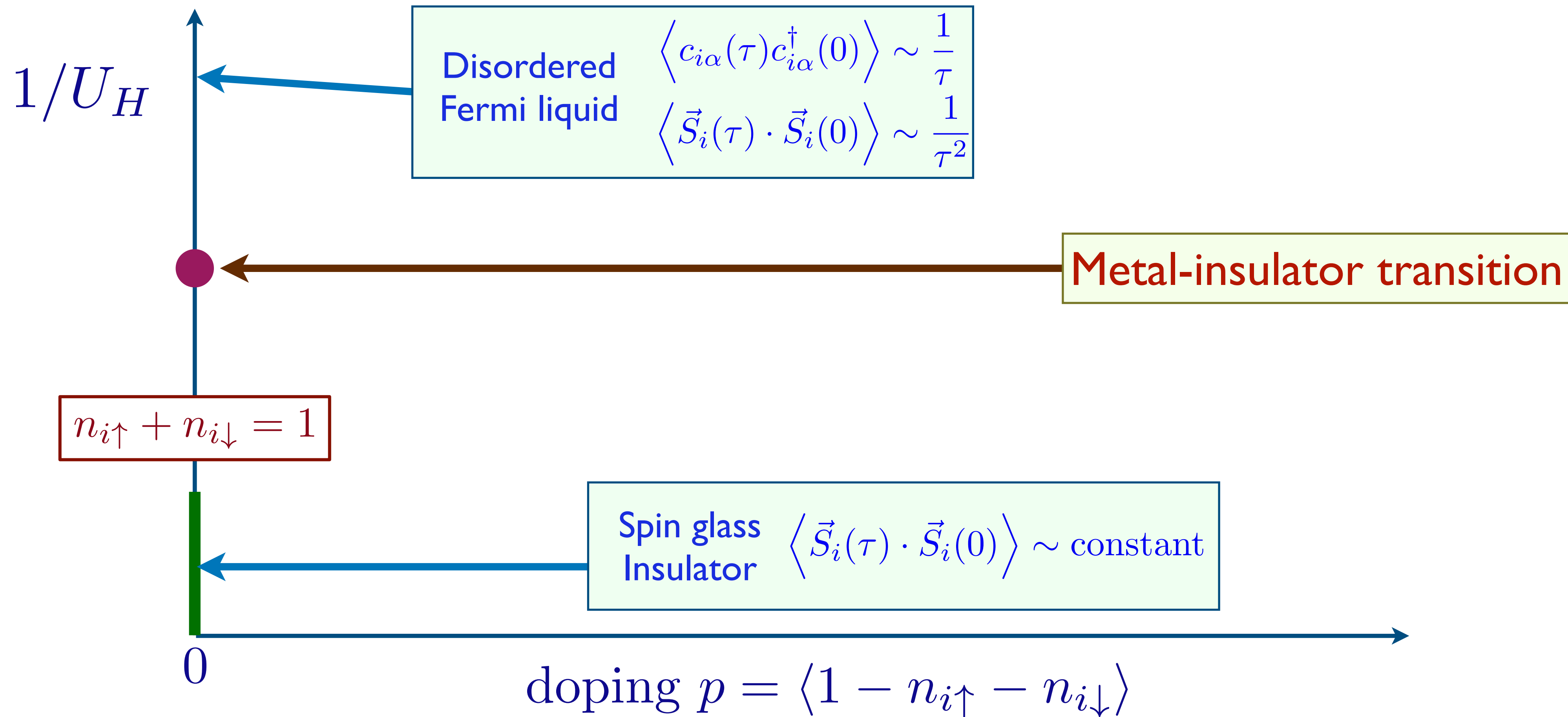
$$H = -\frac{1}{\sqrt{N}} \sum_{i,j=1}^N t_{ij} c_{i\alpha}^\dagger c_{j\alpha} + \frac{1}{\sqrt{N}} \sum_{i<j=1}^N J_{ij} \vec{S}_i \cdot \vec{S}_j + U_H \sum_{i=1}^N n_{i\uparrow} n_{i\downarrow}$$



L. Arrachea and M. J. Rozenberg,  
PRB **65**, 224430 (2002)

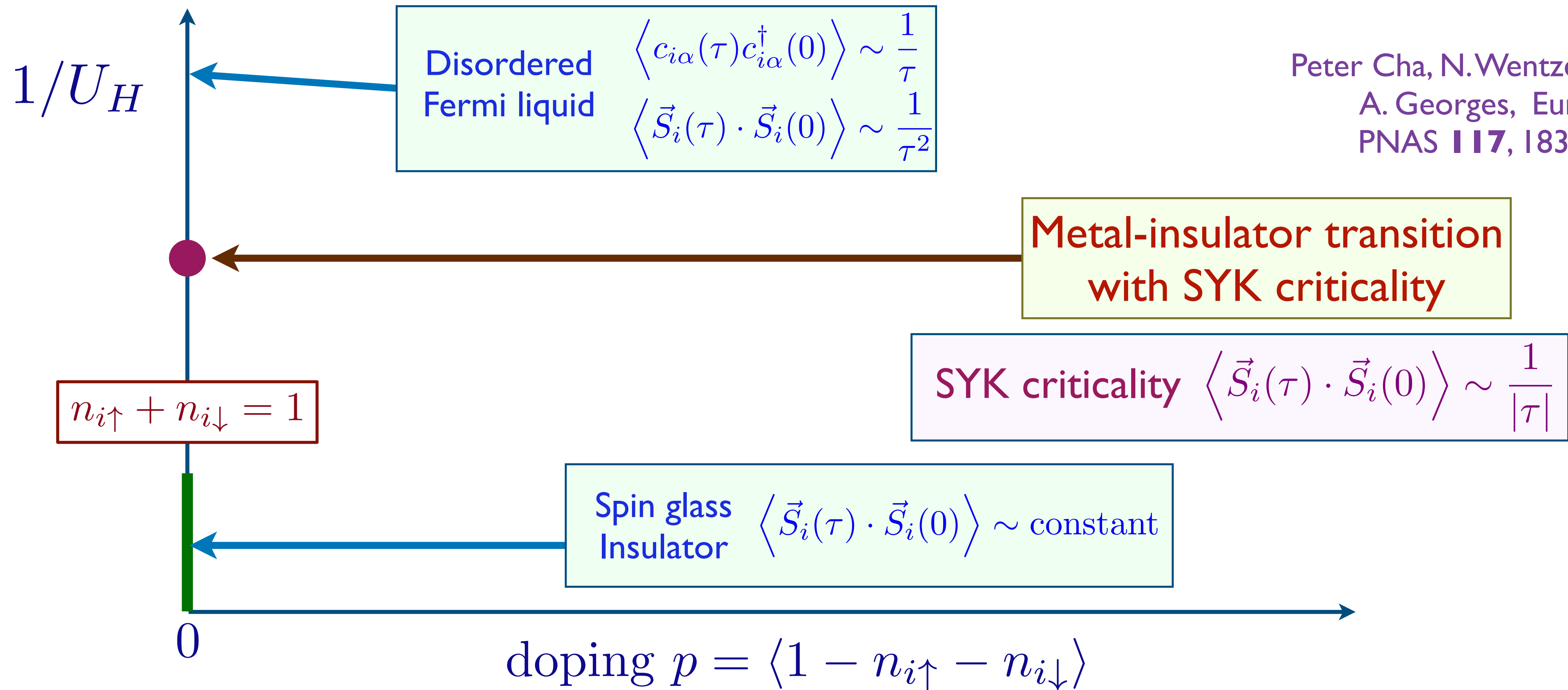
# Random $t$ - $J$ - $U_H$ model

$$H = -\frac{1}{\sqrt{N}} \sum_{i,j=1}^N t_{ij} c_{i\alpha}^\dagger c_{j\alpha} + \frac{1}{\sqrt{N}} \sum_{i<j=1}^N J_{ij} \vec{S}_i \cdot \vec{S}_j + U_H \sum_{i=1}^N n_{i\uparrow} n_{i\downarrow}$$



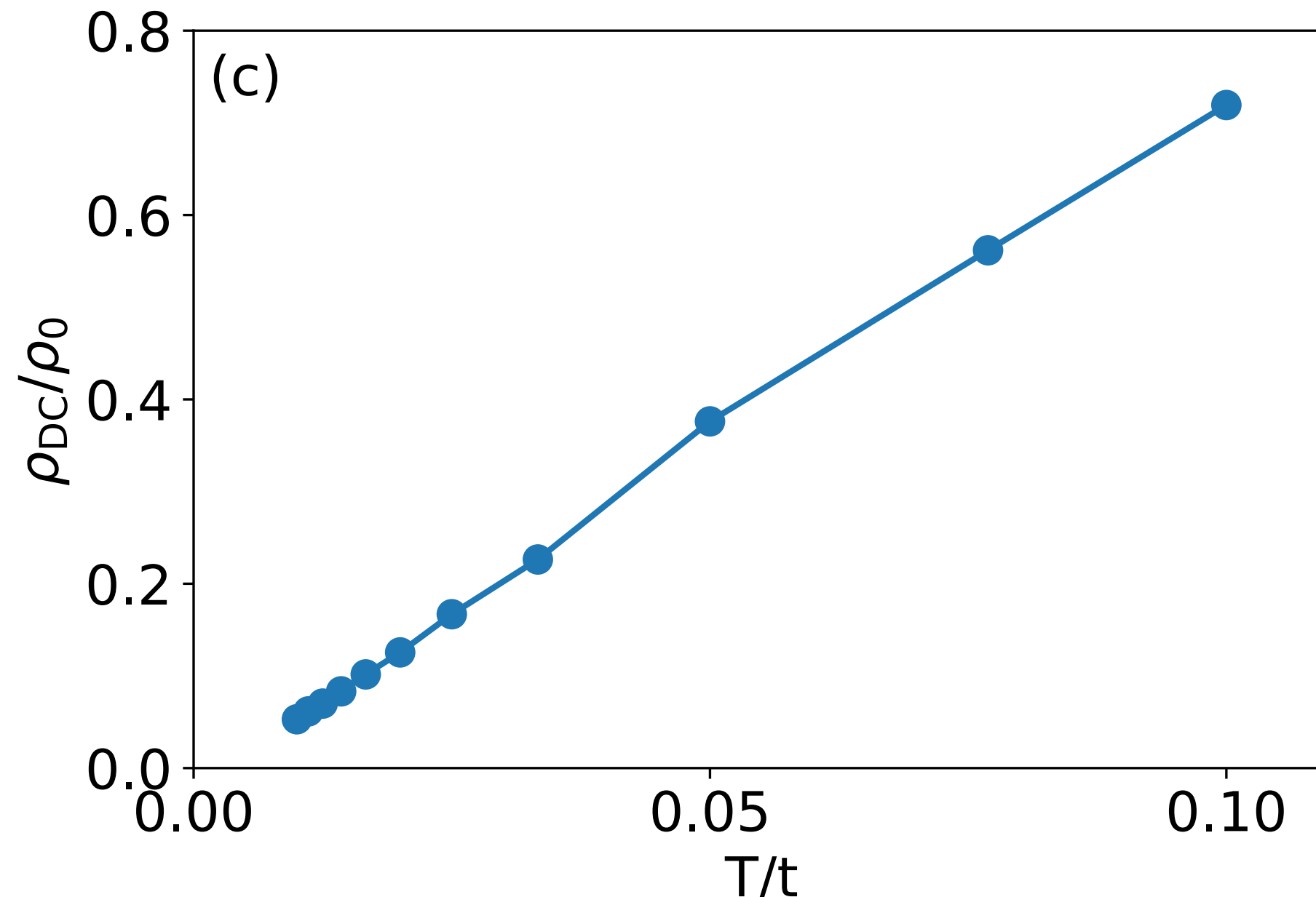
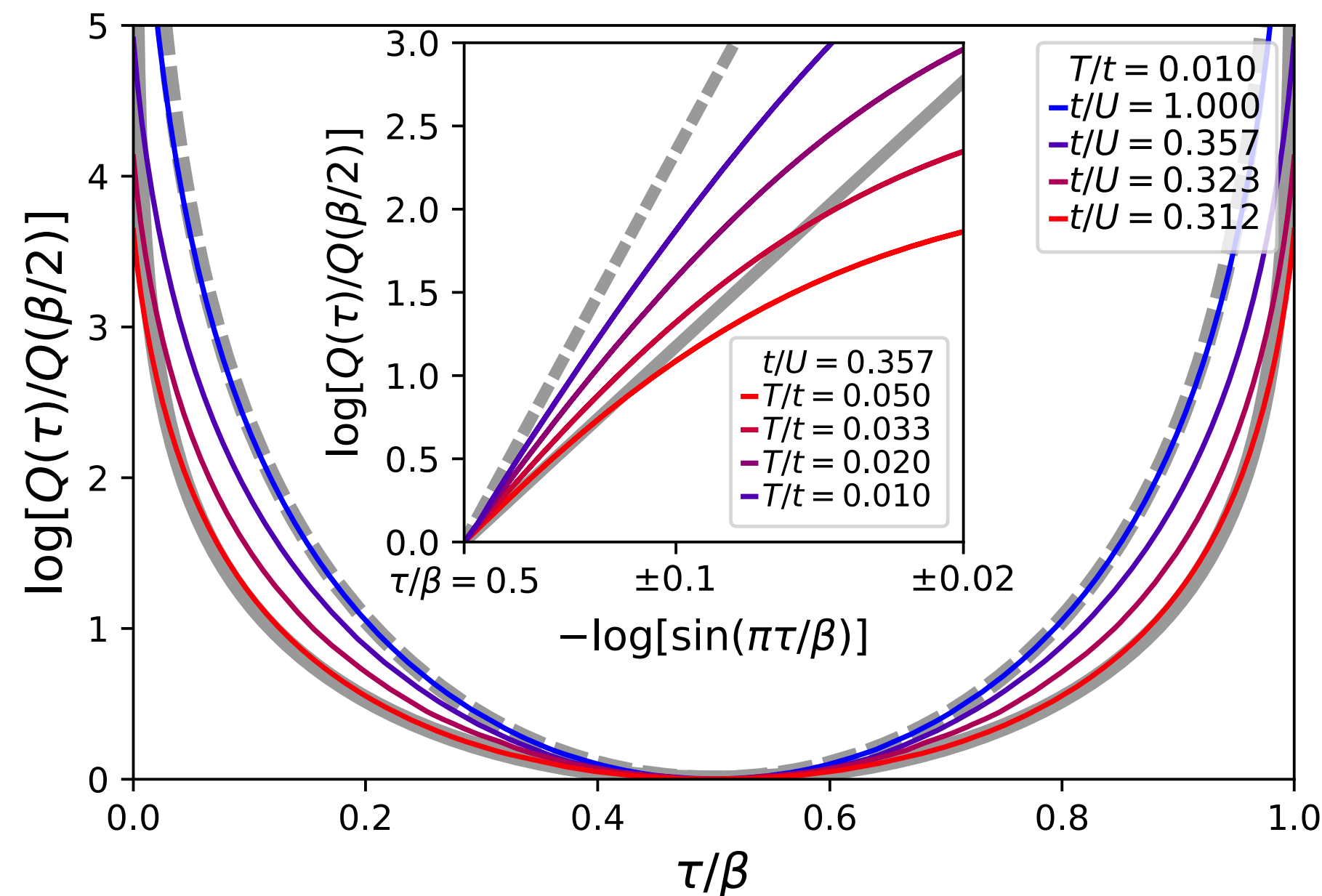
# Random $t$ - $J$ - $U_H$ model

$$H = -\frac{1}{\sqrt{N}} \sum_{i,j=1}^N t_{ij} c_{i\alpha}^\dagger c_{j\alpha} + \frac{1}{\sqrt{N}} \sum_{i<j=1}^N J_{ij} \vec{S}_i \cdot \vec{S}_j + U_H \sum_{i=1}^N n_{i\uparrow} n_{i\downarrow}$$



Peter Cha, N. Wentzell, O. Parcollet,  
 A. Georges, Eun-Ah Kim,  
 PNAS **117**, 18341 (2020)

# Linear resistivity and Sachdev-Ye-Kitaev (SYK) spin liquid behavior in a quantum critical metal with spin-1/2 fermions



Critical spin correlations:

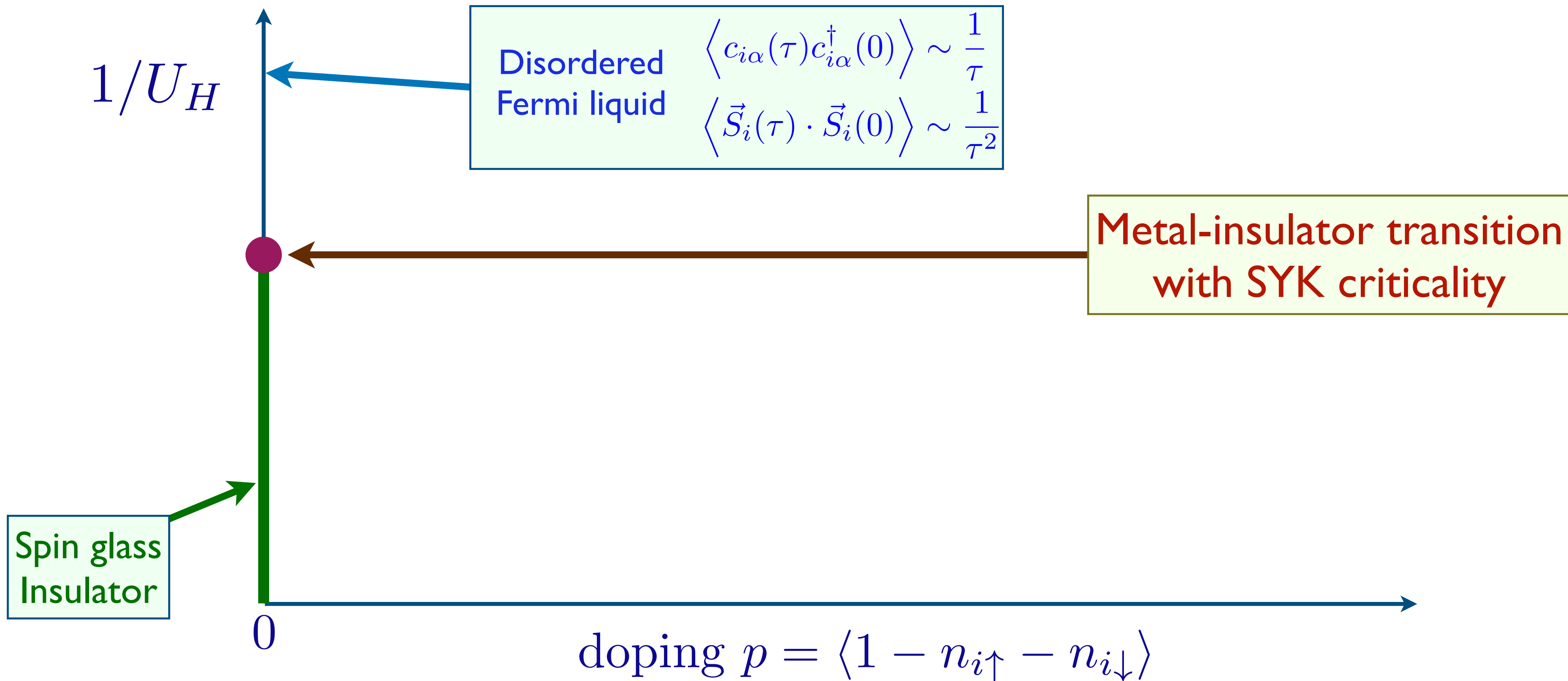
$$\langle \vec{S}(\tau) \cdot \vec{S}(0) \rangle \sim \frac{1}{|\tau|}$$

Resistivity  $\rho \sim T$  to the lowest  $T$  at the critical point

Onset of insulating gap and spin glass order appear to co-occur.

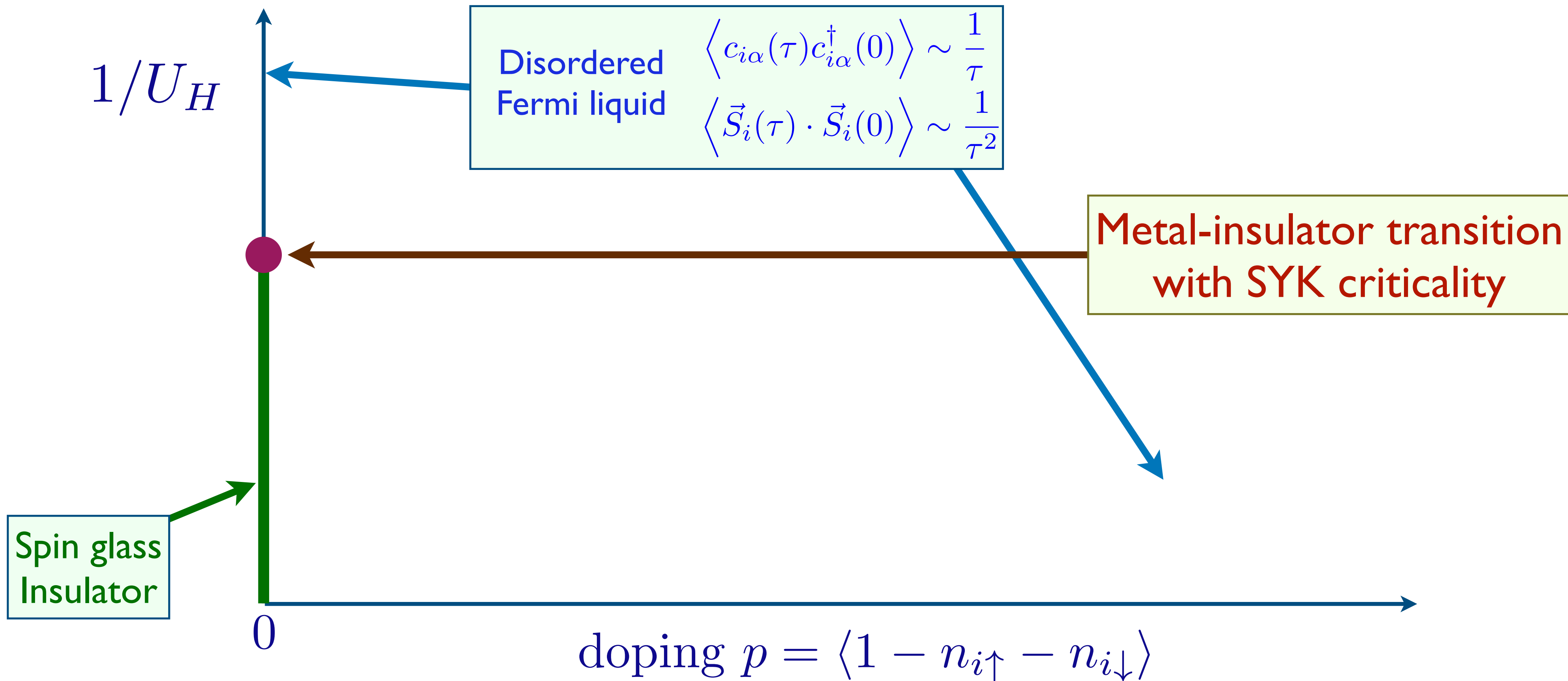
# Random $t$ - $J$ - $U_H$ model

$$H = -\frac{1}{\sqrt{N}} \sum_{i,j=1}^N t_{ij} c_{i\alpha}^\dagger c_{j\alpha} + \frac{1}{\sqrt{N}} \sum_{i<j=1}^N J_{ij} \vec{S}_i \cdot \vec{S}_j + U_H \sum_{i=1}^N n_{i\uparrow} n_{i\downarrow}$$



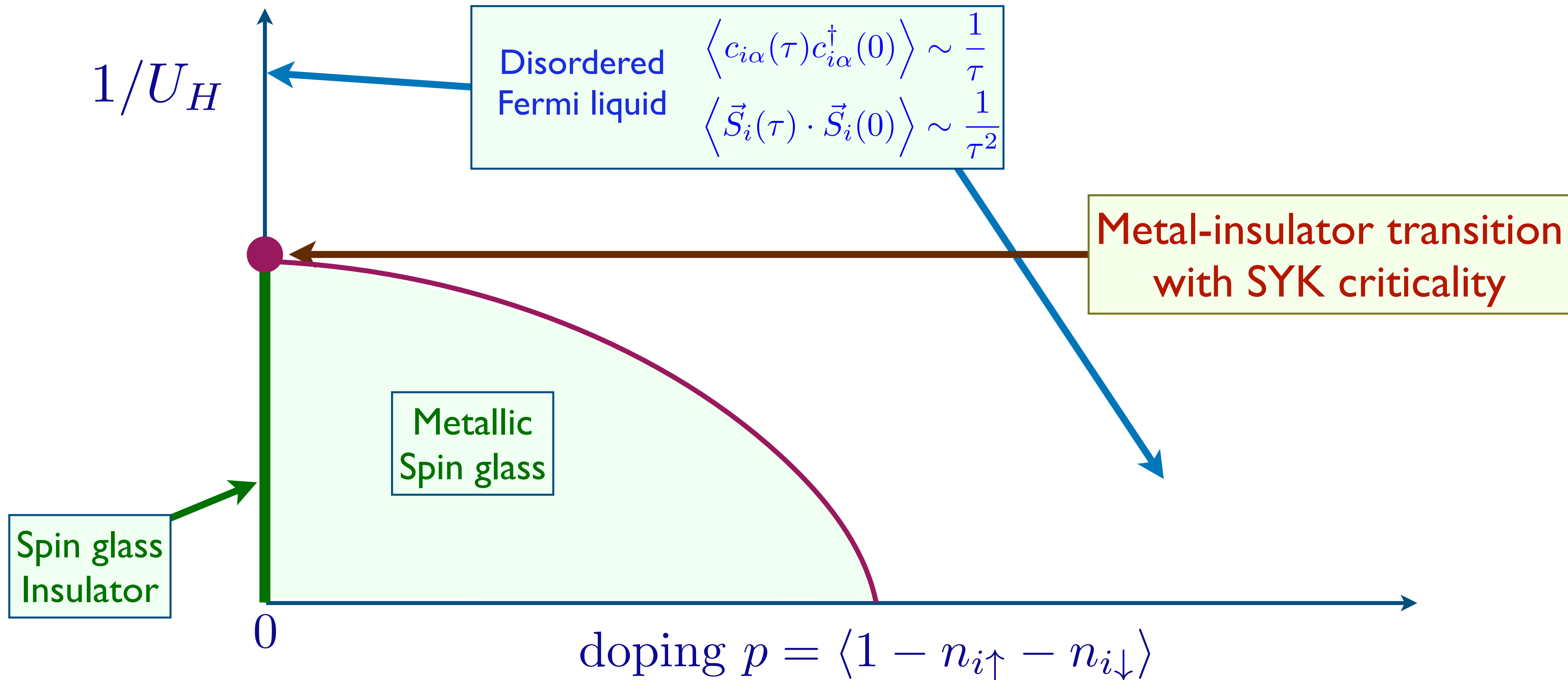
# Random $t$ - $J$ - $U_H$ model

$$H = -\frac{1}{\sqrt{N}} \sum_{i,j=1}^N t_{ij} c_{i\alpha}^\dagger c_{j\alpha} + \frac{1}{\sqrt{N}} \sum_{i<j=1}^N J_{ij} \vec{S}_i \cdot \vec{S}_j + U_H \sum_{i=1}^N n_{i\uparrow} n_{i\downarrow}$$



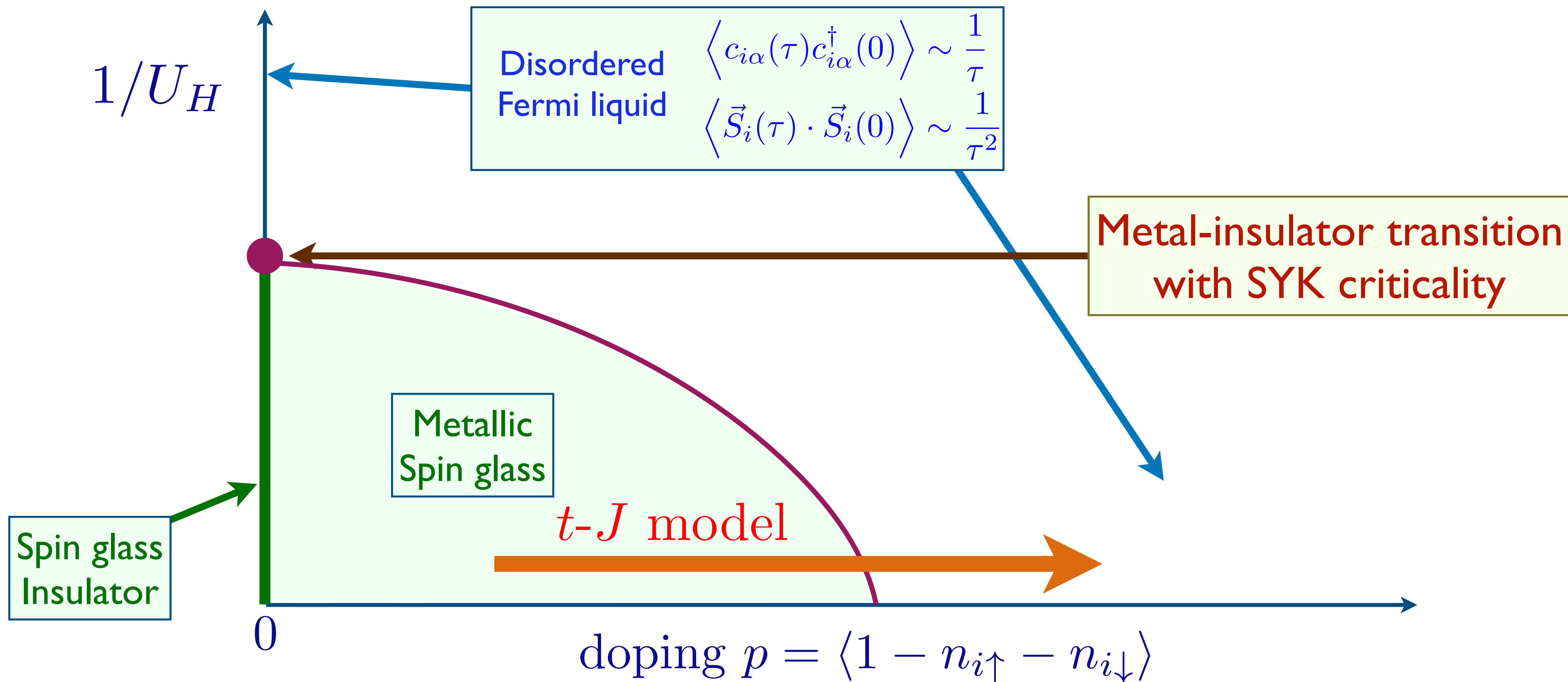
# Random $t$ - $J$ - $U_H$ model

$$H = -\frac{1}{\sqrt{N}} \sum_{i,j=1}^N t_{ij} c_{i\alpha}^\dagger c_{j\alpha} + \frac{1}{\sqrt{N}} \sum_{i<j=1}^N J_{ij} \vec{S}_i \cdot \vec{S}_j + U_H \sum_{i=1}^N n_{i\uparrow} n_{i\downarrow}$$



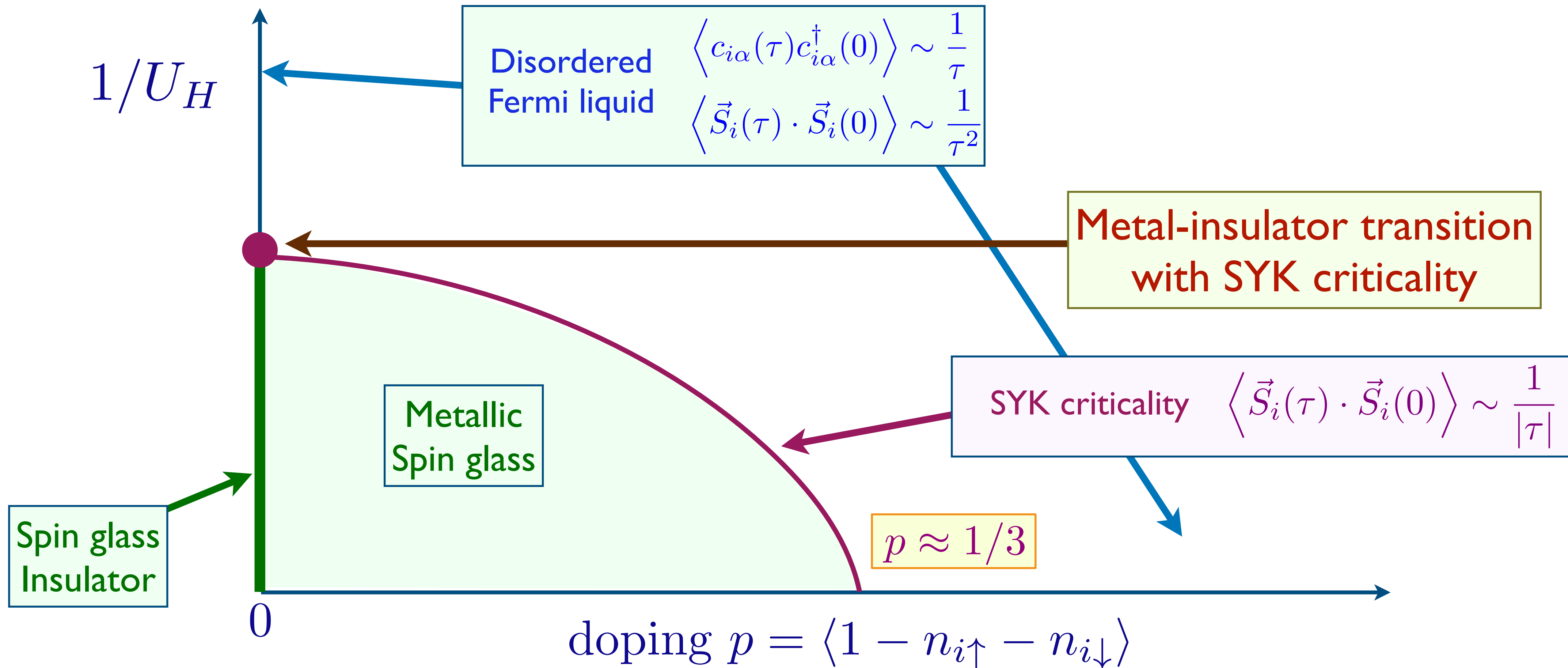
# Random $t$ - $J$ - $U_H$ model

$$H = -\frac{1}{\sqrt{N}} \sum_{i,j=1}^N t_{ij} c_{i\alpha}^\dagger c_{j\alpha} + \frac{1}{\sqrt{N}} \sum_{i<j=1}^N J_{ij} \vec{S}_i \cdot \vec{S}_j + U_H \sum_{i=1}^N n_{i\uparrow} n_{i\downarrow}$$



# Random $t$ - $J$ - $U_H$ model

$$H = -\frac{1}{\sqrt{N}} \sum_{i,j=1}^N t_{ij} c_{i\alpha}^\dagger c_{j\alpha} + \frac{1}{\sqrt{N}} \sum_{i<j=1}^N J_{ij} \vec{S}_i \cdot \vec{S}_j + U_H \sum_{i=1}^N n_{i\uparrow} n_{i\downarrow}$$



## Random $t$ - $J$ model

- Proposed phase diagram of random  $t$ - $J$  model captures key characteristics of cuprates.
- Critical electron Green's function  $G_c(\tau) \sim 1/\tau$  and local spin correlator  $\chi(\tau) \sim 1/|\tau|$ .
- Can be interpreted in terms of fractionalization with spinon and holon correlators  $\sim 1/\sqrt{\tau}$  (deconfined criticality).
- Linear-in- $T$  resistivity down to  $T = 0$  at the critical point from the time reparameterization soft mode (but there could be other singular modes).
- Carrier density  $p$  for  $p < p_c$ , and  $1 + p$  for  $p > p_c$ .
- Extensive zero temperature entropy  $\lim_{T \rightarrow 0} \lim_{N \rightarrow \infty} S/N > 0$ . Related to entropy of extremal black holes.

